THE ROLE OF HEPATOCELLULAR ENOS IN NAFLD DEVELOPMENT

AND HEPATIC MITOCHONDRIAL ADAPTATIONS TO EXERCISE

_____

A Dissertation

presented to

the Faculty of the Graduate School

at the University of Missouri-Columbia

_____

In Partial Fulfillment

of the Requirements for the Degree

Doctor of Philosophy

_____

by

RORY P. CUNNINGHAM

Dr. R. Scott Rector, Dissertation Supervisor

December 2020

The undersigned, appointed by the dean of the Graduate School, have examined the dissertation entitled

THE ROLE OF HEPATOCELLULAR ENOS IN NAFLD DEVELOPMENT

AND HEPATIC MITOCHONDRIAL ADAPTATIONS TO EXERCISE

presented by Rory P. Cunningham,

a candidate for the degree of Doctor of Philosophy,

and hereby certify that, in their opinion, it is worthy of acceptance.

Associate Professor Scott Rector

Associate Professor Victoria Vieira-Potter

Professor Jill Kanaley

Professor Frank Booth

ACKNOWLEDGEMENTS

First and foremost, I would like to thank my primary supervisor Dr. Scott Rector for his guidance and mentorship throughout my entire time at The University of Missouri. As stressful as a doctorate degree can be, I thought Dr. Rector found the perfect balance between maintaining productivity and managing expectations and workload. I always felt comfortable bringing up any issues and importantly never worried about bringing data that went the opposite of our hypothesis! I would like to thank Dr. Jill Kanaley for her guidance and thoughts on post-student life. I never shied from bouncing any career options and ideas off her, and she has been very helpful in choosing my next career step. I would also like to thank and acknowledge Dr. Victoria Vieira-Potter and Dr. Frank Booth in helping to shape my doctorate experience and ultimately my dissertation studies. I always enjoyed my meetings with Dr. Vieira-Potter, and left with a smile and a new way of thinking about a certain piece of data. I'd like to thank Dr. Booth for his renowned expertise and keeping me on track with his 'big picture' questions, and was always good for a couple of jokes in there to keep things light. It was a privilege to have all of these excellent scientists on my committee.

Importantly, these studies could not have been completed without the help of my lab mates and manager. Grace Meers was instrumental in not only teaching me all the techniques in the lab (while I stretched her patience thin), but collecting vital data for my dissertation. Mary Moore always responded positively to my threats of taking her name off all my papers if she didn't start pulling her weight, but I am very grateful to have had such a good friend in the lab who was so generous with her time. I'd also like to thank

TABLE OF CONTENTS

ABBREVIATIONS

AAV - adeno associated virus

Adv - adenoviral

ALT - alanine aminotransferase

AMPK - AMP-activated protein kinase

ASMs - acid soluble metabolites.

AUC - area under the curve

BNIP3 - BCL2 interacting protein 3

C - complex

CD - control diet;

cGMP - cyclic guanosine-3′,5′-monophosphate

DRP1 - dynamin related protein 1

eNOS - endothelial nitric oxide synthase

eNOS$^{fl/fl}$ – eNOS floxed mouse

eNOS$^{hep-/-}$ - eNOS hepatocyte-specific knockout mouse

EX – voluntary wheel running exercise

GTT - glucose tolerance test

H&E - haemotoxylin and eosin

ITT - insulin tolerance test

LC3 – light chain 3

NAFLD - nonalcoholic fatty liver disease

NAS - NAFLD activity score

NASH - nonalcoholic steatohepatitis

NO - nitric oxide

NRF2 - Nuclear Respiratory Factor-2

OCR - oxygen consumption rate

OLETF - Otsuka Long-Evans Tokushima Fatty rats

OPA1 - dynamin-like 120 kDa protein, mitochondrial

OXPHOS – oxidative phosphorylation

PCoA - palmitoyl-CoA

PGC1α - peroxisome proliferator-activated receptor gamma coactivator 1-α

PINK1 - PTEN-induced kinase 1

PTT - pyruvate tolerance test

RP - retroperitoneal.

TCA- Triacarboxylic Acid

TEM - transmission electron microscopy

TFAM - mitochondrial transcription factor A

TGs – triglycerides

ULK1 - Unc-51 Like Autophagy Activating Kinase 1

VWR – voluntary wheel running

WD - western diet.

WT – wild-type

β-HAD - 3-hydroxyacyl-CoA dehydrogenase

LIST OF FIGURES

LIST OF TABLES

ABSTRACT

Whole body loss of endothelial nitric oxide synthase (eNOS) worsens hepatic mitochondrial function and exacerbates nonalcoholic fatty liver disease/steatohepatitis (NAFLD/NASH) development and progression. However, the precise role of eNOS in hepatocytes in the contribution to NAFLD has not been established. Here, we use gain- and loss- of-function approaches including a hepatocyte-specific eNOS knockout mouse model (eNOS$^{hep-/-}$), and lifestyle interventions (diet and exercise), to investigate the role of hepatocellular eNOS in NAFLD/NASH development and hepatic mitochondrial adaptations to exercise. Ablation of hepatocellular eNOS via genetic and viral knockout exacerbated hepatic steatosis and inflammation, decreased hepatic mitochondrial fatty acid oxidation and respiration, and impaired mitophagy. Conversely, overexpressing hepatocellular eNOS via viral approaches increased hepatocyte respiration, markers of mitophagy, while attenuating NASH progression. Interestingly, these detriments were not rescued by BNIP3 overexpression or nitric oxide (NO) donors in eNOS deficient hepatocytes. In addition, elevated H_2O_2 emission and hepatic steatosis in eNOS$^{hep-/-}$ mice was completely ablated with 10 weeks of voluntary wheel running exercise. Interestingly, eNOS$^{hep-/-}$ male mice had a blunted exercise-induced increase in hepatic fatty acid oxidation. eNOS$^{hep-/-}$ mice also had impaired markers of energy sensing ability of the cell and attenuated activation of the autophagy initiating factor ULK1. While mitochondrial respiration and markers of mitochondrial content were not increased with exercise, female mice showed markers of mitochondrial biogenesis. Collectively, these data uncover the important and novel role of hepatocellular eNOS in exercise-induced hepatic mitochondrial adaptations, and help to further the understanding behind the mechanistic role of eNOS in NAFLD development.

CHAPTER 1 – Background and Aims

Nonalcoholic fatty liver disease

Nonalcoholic fatty liver disease (NAFLD) is a progressive disease of the liver that ranges on a wide pathological spectrum from simple hepatic steatosis to a more serve nonalcoholic steatohepatitis (NASH) phenotype, which can progress to fibrosis and cirrhosis (2). Numerous factors are involved in the progression of NAFLD, including changes in lipid metabolism, insulin resistance, inflammatory cytokines, and oxidative stress (3). NAFLD has a high incidence rate, with reports in the general population ranging from 10-30% and as high as 80-100% in people with obesity (4, 5). These rates exhibit gender-specific differences, with men at a significantly higher risk of developing NAFLD than premenopausal women (6, 7). NAFLD progression is the most rapidly increasing indication for liver transplantation in the United States (8), and now can be considered a multisystem disease affecting many extra-hepatic organs. Indeed, NAFLD is an independent risk factor for cardiovascular, liver-related, and all-cause mortality (9, 10), and doubles the risk of type 2 diabetes mellitus development (11). Currently, there are no FDA-approved pharmacological treatments for NAFLD.

Mechanisms of NAFLD development

Despite the prevalence of NAFLD, the pathophysiology of disease progression is not well understood. The mechanisms of NAFLD and NASH development are complex and multifactorial, with the most widely accepted model being the multiple-hit hypothesis (2, 12). Here, the interaction between dietary, environmental, and genetic factors as well as

inter-organ cross talk all contribute to the pathogenesis of NAFLD. Insulin resistance

(IR) at the adipose tissue level prevents insulin-stimulated suppression of lipolysis,

causing free fatty acids (FFA) to be ectopically taken up and converted to triglycerides by

the liver, along with excess dietary lipids. Additionally, hepatic IR disrupts the insulin-

mediated suppression of hepatic glucose output. The combination of hepatic and adipose

tissue IR result in elevated serum insulin and glucose concentrations - potent stimulators

of *de novo* lipogenesis (DNL), where lipids are synthesized from dietary carbohydrates.

Indeed, as much as ~25% of liver triglycerides can be attributed to DNL in NAFLD

patients (13). This buildup of triglycerides in the liver can lead to hepatic lipotoxicity and

IR, increasing hepatic inflammatory pathways. Additionally, dysbiosis of the gut

microbiome have been linked with NAFLD development and progression (14, 15), with

gut-derived endotoxins and altered bile acids further exacerbating hepatic inflammation

(16).

Hepatic mitochondrial dysfunction and NAFLD

While the mechanisms behind NAFLD development have not been fully elucidated,

mounting evidence suggests that hepatic mitochondrial dysfunction is tightly linked to

disease progression (17-19). Characteristics of hepatic mitochondrial dysfunction in the

setting of NAFLD/NASH progression include decreased electron transport chain (ETC)

content, abnormal morphology, and reduced respiration and β-oxidation (20). The

inability of hepatic mitochondria to oxidize free fatty acids that enter the liver contribute

to liver triglyceride accumulation. This coupled with hepatic inflammation lead to a

decrease in mitochondrial function and generation of reactive oxygen species and inflammatory cytokine production, further exacerbating NAFLD progression. However, there is some controversy surrounding this timing of hepatic mitochondrial dysfunction during NAFLD development. In rodent models, a decline in hepatic mitochondrial function is observed early in fatty liver development; our group has shown that mitochondrial dysfunction in the liver even precedes hepatic steatosis development (21). In human NAFLD/NASH development it is not as clear - previous studies have reported a compensatory increase in hepatic mitochondrial function and tricarboxylic acid cycle (TCA) cycle flux during fatty liver development in humans (22, 23), but this is lost during NASH progression (24, 25). Moreover, NASH patients present with porous mitochondria and elevated hepatic oxidative stress, along with impaired mitochondrial biogenesis and decreased ETC complexes (24). Despite debate over its timing during NAFLD/NASH development, mitochondrial dysfunction is clearly implicated in exacerbating disease progression, and therapies that target hepatic mitochondria may provide novel avenues for NAFLD/NASH treatment.

Exercise increases hepatic mitochondrial function and reduces NAFLD

Lifestyle interventions such as diet and exercise remain the cornerstone of NAFLD therapy. Exercise has been reported to improve NAFLD outcomes via improved lipid metabolism, decreased oxidative stress, and inflammation (26), although the exact mechanisms are elusive. Regarding improved lipid metabolism, exercise may reduce liver fat through improved lipid export from the liver (27), reduced postprandial hepatic lipogenesis (28), and decreased markers of DNL (29, 30), among other pathways.

3

Importantly, exercise-induced improvements in NAFLD may also be seen in the absence of weight loss (31, 32). Our group has demonstrated that exercise brought about additional benefits beyond weight loss alone using a rodent model (30). Furthermore, our group has shown that along with improvements in NAFLD outcomes, exercise increases hepatic mitochondrial content and function (29, 30, 33, 34). Both acute and chronic exercise has been reported to improve hepatic autophagy and mitophagy (cellular process to clear aberrant and dysfunctional mitochondria) (35, 36). Taken together, these results indicate that exercise is a powerful stimulus for improving hepatic mitochondrial health and NAFLD outcomes. However, the precise mechanisms by which exercise mediates these beneficial changes in liver mitochondria are yet to be elucidated. One of the aims of the proposed study was examining the role of hepatic endothelial nitric oxide synthase (eNOS) in these adaptations.

Nitric Oxide

Nitric oxide (NO) is an autocrine and paracrine signaling gas that has many diverse functions and molecular targets, such as regulating neurotransmission, vascular tone, gene transcription, mRNA translation, and post-translational modification [reviewed in detail (37, 38)]. NO is produced by the nitric oxide synthase (NOS) enzyme, which consists of three isoforms; neuronal NOS (nNOS), inducible NOS (iNOS), and endothelial NOS (eNOS). All three isoforms catalyze the production of NO by converting L-arginine to L-citrulline, with oxygen, reduced nicotinamide-adenine-dinucleotide phosphate (NADPH), and tetrahydrobiopterin (BH4) used as essential substrates and cofactors (39). In environments of increased oxidative stress such as obesity, BH4 can be

oxidized and its bioavailability reduced. This switches the product of eNOS from NO to superoxide, in a process called eNOS uncoupling (40).

The biological role of NO is often concentration dependent; pathological levels (µM) are typically produced by iNOS as an immune defense mechanism when macrophages are induced leading to cytotoxicity (38). Alternatively, physiological levels of NO (nM) are constitutively produced by nNOS and eNOS in a calcium-calmodulin dependent manner (38), although eNOS may also be activated in a calcium independent manner by phosphorylation of the enzyme (41, 42). At these physiological levels, NO derived from nNOS and eNOS performs important regulatory functions such as vasodilation, apoptosis, inhibits platelet aggregation, and act as neurotransmitters, among other functions (37, 38). This dissertation will focus on eNOS and eNOS derived NO and the potential role that both enzyme and gas play in NAFLD development and progression.

eNOS and NAFLD/NASH

The vast majority of studies examining eNOS in relation to NAFLD/NASH development have focused on its role in hepatic blood flow and vascular resistance. Portal hypertension is a major complication in liver disease caused by increased intrahepatic vascular resistance mediated in part by eNOS derived NO (42); cirrhotic livers also present with significantly reduced hepatic eNOS activity (43, 44), while our lab has also demonstrated reduced hepatic eNOS activity after 18 weeks of western diet (WD) feeding. Furthermore, whole body eNOS null mice have increased susceptibility to high-fat-diet induced NASH (45). In addition, we have previously shown that chronic systemic

NOS inhibition exacerbates NAFLD development (46). Moreover, we have shown that reduced eNOS activation is associated with NAFLD progression (47). Importantly, loss of eNOS activation, as well as NAFLD development, were prevented with chronic voluntary wheel running exercise (47), indicating a potential role for exercise-induced elevations in eNOS activity in liver health. Recently, our group demonstrated the whole body eNOS null mice were more predisposed to western diet-induced hepatic inflammation and fibrosis, suggesting a role of eNOS in NASH susceptibility (1).

The whole body eNOS null model demonstrates a protective role for eNOS in NAFLD development. However, studies fail to define the role of hepatocyte-specific eNOS *in vivo*, as it is also present in other cell types within the liver. To address this, using the homozygous eNOS floxed mouse (eNOS$^{fl/fl}$) (48), our group has successfully generated hepatocyte-specific eNOS knockout (eNOS$^{hep-/-}$) mice by crossing eNOS$^{fl/fl}$ with homozygous Albumin-Cre transgenic mice. Shown in **Figure 1.1** is the deletion of eNOS
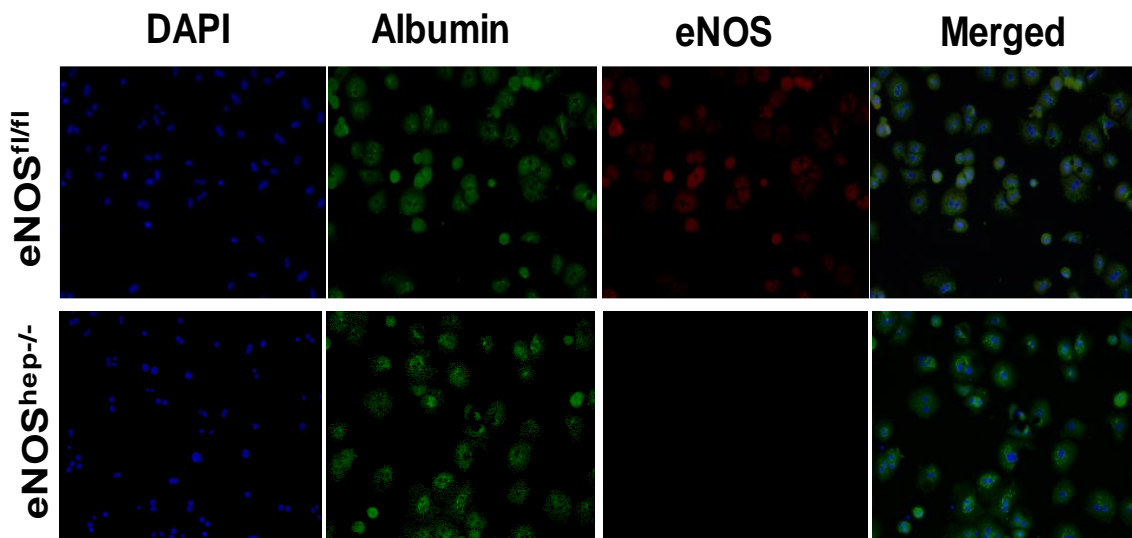
Figure 1.1. Fluorescence microscopy of isolated primary hepatocytes, confirming deletion of hepatocellular eNOS in eNOS$^{hep-/-}$ mice vs eNOS$^{fl/fl}$. Nuclei were stained with DAPI (blue), hepatocytes stained with albumin (green), and eNOS stained by anti-eNOS antibody (red) (N=4-5 per genotype).

in cultured primary hepatocytes in eNOS$^{hep-/-}$ mice compared with eNOS$^{fl/fl}$ mice.

Using this novel mouse model, we have generated preliminary data in a small subset of animals identifying a direct role of hepatocellular eNOS in NAFLD development. Here, it appears eNOS$^{hep-/-}$ mice develop hepatic steatosis on a low-fat diet with accompanying reductions in hepatic mitochondrial fatty acid oxidation and maximal uncoupled mitochondrial respiration compared with eNOS$^{fl/fl}$ control mice (**Figure 1.2A-C**). These data demonstrate for the first time that hepatocyte-specific deletion of eNOS impairs hepatic mitochondrial function and exacerbates hepatic steatosis. The proposed study will be the first to examine whether hepatocellular eNOS is required for maintaining mitochondrial function in NAFLD development. In this dissertation, I expand upon these preliminary findings by seeing if these results hold true with more animals added to the small subset shown here, as well as challenging these mice with a western diet.
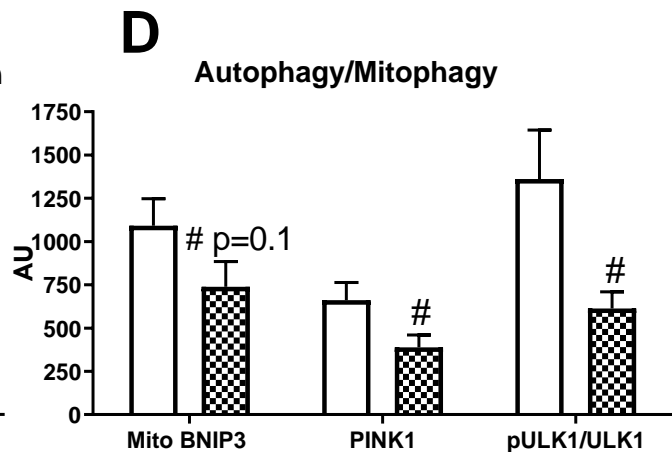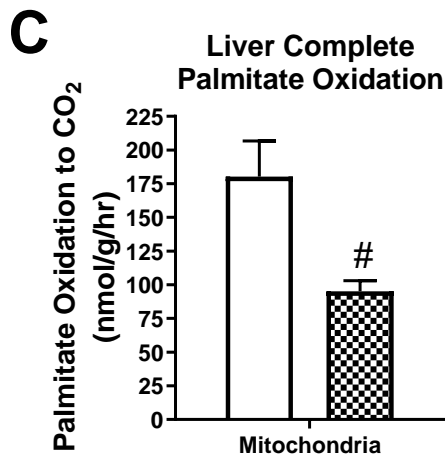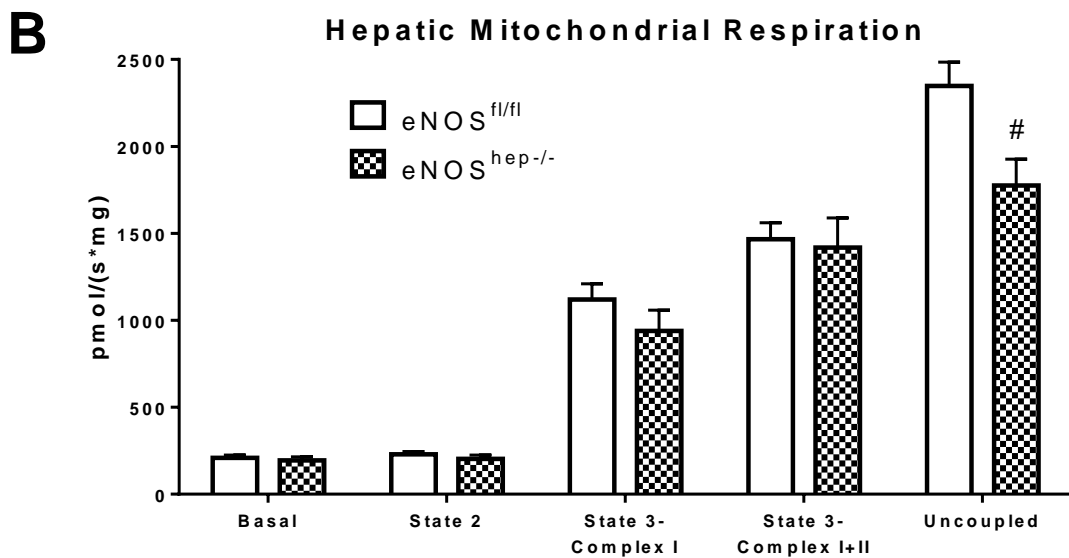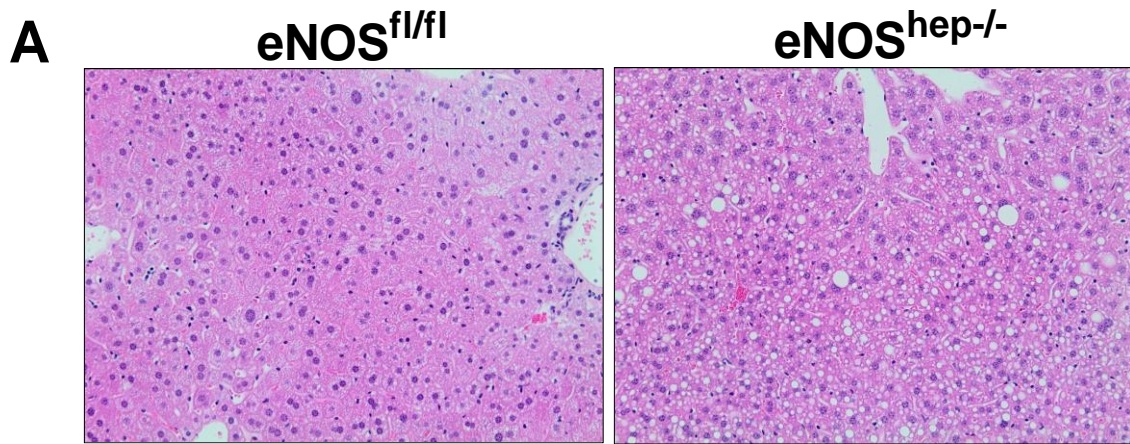
Figure 1.2. Elevated steatosis and decreased mitochondrial function in *eNOS^hep-/-* vs *eNOS^fl/fl* mice after 16 weeks of CD: A) H&E staining, B) hepatic mitochondrial respiration, C) complete liver palmitate oxidation in isolated mitochondria, D) protein markers of autophagy/ mitophagy. All data presented as means ± SE (n= 9-11). # indicates significantly different than *eNOS^fl/fl* mice (p≤0.05).

eNOS, and mitochondrial function

 The link between eNOS derived NO and its regulation of mitochondrial function are well established (49-54). In a seminal paper by Nisoli et al, the addition of an NO donor to cultured brown adipocytes induced markers of mitochondrial biogenesis and content in a cyclic GMP and peroxisome proliferator receptor γ coactivator α (PGC1α) dependent manner (50). In the same study, cold exposure-induced mitochondrial biogenesis in brown adipose tissue was significantly attenuated in whole body eNOS null mice, while eNOS null mice also presented with reduced markers of mitochondrial content in brain, heart, and liver tissue (50). Furthermore, calorie restricted-induced mitochondrial biogenesis is severely attenuated in eNOS null mice (52). The reverse is also true – global eNOS overexpression prevented diet induced obesity while increasing markers of mitochondrial biogenesis and activity in adipose tissue (55). Preliminary observations from our lab further validate the role of eNOS in mitochondrial function – deletion of hepatocellular eNOS resulted in reduced hepatic mitochondrial respiration and fatty acid oxidation (**Figure 1.2B-C**). Moreover, hepatocytes isolated from low fat diet fed eNOS$^{hep-/-}$ mice have decreased respiration compared to eNOS$^{fl/fl}$ mice (not shown), while *in vivo* overexpression of hepatocellular eNOS increased respiration in isolated hepatocytes (**Figure 1.3B-C**). Taken together, these data highlight the beneficial role of eNOS in mitochondrial biogenesis and function. These preliminary data demonstrate our ability to increase eNOS expression in hepatocytes, and that overexpressing it may provide beneficial results. This dissertation investigated the role of hepatocellular eNOS in NAFLD/NASH development.
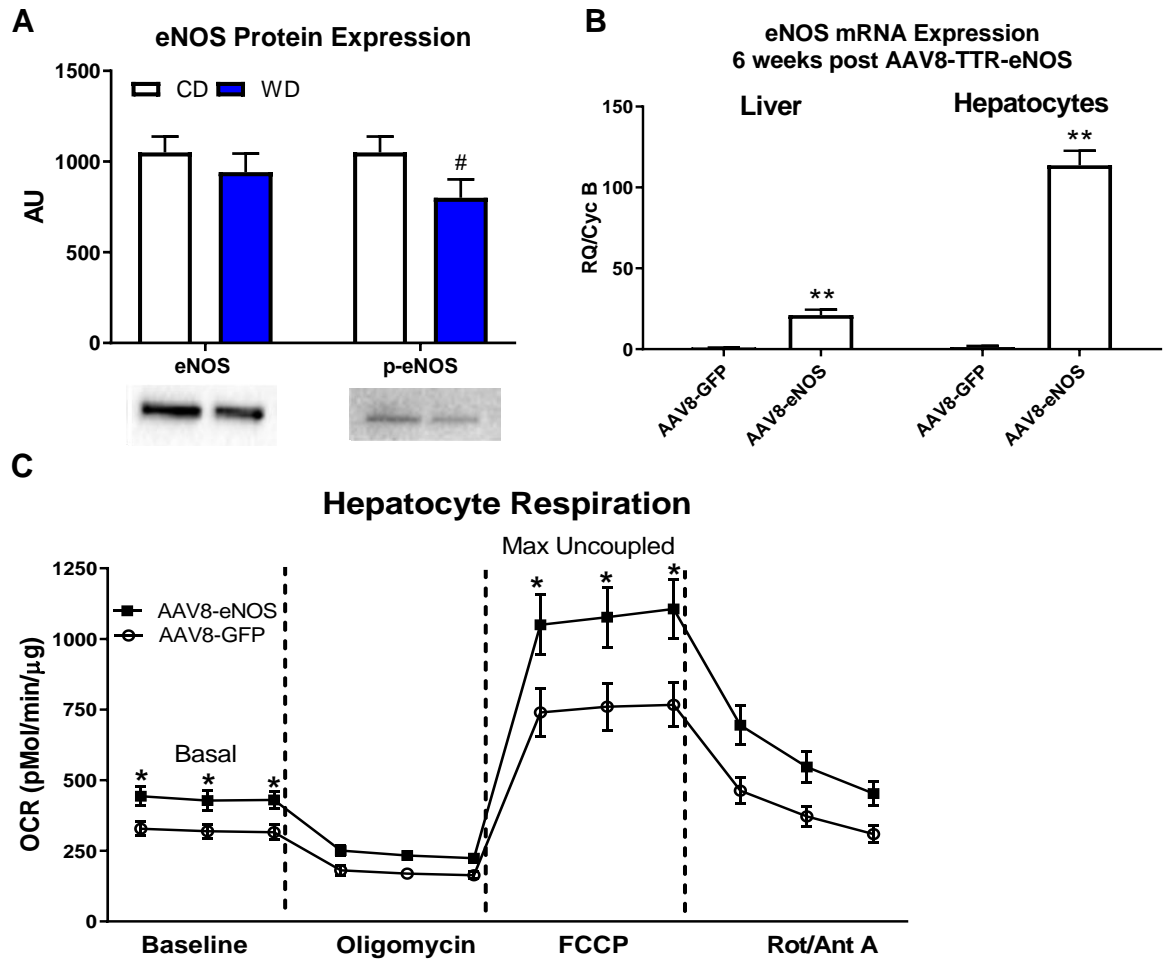
Figure 1. 3: Manipulation of hepatic eNOS with via AAV overexpression or WD: A) hepatic eNOS protein in WT mice fed CD or WD for 18 weeks, B) overexpression of eNOS in whole liver and isolated primary hepatocytes, C) hepatocyte respiration. All data presented as means ± SE (n= 8). *# significantly different than CD ($p<0.05$); *, ** significantly different from AAV-GFP ($p<0.05$) and ($p<0.001$), respectively.

eNOS and mitophagy

While there is clear evidence for a role of eNOS in the process of mitochondrial biogenesis, less is known about the ability of eNOS to regulate mitochondrial turnover. This turnover hinges on the intimately linked processes of biogenesis and autophagy - where dysfunctional, aberrant mitochondria are removed via selected autophagy (mitophagy) and replaced in an effort to maintain mitochondrial homeostasis within the cell (56). Indeed, impaired hepatic mitophagy via loss of BCL2 interacting protein 3

(BNIP3), a key protein in the docking of dysfunctional mitochondria to the autophagosome, results in accumulation of dysfunctional mitochondria and elevated hepatic steatosis (57, 58).

The data on eNOS and autophagy/mitophagy are limited; however, there is evidence for NO regulation of autophagy. NO has consistently been shown to be a potent activator of the metabolic sensor enzyme AMP-activated protein kinase or AMPK (59, 60). This directly promotes autophagy/mitophagy by the AMPK-induced activation of Unc-51 Like Autophagy Activating Kinase 1 (Ulk1) at Ser 317 and Ser 777 (61, 62) – a key initiating step in the autophagosome formation. Indeed, NO stimulates autophagy in breast cancer cells by suppression of mTORC1 (Ulk1 inhibitor) and activation of AMPK (63). This resulted in elevated light chain 3 (LC3) II/I ratio and decreased p62 levels, indicative of increased autophagosome formation and ultimately its targeted degradation. Whether NO is capable of regulating autophagy/mitophagy in hepatocytes remains to be resolved.

Recent work from our lab has identified hepatocellular eNOS as a novel regulator of mitochondrial homeostasis and maintaining mitophagic capacity (**Figure 1.4**) (1). Hepatic mitochondria from eNOS null mice displayed decreased markers of mitochondrial biogenesis and autophagy/mitophagy. In addition, in vitro siRNA-induced knockdown of eNOS in primary hepatocytes reduced fatty acid oxidation and impaired the induction of BNIP3 upon mitophagic stimulation. Preliminary data from our lab also demonstrated $eNOS^{hep-/-}$ mice present with reductions in key proteins involved in mitophagy and autophagy in the liver, including BNIP3, PTEN-induced kinase 1

(PINK1) and phosphorylated pUlk1/Ulk1 compared to *eNOS^{fl/fl}* mice (**Figure 1.2D**).

These data indicate that hepatocellular eNOS deficiency may compromise hepatic

mitophagy, potentially leading to mitochondrial dysfunction. This dissertation seeks to

elucidate the role of *in vivo* hepatocellular eNOS in the process of maintaining a healthy

mitochondrial pool in the liver, and examined more dynamic measurements of

mitophagic capacity as opposed to the static measures shown in the preliminary data.
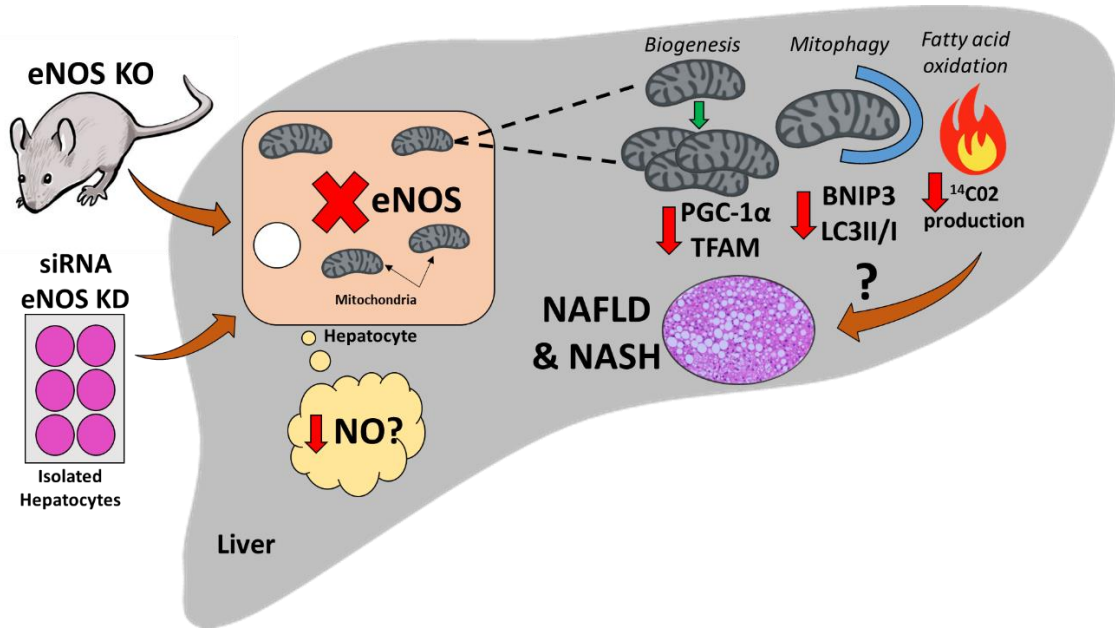
Figure 1.4. Schematic illustration of the potential role that hepatocellular endothelial nitric oxide synthase (eNOS) may play in nonalcoholic fatty liver disease (NAFLD) development. Genetic ablation of eNOS in mice, as well as small interfering RNA (siRNA) knockdown (KD) of eNOS in isolated primary hepatocytes result in hepatocytes lacking eNOS. This leads to a reduction in markers of hepatic mitochondrial biogenesis [PPARγ coactivator-1α (PGC-1 α), mitochondrial transcription factor A (TFAM)], and also markers of autophagy/mitophagy [BCL-2-interacting protein-3 (BNIP3), 1A/1B light chain 3B (LC3)], and decreased fatty acid oxidation in primary hepatocytes (as measured by complete $^{14}CO_2$ production (1). Whether this process is governed by a reduction in nitric oxide (NO) is yet to be determined. This impairment in hepatic mitochondrial dynamics can lead to mitochondrial dysfunction, and ultimately may cause/exacerbate NAFLD development.

Sex differences with hepatic mitophagy

The is a paucity of literature examining sex differences in hepatic mitophagy. Female

rodents are known to be protected against hepatic steatosis development, while showing

inherent differences in hepatic mitochondrial metabolism (64, 65). Despite this, the

mechanisms conferring this protection against NAFLD development is unresolved. Our

group has demonstrated that female mice are not only protected from hepatic steatosis

compared to male mice, but also displayed elevated markers of mitochondrial biogenesis

and mitophagy, regardless of maternal condition (66). Similarly, we have shown that

female rats have higher markers of mitochondrial biogenesis (TFAM), mitophagy (LC3-

II/I, ATG12:5), and cellular energy homeostasis (AMPK) compared to males, regardless

of diet (67). Other studies have shown female mice possess elevated hepatic

mitochondrial content, respiratory capacity, and lower reactive oxygen species emission

compared to male mice, regardless of physical activity (68-70). As such, females had a

lower need for mitophagy, reflected in lower mitophagy flux. Whether these differences

are mediated by hepatocellular eNOS is unknown.

eNOS and exercise-induced mitochondrial adaptations

Interestingly, exercise-induced adaptations in mitochondrial health may be dependent on

eNOS. In fact, six weeks of swim training increased mitochondrial biogenesis,

mitochondrial DNA content, and glucose uptake in subcutaneous adipose tissue of wild-

type but not eNOS knockout mice (53). Similarly, genetic ablation of eNOS attenuated

exercise-induced increases in mitochondrial biogenesis and function in cardiomyocytes

(54). Collectively, these studies indicate that exercise promotes eNOS dependent

improvements in mitochondrial biogenesis and function. Whether this phenomenon is

also seen in the liver is unknown. These proposed studies aim to determine if

hepatocellular eNOS is required for exercise-induced improvements in hepatic mitochondrial biogenesis and function.

One of the major concerns regarding exercise studies in whole body eNOS knockout mice is a severe reduction in exercise capacity (71). However, preliminary observations from our lab indicate that eNOS$^{hep-/-}$ mice voluntarily run similar distances as control eNOS$^{fl/fl}$ mice (**Figure 1.5**).   In addition, eNOS$^{hep-/-}$ mice had similar body composition and training adaptations as seen in eNOS$^{fl/fl}$ mice following 10 weeks of VWR (**Figure 1.5**). These effects were only seen in a small subset of female mice, and the proposed studies examine sex effects by using both male and female eNOS$^{fl/fl}$ and eNOS$^{hep-/-}$ mice. Equating training volume and body composition is paramount in determining the effects of exercise *per se* in eNOS$^{hep-/-}$ mice on measures of mitochondrial health and hepatic steatosis.
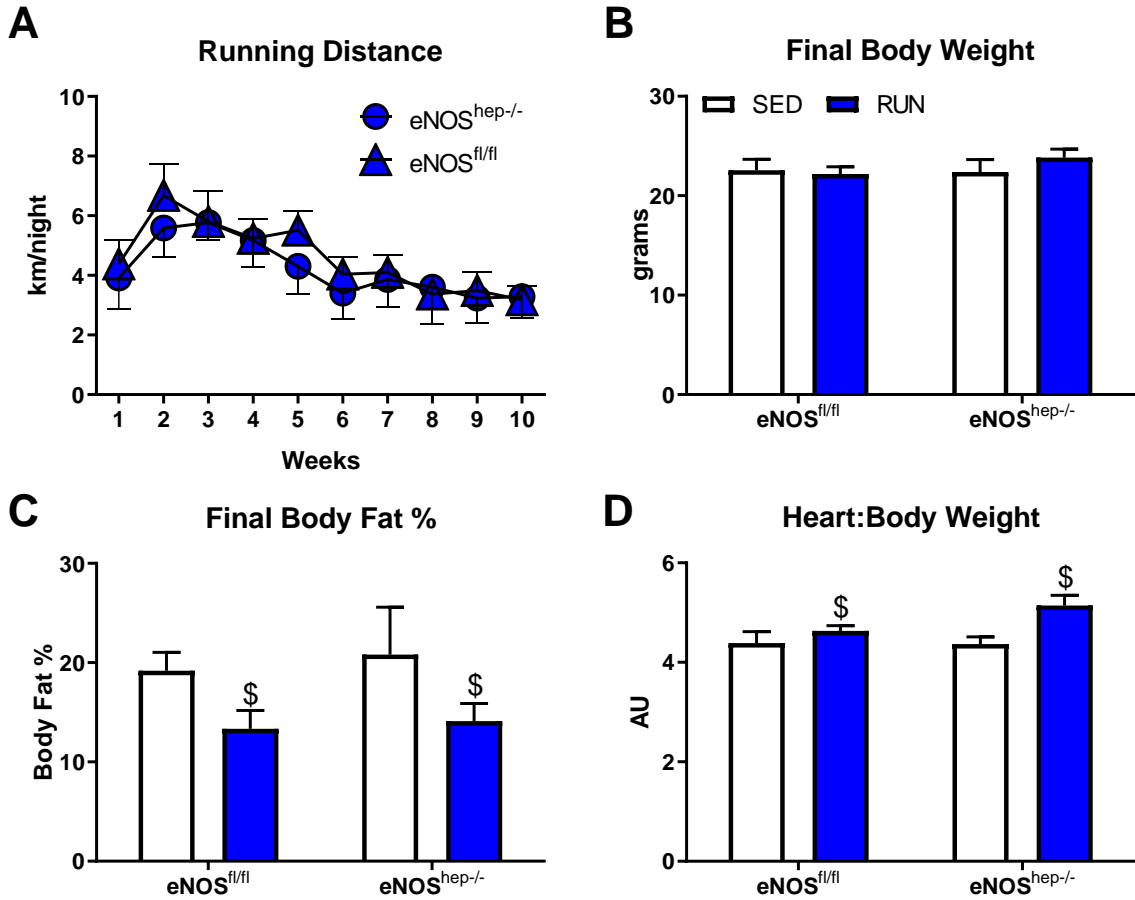
Figure 1.5. Animal characteristics from eNOS[hep-/-] and eNOS^{fl/fl} female mice after 10 weeks of VWR (n=5-9 per group). A) Average running distance per night, B) final body weight, C) final body fat %, and D) heart:body weight ratio. All data presented as means ± SE; $ indicates significantly different than SED ($p \leq 0.05$).

Based on the aggregate of the data including our preliminary studies, I hypothesize that hepatocellular eNOS is necessary for maintaining hepatic mitochondrial function and prevention of hepatic steatosis. Additionally, I hypothesize that hepatic mitochondrial adaptations to exercise are mediated in part, by hepatocellular eNOS. To test this central hypothesis, I propose the following specific aims:

Aim 1: To determine the significance of hepatocellular eNOS in NASH susceptibility. Here, male hepatocyte-specific eNOS knockout (eNOS$^{hep-/-}$) and eNOS floxed (eNOS$^{fl/fl}$) mice were fed a western diet (WD) or a control diet (CD) for 16 weeks to induce NASH. Additionally, WD-induced obese or CD fed C57BL/6 male mice were administered a hepatocyte-specific adeno-associated virus (AAV) to overexpress eNOS or an AAV-GFP control before remaining on their respective diets for a further 10 weeks. *Hypothesis:* that eNOS$^{hep-/-}$ mice will display exacerbated NASH development, while that hepatocyte-specific eNOS over expression will attenuate WD-induced NASH, compared to their respective controls.

Aim 2: To determine if the protective role of hepatocellular eNOS on hepatic mitochondrial function and turnover during NASH development is sex dependent. Here, male and female eNOS$^{hep-/-}$ and eNOS$^{fl/fl}$ mice were fed a CD or WD for 16 weeks. *Hypothesis:* that eNOS$^{hep-/-}$ females will present with an exacerbated NAFLD phenotype compared to eNOS$^{fl/fl}$ females. Regardless of genotype, male mice will have an exacerbated NAFLD phenotype compared to females, i.e. – eNOS$^{hep-/-}$ males will develop the most severe NALD phenotype, with eNOS$^{hep-/-}$ females brought to the NAFLD phenotype of eNOS$^{fl/fl}$ males, while eNOS$^{fl/fl}$ females will have the lowest hepatic steatosis and highest mitochondrial function and turnover.

Aim 3: To determine if hepatocellular eNOS is required for exercise-induced hepatic mitochondrial adaptations. Here, male and female eNOS$^{hep-/-}$ and eNOS$^{fl/fl}$ control mice fed a low-fat diet were exposed to either sedentary or voluntary wheel running conditions for 10 weeks. *Hypothesis:* that the lack of hepatocellular eNOS will

prevent exercised-induced increases in hepatic mitochondrial content, function, and

turnover and attenuate exercise-induced prevention of hepatic steatosis.

Impact: Currently, there are no FDA-approved pharmacological treatments for NAFLD.

These expected results would demonstrate the requirement of hepatocellular eNOS, at

least in part, for maintaining hepatic mitochondrial function and turnover in the

prevention of NAFLD development and progression. Identifying a novel role for

hepatocellular eNOS would significantly improve our understanding of hepatic

mitochondrial dysfunction in the setting of NAFLD and NASH development and provide

novel targets for future pharmacological interventions.

Innovation

The mechanisms behind mitochondrial dysfunction in NAFLD development and

progression have not been fully elucidated. Preliminary studies from our lab suggest that

hepatocyte-specific deletion of eNOS impairs mitochondrial function and exacerbates

hepatic steatosis (**Figure 1.2**). In other tissues, it appears that exercise-induced

improvements in mitochondrial health are eNOS dependent (53, 54). Given these data,

the innovative aspects of the proposed study are as follows:

- Given our preliminary data demonstrating an exacerbated NAFLD phenotype in
  eNOS[hep-/-] mice, this study is the first to investigate the role of hepatocellular
  eNOS in NAFLD development *in vivo*.
- Additionally, this study examined potential sex differences in eNOS[hep-/-] mice,
  and *whether the observed phenotype seen in* eNOS[hep-/-] *mice is sex dependent.*

- To date, no studies have examined *whether hepatocellular eNOS is necessary for the exercise-induced benefits in the liver.* Here for the first time, we examined the role of hepatocellular eNOS in exercise-induced adaptations in the liver.

In short, this dissertation used the novel eNOS$^{hep-/-}$ mouse model that our lab has developed to further elucidate the role of eNOS in the liver in NAFLD/NASH development and progression. Furthermore, these data will have a powerful impact on our understanding of hepatic mitochondrial adaptations to exercise.

CHAPTER 2 - Manipulation of hepatocellular eNOS uncovers its vital role in NAFLD and NASH development

Rory P. Cunningham[1,3], Mary P. Moore[1,3], Grace M. Meers[1, 3], Vivien Jepkemoi[1], Luigi Boccardi[1], Takamune Takahashi[4], Ryan D. Sheldon[5], Jamal A. Ibdah[1,2], John P. Thyfault[6,7], R. Scott Rector[1,2,3]

[1]Research Service, Harry S Truman Memorial Veterans Medical Center, Columbia, Missouri 65212, USA; [2]Departments of Medicine-Division of Gastroenterology and Hepatology, [3]Nutrition and Exercise Physiology, University of Missouri, Columbia, MO 65211, USA; [4]Division of Nephrology and Hypertension, Vanderbilt University School of Medicine, Nashville, Tennessee 37232, USA; [5] Metabolic and Nutritional Programming, Center for Cancer and Cell Biology, Van Andel Institute, Grand Rapids, MI 49503, USA; [6]Molecular and Integrative Physiology, University of Kansas Medical Center, Kansas City, KS 66160, USA; [7]Kansas City VA Medical Center, Kansas City, MO 64128, USA.

Address of Correspondence:

        R. Scott Rector, PhD
        Research Health Scientist and Associate Professor
        Harry S Truman Memorial VA Hospital
        Departments of Medicine - Division of Gastroenterology
        and Hepatology and Nutrition and Exercise Physiology
        University of Missouri-Columbia
        Columbia, MO 65212
        Tel: 573-884-0979
        Fax: 573-884-4595
        Email: rectors@health.missouri.edu

ABSTRACT

Whole body loss of endothelial nitric oxide synthase (eNOS) worsens hepatic mitochondrial function and exacerbates nonalcoholic fatty liver disease/steatohepatitis (NAFLD/NASH) development and progression. However, the precise role of eNOS in hepatocytes in the contribution to NAFLD has not been established. Here, we use gain- and loss- of-function approaches including a hepatic-specific eNOS knockout mouse model to investigate the role of hepatocellular eNOS in NAFLD and NASH development. Ablation of hepatocellular eNOS via genetic and viral knockout results in exacerbated hepatic steatosis and inflammation, decreased hepatic mitochondrial fatty acid oxidation and respiration, and an impaired mitophagy response. Conversely, overexpressing hepatocellular eNOS via viral approaches increased hepatocyte respiration, markers of mitophagy, while attenuating NASH progression. Detrimental effects of eNOS deficiency in hepatocytes was not rescued with nitric oxide donors and BCL2 interacting protein 3 (BNIP3) overexpression *in vitro*. Here we demonstrate for the first time that hepatocyte-specific deletion of eNOS impairs hepatic mitochondrial function and exacerbates NAFLD development. Further, we identify an additional role of hepatocellular eNOS in mitochondrial quality control and attenuating inflammation during NASH development and progression. Further studies are necessary to determine the mechanisms by which hepatocellular eNOS regulates hepatic mitochondrial homeostasis and mitigates the spectrum of NAFLD development.

INTRODUCTION

Nonalcoholic fatty liver disease (NAFLD) is comprised of a spectrum of liver injury ranging from excess lipid accumulation in the liver (steatosis), to steatohepatitis (NASH) and fibrosis, to its end stage of cirrhosis and hepatocellular carcinoma. NAFLD affects >75% of individuals with overweight or obesity (72), and its progression to NASH is the most rapidly increasing indication for liver transplantation in the United States (8). NAFLD is considered an independent risk factor for cardiovascular, liver-related, and all-cause mortality (9, 10), with no current FDA-approved pharmacological treatments. A hallmark of NAFLD progression is the decline in function of hepatic mitochondria, including increased reactive oxygen species and decreased oxidative capacity (18, 20, 24), while we have shown that mitochondrial dysfunction precedes insulin resistance and hepatic steatosis in rodents(21). However, the precise mechanisms of hepatic mitochondrial dysfunction during NAFLD development and progression to NASH remain unresolved.

Endothelial nitric oxide synthase (eNOS) represents one potential mediator of maintaining mitochondrial function in the liver, given its well established role in regulating mitochondrial biogenesis (49-52). Further, previous studies clearly demonstrate the importance of eNOS in exercised-induced improvements in mitochondrial function in adipose and cardiac tissue (53, 54). In addition, whole body loss of eNOS worsens hepatic mitochondrial function and increases NAFLD susceptibility (45, 73) and our group has shown that reduced hepatic eNOS activity is linked with NAFLD progression to NASH (47). Moreover, we have previously

demonstrated that systemic NOS inhibition causes hepatic mitochondrial dysfunction and accelerates NAFLD development (46). Recent work from our lab has identified hepatocellular eNOS as a novel regulator of mitochondrial homeostasis within the liver. Hepatic mitochondria from eNOS null mice displayed decreased markers of mitochondrial turnover, while *in vitro* siRNA-induced knockdown of eNOS in primary hepatocytes reduced fatty acid oxidation and impaired the induction of BCL-2/adenovirus E1B 19-kDa protein-interacting protein-3 (BNIP3) upon mitophagic stimulation (1). However, *in vivo* manipulation of hepatocellular eNOS as it pertains to the development and progression of NAFLD has not been attempted.

Here, we have generated a hepatocyte-specific eNOS null murine model to elucidate the role of hepatocellular eNOS in NAFLD/NASH development. With both *in vivo* and *in vitro* manipulation, our novel results demonstrate that hepatocellular eNOS is required for adequate mitochondrial function and turnover within the liver and the prevention of NAFLD development and NASH progression. These data further uncover the role of hepatocellular eNOS in NAFLD pathogenesis, and may provide a potential novel target for future therapies.

RESEARCH DESIGN AND METHODS

Genetic ablation of hepatocellular eNOS

Hepatic-specific eNOS knockout (KO) (eNOS$^{hep-/-}$) mice have been generated by crossing homozygous eNOS floxed (eNOS$^{fl/fl}$) mice on a C57BL/6J background (48), with albumin-Cre recombinase transgenic mice (Jackson Labs no. 002684; Bar Harbor, ME)

At 10 weeks of age, male and female eNOS^{fl/fl} and eNOS^{hep-/-} mice received either a semi-purified control diet (CD; no. D12110704; Research Diets, New Brunswick, NJ) containing 10% kcal fat, 70% kcal carbohydrate (3.5% kcal sucrose), and 20% kcal protein, or a Western style high-fat, high-sucrose diet with cholesterol (WD; D09071604, Research Diets) containing 44.9% kcal fat, 35.1% kcal carbohydrate (17% sucrose), 20% kcal protein, and 1% wt/wt cholesterol for 16 weeks. This resulted in a total of 4 groups (n = 13-17/group): CD-eNOS^{fl/fl,} WD-eNOS^{fl/fl}, CD-eNOS^{hep-/-}, WD-eNOS^{hep-/-}.

Adeno-associated viral (AAV) knockdown of hepatocellular eNOS

To manipulate hepatocellular eNOS via alternative approaches, we have used both AAV-shRNA and AAV-Cre injection approaches to knockdown eNOS in the hepatocyte *in vivo*. These were driven by either a thyroxine binding globulin (TBG) or transthyretin (TTR) promotor to specifically target hepatocytes. All AAV-shRNA and AAV-Cre viruses were purchased from Vector Biolabs (Malvern, PA), and all administered via tail-vein injection. To determine the effects of short-term eNOS knockdown to mice on a CD, we injected male eNOS^{fl/fl} mice with an AAV8-TBG-Cre virus (1×10^{12} gene copies (GC)/ml, Lot #CS1294), and fed them a CD for 6 weeks vs AAV-TBG-Scr control (1×10^{12} GC/ml, Lot #CS1325L). To investigate the effect of hepatocellular eNOS deletion on short-term WD feeding and mitophagic flux, wild-type C57BL/6J mice were injected with either an AAV8-TTR-GFP-mNOS3-shRNA (1×10^{11} GC/ml, Lot #2015-1130) or an AAV8-TTR-GFP-Scr-shRNA (1×10^{11} GC/ml, Lot #2016-0808) to serve as control. Mice were then fed a WD for 2 weeks before mitophagic flux testing via leupeptin injections, described in more detail below (n = 3-4/group).

23

Adenoviral and AAV overexpression of hepatocellular eNOS

To determine the effect of hepatocellular eNOS overexpression *in vitro*, primary

hepatocytes were isolated from female eNOS$^{fl/fl}$ mice (20-22 weeks of age) and

transfected with either adenoviral (Adv) β-Galactosidase (β-Gal) control or Adv eNOS

overexpression expressed in plaque forming units (PFU)/ml; 1x10^4, 1x10^5, 1x10^6

(Vector Biolabs, Lot #20170516T#2). For *in vivo* overexpression studies, male wild-type

C57/Bl6J were obtained from Jackson Laboratories (no. 002684; Bar Harbor, ME) at 8

weeks of age. For short-term overexpression studies, at 10 weeks of age animals on a CD

were injected with either an AAV8-TTR-eNOS overexpression virus (1x10^{11} GC/ml, Lot

#170605#16) or AAV8-TTR-GFP (1x10^{11} GC/ml, Lot #161219-170614) to serve as a

control, and maintained on CD for 6 weeks. For longer-term overexpression studies, at 10

weeks of age animals were randomly selected to receive either CD or WD as described

above, for 20 weeks to induce NASH. After 20 weeks on their respective diets, mice were

randomly injected with either an AAV8-TTR-eNOS or AAV8-TTR-GFP scramble

control (as described above) and maintained on their diets for an additional 10 weeks.

This resulted in a total of 4 groups (n = 10/group): AAV-GFP-CD, AAV-eNOS OE-CD,

AAV-GFP-WD, AAV-eNOS OE-WD.

Adenoviral BNIP3 overexpression and NO donor rescue in primary hepatocytes

To determine the effect of hepatocellular eNOS deficiency on respiration *in vitro*, and

whether any decrements in respiration were mediated by BNIP3 or NO, primary

hepatocytes were exposed to Adv BNIP3 overexpression or NO donors. Primary

hepatocytes were isolated from female eNOS$^{fl/fl}$ mice (20-22 weeks of age) and

transfected with either i) adenoviral (Adv) β-Gal control or Adv BNIP3 overexpression

expressed in plaque forming units (PFU)/ml; 1x10^3 - 1x10^6 (Vector Biolabs, Lot #20160405T#10); ii) cells were left untreated or administered an NO donor (DETA NONOate, Cayman Chemical50uM, #82129), at either 50uM or 100uM, before functional outcomes were performed as described below.

Animal care and terminal procedures

For all animal experiments, room temperature was kept constant at 21-22°C with a 12:12 light/dark cycle. Food intake and body weight of the animals was recorded weekly, and body composition (4in1-1100 Analyzer; EchoMRI, Houston, TX) measured monthly. Food consumption was measured by taking the difference in grams of food given and grams of food remaining 7 days later and multiplying total grams consumed by energy content per gram of the diet (CD; 3.5kcal/gram, WD; 4.75kcal/gram) and dividing by 7 to give kilocalories per day. On the day of euthanasia, mice were fasted overnight for 12 hr (2000-0800), before being anesthetized with pentobarbital sodium (50 mg/kg). Blood was collected via cardiac puncture, and the animals were euthanized via removal of the heart. Livers were quickly excised from anesthetized mice and prepared for mitochondrial isolation, nuclear extraction, homogenization for palmitate oxidation, and fixed in 10% formalin or snap-frozen in liquid nitrogen for later processing as described in detail in the following sections. All animal protocols were approved by the University of Missouri and the Harry S Truman Animal Care and Use Committees.

Glucose, insulin, and pyruvate tolerance testing

A subset of CD and WD-fed eNOS$^{fl/fl}$ and eNOS$^{hep-/-}$ male mice (22-30 weeks of age) were used for glucose, insulin, and pyruvate tolerance tests, to determine the effects of

hepatocellular eNOS deficiency on whole body glucose homeostasis. For all testing, mice were fasted in single cages with fresh bedding and *ad libitum* access to water. For glucose tolerance testing (GTT), mice were fasted overnight for 15 hr prior to baseline testing. At the end of the fast, the tail was nicked and blood sampled via a glucometer (Alpha Trak, Abbott Labs), to determine baseline blood glucose concentrations. Mice were then administered a sterile solution of 50% dextrose (2g/kg of body weight) via intra peritoneal (IP) injection, as previously performed (74). Blood glucose measures were taken at 15, 30, 45, 60, and 120 min post glucose injection. For insulin tolerance testing (ITT), mice were fasted 3 hr prior to baseline testing, from the start of their light cycle. After baseline glucose measurement, mice were administered insulin (Humulin R; 100 U/ml) made in a 3% BSA sterile saline (0.9% NaCl, Hospira; NDC 0409-4888-20) solution at a dose of 0.75U insulin/kg of body weight via IP injection. Blood glucose measurements were taken at the same intervals as GTT. Mice were fasted 5 hr prior to pyruvate tolerance testing (PTT) at the start of their light cycle. After baseline glucose measured, mice were administered a pyruvate solution (0.2g/mL of sterile saline) at a dose of 2g/kg of body weight via IP injection. Blood glucose was measured at the same intervals as GTT and ITT. All area under the curves were calculated using the trapezoidal method.

Primary hepatocyte isolation and MACS purification

A separate cohort of CD-fed WT and eNOS$^{fl/fl}$ and eNOS$^{hep-/-}$ mice was used for primary hepatocyte studies. Primary hepatocytes were isolated from female mice between 20-22 weeks of age by using the two-step collagenase method as described previously (1, 75, 76). The cell suspension was filtered through a 100 micron filter and centrifuged at 50 g

for 6 min at 4°C. The resultant crude isolated hepatocyte pellet from the centrifuge was

resuspended in a 43.5% Percoll solution [11 mL Percoll, 11 mL growth media (Williams

E, Invitrogen), 10% FBS, 4 mM L-glutamine, 100 U penicillin-100 mg streptomycin, 2

ng/mL rat EGF, 100 nM insulin, 100 nM dexamethasone, 0.1% BSA, and 10 mM sodium

pyruvate, and 3.3 mL PBS] and centrifuged at 40 g for 15 min at 4°C without braking.

Trypan blue and a manual hemocytometer were used to determine cell viability and

number. In order to obtain a purer isolation of hepatocytes only, magnetic activated cell

sorting was used. Described previously by our group (1) and originally modified from

Azimifar et al. (77), 10^8 cells were pelleted at 300 g for 10 min at 4°C. The cell pellet was

resuspended in 80 µL of degassed magnetic-activated cell sorting (*MACS*) working buffer

(PBS, 0.5% BSA, 2 mM EDTA, pH 7.2), 10 µL of CD146 (for removal of endothelial

cells) microbeads, and 10 µL of CD11b (for removal of Kupffer cells and macrophages)

microbeads (Miltenyi Biotec, Auburn, CA) and incubated on ice for 15 min. The cells

were then washed with 2 mL of MACS working buffer and centrifuged at 300 g for 10

min at 4°C. The supernatant was aspirated, and the pellet was resuspended in 500 µL of

MACS working buffer. The large cell column was washed with 500 vols of MACS

working buffer, the cells were then applied to the column, and the flow-through was

collected containing the unlabeled cells, the column was then washed three times with

500 µL of MACS working buffer and combined with the unlabeled cell flow-through.

Immunofluorescence was performed on a subset of MACS-purified primary hepatocytes

for confirmation of the removal of Cd11b^{+} and CD146^{+} cells and lack of eNOS in

hepatocytes from eNOS[hep-/-] mice as described below. Otherwise, MACS-purified

primary hepatocytes were plated on type 1 collagen-coated plates and either treated

immediately with a virus or small interfering (si)RNAs or plated for 48 hr before examination of other outcomes. Growth media [Williams Media E (no. 12551-032, ThermoFisher), 10% FBS, 4 mM L-glutamine, 1% penicillin-streptomycin (no. 15140122, ThermoFisher), 20 ng/mL mouse epidermal growth factor (EGF), insulin, transferrin, and selenium (ITS), 100 nM dexamethasone, 10 mM sodium pyruvate, 0.1% BSA] was exchanged daily throughout culture.

Immunofluorescence of MACS-purified primary hepatocytes

MACS-purified primary hepatocytes were plated onto collagen coated glass chamber slides for 24 hr in growth media. Modified from Werner et al. (78), and described previously (1), cells were fixed with prechilled methanol-acetone (1:2 vol/vol) for 10 min on ice, washed with PBS, permeabilized with 0.3% Triton X-100 for 30 min, and then washed with PBS. The slides were then blocked with 2% BSA for 1 hr. In order to confirm the presence of eNOS and the success of our MACS of primary hepatocytes, the following primary antibodies were diluted 1:1,000 and incubated overnight at 4°C: albumin (Antibodies-Online, Atlanta, GA), eNOS (BD Bioscience, San Jose, CA), CD146, and CD11b (Novus Biologicals, Littleton, CO). After a washing with PBS, the slides were incubated with the appropriate secondary antibody diluted 1:1,000 for 3 hr at 4°C in the dark. The slides were washed with PBS, stained with DAPI for 1 min, washed with PBS, and mounted with Mowiol mounting media (3.6 M glycerol, 4.3 mM Mowiol 4-88, 130 mM Tris). Exclusion of the primary antibody was used as negative control. For confirmation of the removal of Cd11b$^+$ and CD146$^+$ cells, back-end immunofluorescence for CD11b and CD146 was used in purified hepatocytes.

Primary hepatocyte respiration

Cellular oxygen consumption in primary hepatocytes were assessed using a Seahorse

XF24 analyzer (Agilent, Santa Clara, CA) , as described previously with slight

modifications (79). Hepatocytes were plated in growth media on collagen coated 24 well

XF24 cell culture microplates at 15,000 cells per well. Cells were immediately treated

with Adv or control media for 6 hr. Cells then rested overnight in growth media. The

growth media was then removed and starvation media (William Media E, 20 mM

glutamine, 0.1% FBS) was then placed on the cells overnight. On the third day seahorse

media conditioned with 1mM sodium pyruvate, 2mM glutamine, and 10mM glucose

(need to add mM concentrations of chemicals) at a pH of 7.4 was used to wash the cells

twice. To allow cells to pre-equilibrate with the seahorse media, they were incubated at

37 °C without CO_2 for 1 hr. Oligomycin (1uM), FCCP (0.5uM) or rotenone/antimycin A

(0.5uM) (Sigma) were diluted in growth media and loaded into port-A, port-B and port-

C, respectively. Basal level of oxygen consumption rate (OCR) was measured three

times, and then after sequential injections of port-A, port-B and port-C OCR was

measured again three times after each injection to determine mitochondrial or non-

mitochondrial contribution of OCR. Experiments were repeated 5 times with different

cell preparations. Mitochondrial oxidative phosphorylation was determined by OCR

before oligomycin injection minus OCR after oligomycin injection. Mitochondrial proton

leak was determined by OCR after oligomycin injection minus OCR after rotenone

injection. Non-mitochondrial OCR was determined by OCR after rotenone injection

minus OCR of wells without cells. Mitochondrial reserve oxidative capacity was

determined by OCR after FCCP injection minus OCR before oligomycin injection.

Hepatocyte processing for Western blot and qPCR

In preparation of hepatocytes for Western blot analysis, cells were washed with ice-cold PBS and lysed with cell lysis buffer [1% Triton X-100, 100 mM NaCl, 20 mM Tris, 2 mM EDTA, 10 mM $MgCl_2$, 10 mM NaF, 40 mM β-glycerol phosphate, protease inhibitor (Roche), and phosphatase inhibitors (Sigma)]. Samples were sonicated and centrifuged at 15,000 g for 15 min, and the supernatant was collected and evaluated for total protein content using BCA. Cells prepared for RNA extraction were washed with ice-cold PBS and lysed in buffer RLT (Qiagen) with 1% (vol/vol) β-mercaptoethanol and sonicated. RNA was isolated using the RNeasy mini kit (Qiagen) per the manufacturer's instructions.

Primary hepatocyte fatty acid oxidation

For determination of fatty acid oxidation in isolated primary hepatocytes, [1-^{14}C] radiolabeled palmitate was used as described previously (76, 80), with minor modifications. After serum starvation for 24 hr, 12-well plates were washed with warm PBS, and the cells were incubated with ^{14}C-labeled FAO reaction media consisting of starvation media (William Media E, 20 mM glutamine, 0.1% FBS), 0.5 μCi/ml [1-^{14}C]palmitate, 100 μM palmitate, 0.25% BSA, 1 mM carnitine, and 12.5 mM HEPES (pH ~7.4) at 37°C for 3 hr in triplicate. The media from each well was collected after 3 hr, and an aliquot was dispensed into the sealed trapping device. The $^{14}CO_2$ was driven from the media aliquot by adding perchloric acid and trapped in a microtube of NaOH in the well, which was then collected, and a liquid scintillation counter was used to determine complete FAO to CO_2. The acidified media was collected, refrigerated overnight, and

centrifuged (16,000 g, 4°C). An aliquot of the acidified media was analyzed by liquid

scintillation counting to determine the acid-soluble metabolites (ASMs) of FAO, a

marker of incomplete oxidation to CO_2. The cells were rinsed three times with ice-cold

Krebs-Henseleit buffer and lysed with SDS lysis buffer. The protein concentration of the

lysate was determined by BCA assay.

Mitochondrial isolation

Hepatic mitochondria were isolated as previously described (30, 34). Briefly, roughly 100

mg of fresh liver tissue was minced and homogenized using a Teflon pestle in

mitochondrial isolation buffer (220 mM mannitol, 70 mM sucrose, 10 mM Tris base, 1

mM EDTA, pH 7.4). The sample was centrifuged at 1,500 *g* for 10 min. The supernatant

was retained and underwent a series of three centrifugations (6,000–8,000 *g*), while the

resultant pellet was resuspended with gentle glass-on-glass homogenizations. Sample was

maintained at 4°C throughout the isolation protocol. The final pellet was suspended in

mitochondrial incubation buffer (110 mM sucrose, 60 mM KMES, 20 mM glucose, 20

mM HEPES, 10 mM KH_2PO_4, 3 mM $MgCl_2$, 0.5 mM EGTA, pH 7.4), and let rest for 30

min before being used for determining protein content via BCA, mitochondrial

respiration, [1-^{14}C] palmitate oxidation, or stored at −80°C for Western blot analysis.

Mitochondrial respiration

In the both the eNOS$^{fl/fl}$ vs eNOS$^{hep-/-}$ and eNOS overexpression studies, hepatic

mitochondrial respiration and H_2O_2 production was assessed in isolated hepatic

mitochondria using high-resolution respirometry (Oroboros Oxygraph-2k; Oroboros

Instruments; Innsbruck, Austria), with all values were corrected to total mitochondrial

protein loaded. Respiration and H_2O_2 production , measured via oxygen consumption and Amplex^{TM} UltraRed reagent, respectively (#A36006, Thermo Fisher Scientific), was assessed by the addition of isolated mitochondria and various substrates to the Oroboros as described previously (1, 30, 33, 34). For respiration, isolated mitochondria (100-150 µg mitochondrial protein) were initially placed in respiration chambers in respiration media (MiR05; sucrose, 100 mM; K-lactobionate, 60 mM; EGTA, 0.5 mM; $MgCl_2$, 3 mM; taurine, 20 mM; KH_2PO_4, 10 mM; HEPES, 20 mM; adjusted to pH 7.1 with KOH at 37C; and 1 g/L fatty acid free BSA) for assessment of baseline respiration (Basal). Oxygen flux was measured by addition of glutamate (5 mM) and malate (2 mM) to the chambers in the absence of ADP for assessment of State 2 respiration. Once respiration had stabilized, serial additions of ADP were added (125 µM total) to stimulate and quantify oxidative phosphorylation (OXPHOS) with electron flux through complex I (State 3 – Complex I). Complex I and II respiration were assessed by the addition of 7.5 mM of succinate to the chamber (State 3 – Complex I+II). Following this, maximal uncoupled respiration was achieved by serial additions of 0.125 µM FCCP (Carbonyl cyanide 4-(trifluoromethoxy) phenylhydrazone) (Uncoupled). Increases in maximal uncoupled respiration >20% following the addition of reduced cytochrome c (2 µM) was used for mitochondrial preparation quality control. For H_2O_2 production, Amplex^{TM} UltraRed reagent (4µl) (#A36006, Thermo Fisher Scientific) and horseradish peroxide (HRP) (8µl) were added to the chamber before the addition of 100-150 µg of isolated mitochondrial protein. In the presence of the HRP, the Amplex^{TM} UltraRed reagent reacts with H_2O_2 to produce a red-fluorescent product which can be quantified and used as a surrogate marker for H_2O_2 emission. After baseline respiration is stabilized, 20 µM of

palmitoyl-CoA was added to the chamber, followed by serial additions of 10 µM of palmitoyl-CoA until a maximal response was achieved. Each substrate condition was tested in a technical replicate from a single mitochondrial preparation per mouse.

Hepatic fatty acid oxidation

Using isolated hepatic mitochondria and whole liver homogenate, hepatic fatty acid oxidation capacity was determined by the addition of $[1\text{-}^{14}C]$ palmitate, as previously described (34). Briefly, the amount of $^{14}CO_2$ produced in 1 hr was trapped in a sodium hydroxide solution. Perchloric acid will then be added to stop the reaction and incubation will continue for another hr. $^{14}CO_2$ (a measure of complete oxidation), and the $1\text{-}^{14}C$ containing acid-soluble metabolites (a measure of incomplete oxidation) were measured with a liquid scintillation counter.

Western blots

Western blot analyses were completed in whole liver homogenate, isolated hepatic mitochondria, and hepatocyte lysates. In preparation, sample protein concentration was determined by Pierce BCA protein assay (no. 23225, ThermoFisher Scientific). Primary antibodies used are as follows: eNOS (no. 610297; BD Biosciences, San Jose, CA), oxidative phosphorylation (OXPHOS) mitochondrial profile (ab110413; Abcam, Cambridge, MA), peroxisome proliferator-activated receptor gamma coactivator 1-α (PGC1α, no. WH0010891M3, Millipore-Sigma, Burlington, MA), mitochondrial

transcription factor A (TFAM; Santa Cruz Biotechnology, Dallas, TX), Bnip3 (no. 3769; Cell Signaling Technology, Danvers, MA), 1A/1B light chain 3B (LC3; no. 4108S, Cell Signaling), p62 (no. 5114; Cell Signaling Technology), Unc-51 Like Autophagy

Activating Kinase 1 (D8H5) (ULK1, no. 8054S; Cell Signaling Technology), pULK1 Ser555 (D1H4) (no. 5869S, Cell Signaling Technology), Parkin (no. 4211; Cell Signaling Technology), autophagy related 12-5 ATG12-5 (D88H11), (ATG12-5, no. 6904S; Cell Signaling Technology), autophagy related 7 (ATG7, no. 8558S; Cell Signaling Technology), PTEN-induced kinase 1 (PINK1, no. 6946; Cell Signaling Technology), AMP-activated protein kinase (AMPK, no. 2532S; Cell Signaling Technology), pAMPK (Thr172) (no. 2351; Cell Signaling Technology), dynamin related protein 1 (D8H5) (DRP1, no. 5319S; Cell Signaling Technology), pDRP1 (S616) (no. 3455; Cell Signaling Technology), dynamin-like 120 kDa protein, mitochondrial (D6U5N) (OPA1, no. 80471S; Cell Signaling Technology). Primary antibodies were used at 1:1,000 dilution, and secondary antibody at 1:5,000 dilution. Blots were analyzed via densometric analysis (Image Laboratory Beta 3, Bio-Rad Laboratories, Hercules, CA). Total protein was assessed with Amido black (0.1%, Sigma) to control for differences in protein loading and transfer as previously described (34, 67). Blots in primary hepatocytes were normalized to β-actin.

Quantitative real-time PCR

Initially, RNA was extracted from frozen liver tissue or hepatocyte cultures with a commercially available kit (no. 74104, Qiagen), and a cDNA library was synthesized (Promega). A Nanodrop spectrometer was used to assess purity and quality of RNA and

cDNA (model ND-1000, NanoDrop, Thermo Scientific, Wilmington, DE). Quantitative real-time PCR (qPCR) was conducted using Sybr Green reagents (172–5121, BioRad) and primer pairs listed in **Table 2.1** (Sigma), or TaqMan (Thermo Scientific,

Wilmington, DE) for eNOS (Mm01134911_g1) and glyceraldehyde-3-phosphate

dehydrogenase (GAPDH) (Mm99999915_g1) gene expression. PCR product melt curves

were used to assess primer specificity. Data are represented relative to cyclophillin B

(*Ppib*) or *gapdh* using the $2^{-\Delta\Delta CT}$ method.

Liver histology

To histologically determine hepatic steatosis development, the fresh liver placed in 10%

formalin for 24 hr was then imbedded in paraffin, sectioned and stained with

haematoxylin and eosin (H&E) or trichrome (to assess fibrosis) by IDEXX RADIL

(Columbia, MO). NAFLD activity score (NAS) and fibrosis staging of liver sections were

conducted by a trained and blinded observer.

Transmission Electron Microscopy

 To assess structural differences in the mitochondria via transmission electron

microscopy (TEM), a small section of fresh liver (~1-2 mg) was immediately fixed in 2%

paraformaldehyde, 2% glutaraldehyde in 100 mM sodium cacodylate buffer pH=7.35.

Next, fixed tissues were rinsed with 100 mM sodium cacodylate buffer, pH 7.35

containing 130 mM sucrose. Secondary fixation was performed using 1% osmium

tetroxide (Ted Pella, Inc. Redding, California) in cacodylate buffer using a Pelco

Biowave (Ted Pella, Inc. Redding, California) operated at 100 Watts for 1 minute.

Specimens were next incubated at 4°C for 1 hr, then rinsed with cacodylate buffer and

further with distilled water. En bloc staining was performed using 1% aqueous uranyl

acetate and incubated at 4°C overnight, then rinsed with distilled water. A graded

dehydration series was performed using ethanol, transitioned into acetone, and

dehydrated tissues were then infiltrated with Spurr resin for 48 hr at room temperature and polymerized at 60°C overnight. Sections were cut to a thickness of 75 nm using an ultramicrotome (Ultracut UCT, Leica Microsystems, Germany) and a diamond knife (Diatome, Hatfield PA). Images were acquired with a JEOL JEM 1400 transmission electron microscope (JEOL, Peabody, MA) at 80 kV on a Gatan Ultrascan 1000 CCD (Gatan, Inc, Pleasanton, CA). Post primary fixation, all tissue preparation and imaging were performed at the Electron Microscopy Core Facility, University of Missouri.

Mitophagy measurements

Static measurements of mitophagy proteins do not give an accurate indication of mitophagic flux. Leupeptin is a membrane-permeable thiolprotease inhibitor that impairs the enzymatic and proteolytic activity of the lysosome, preventing the degradation and allowing accumulation of autophagosomes and their associated proteins (81). Mitophagic flux measurements were carried out in a separate cohort of CD and WD fed eNOS^{fl/fl} and eNOS[hep-/-] male mice, and hepatocellular eNOS shRNA knockdown WD fed male mice, at separate times, and underwent *in vivo* intraperitoneal leupeptin injections as described previously (82). Briefly, mice from all groups were IP injected with either 40 mg/kg leupeptin (Sigma #9783, St. Louis MO) or an equal volume of saline 18 hr prior to sacrifice. Mice then had their food pulled 12 hr prior to the terminal experiment the following morning. At 4 hr prior to sacrifice, an additional 20 mg/kg of leupeptin or equal volume of saline was administered via IP injection. Accumulation of key proteins involved in autophogasome assembly and its docking to the mitochondria, LC3-II, p62,

36

and BNIP3, were measured to give an indication of mitophagic flux. These proteins were measured in whole liver and isolated hepatic mitochondria via Western blot.

Enzymatic and serum assays

Further examination of mitochondrial content and function were assessed in whole liver homogenate with enzymatic assays. The rate limiting enzyme of fatty acid β-oxidation, β-hydroxyacyl-CoA dehydrogenase, and citrate synthase activity, a well-established surrogate marker of mitochondrial content, were measured as previously described in whole liver homogenate (34). Quantification of serum alanine aminotransferase (ALT) levels were performed by a commercial laboratory (Comparative Clinical Pathology Services, Columbia, MO) using an Olympus AU680 automated chemistry analyzer (Beckman Coulter, Brea, CA) according to the manufacturer's instructions. Analysis of serum glucose, triglycerides, free fatty acids (FFA) were carried out using an AU680 automated chemistry analyzer (Beckman Coulter, Brea, CA) according to the manufacturer's instructions. Plasma insulin concentrations were determined using a commercially available ELISA (#80-INSMS-E01, Alpco Diagnostics, Salem, NH).

Nitric oxide production

The half-life of NO is short, ranging from less than 1 second to ~30 seconds (83), making accurate real-time measurements difficult. As such, surrogate markers of NO production were used to determine if eNOS deficiency resulted in tangible changes in hepatocellular NO activity. A nitrate/nitrite fluorometric assay kit (Cayman Chemical #780051, Ann Arbor, MI) was used to detect the end productions of NO oxidation in primary

37

hepatocytes supernatant from CD-fed eNOS$^{fl/fl}$ and eNOS$^{hep-/-}$ mice, as performed

previously (84), and according to the manufacturer's instructions. Briefly, nitrate was

converted to nitrite using nitrate reductase, followed by the addition of an acidic solution

and NaOH to enhance the detection of the fluorescent product. NO is known to stimulate

the activity of soluble guanylate cyclase (sGC), resulting in elevated cyclic guanosine-

3′,5′-monophosphate (cGMP); hence, cGMP is a well-established marker of NO

production. A cGMP ELISA kit (Cayman Chemical #581021, Ann Arbor, MI) was used

to detect cGMP levels in primary hepatocyte lysate and their cell culture media as

performed previously (84), and according to the manufacturer's instructions. Briefly,

samples and standards were acetylated to increase the sensitivity of the assay. The

samples were then incubated with a cGMP tracer for 18 hr, followed by addition of a

reagent that caused an enzymatic reaction to produce a distinct yellow color. The

intensity of this color as determined spectrophotometrically, and gives an indication of

the amount of cGMP in the sample.

Metabolomics

Metabolomic analysis was carried out via ion-paired liquid chromatography/mass

spectrometry (LC/MS) metabolite profiling on frozen whole liver from eNOS$^{fl/fl}$ and

eNOS$^{hep-/-}$ mice, as previously described with slight modifications (85). Briefly,

metabolites were extracted by the addition of extraction solvent (80% methanol) kept at -

20°C directly to frozen liver sample at a concentration of 40 mg frozen liver/mL of

extraction solvent. Extracts were vortexed for 15 seconds, sonicated in a water bath

sonicator for 5 min, and then incubated on ice for 10 min. Protein was pelleted by

centrifugation at 17,000g for 10 min at 4C. 800 μL of supernatant (4 million cell equivalents) was transferred to a fresh Eppendorf tube and dried in a rotor speedvac. For LCMS analysis samples were resuspended in 50μL of LCMS grade water. For GCMS analysis samples were incubated at 70C for 15 min in 15uL of 10mg/mL methoxyamine HCL (Sigma# 226904) in pyridine (Millipore #PX2012-7), then 35uL of MTBSFA+1%TMCS (Sigma#M-108) was added and samples were further incubated at 70°C for an additional 90 minutes. Ion-paired LC/MS metabolite profiling was conducted on an Agilent 6470 QQQ mass spectrometer coupled to an Infinity 1290 UHPLC system with a Zorbax RRHD Extend-C18 analytical column (2.1x150 mm, 1.8μm; Agilent# 759700-902) and Zorbax Fast Extend-C18 guard column (2.1 mm 1.8μm; Agilent# 821725). 2uL of resuspended cell extracts (160,000 cell equivalents on column) were injected. Mobile phase A was 97% H2O, 3% methanol, 10mM tributylamine (Sigma# 90780), and 15mM acetic acid. Mobile phase B was 100% methanol with 10 mM tributylamine, and 15mM acetic acid. The gradient is as follows: 0-2.5 min 100%A, 2.5-7.5 min ramp to 80%A, 7.5-13min ramp to 55 %A, 13-20 min ramp to 99 %B, 20-24 min hold at 99 %B. Flow rate was held at 0.25 mL/min, and the column compartment heated to 35 C. The mass spectrometer was operated in dynamic MRM mode pre-programmed per with two transitions within a 2-4-minute retention time window per analyte. The ESI source was operated in negative mode with the following conditions: gas 13 L/min at 150C, nebulizer pressure 45 psi, sheath gas 12L/min at 325C, nozzle voltage 500V, and capillary voltage 2000V. After each analytical run the column was re-equilibrated by backflush with 90% acetonitrile (0.8mL/min) for 8 min and 100% A for 8 min (0.4mL/min) to achieve run-to-run retention time consistency. GC/MS metabolite

profiling was conducted on an Agilent 5977B MSD with a 7890 GC with a DuraGuard
J&W DB-5ms GC Column (30m, 0.25mm, 0.25μm, plus DuraGuard, 10m; Agilent #122-
55326). 1uL of derivatized cell extracts were injected (80,000 cell equivalents on
column) into a split/splitless inlet heated to 250C and operated in splitless mode. Column
flow was set to 1mL/min and the oven ramp was 60C for 1 min, then ramped to 320C at
10C/min, and held at 320C for 10 min. The EI source was operated at -70EV and
250C.The MS was set to scan from 50-800m/z with a step of 0.1m/z at a rate of 2hz. 2-3
fragment ions at a standard-verified retention time were used to identify compounds.
Data analysis for both GC and LC profiling were conducted with Agilent MassHunter
Quantitative software (v. 9.0) and peaks were visually inspected by a trained technician
for accuracy. All metabolic profiling and analysis were completed at the Van Andel
Institute (Grand Rapids, MI), by trained technicians.

Statistical analysis

Statistical analyses were completed in SPSS (IBM SPSS Statistics for Windows, Version
24.0. Armonk, NY) with an alpha level of $P < 0.05$ used to determine statistical
significance of all comparisons. *In vivo* studies were analyzed via two-way (2×2)
ANOVA. A Fisher's least significant difference post hoc test was used when a two-way
or one-way ANOVA detected a significant interaction term ($P<0.05$). For *in vitro* studies*,*
data were analyzed with either two-way or one-way ANOVA with or without repeated
measures or paired *t*-test as appropriate. For fatty acid oxidation and respiration in
isolated primary hepatocytes, a biological replicate was defined as cells isolated from a
single mouse, and each condition was tested in technical triplicate and averaged. Data
from such experiments, and *n* size listed in the figure legends are representative of

independent biological replicates. Data were confirmed as normally distributed using

GraphPad Prism 8.1. All data are presented as means ± standard error SEM.

RESULTS

Model Characterization

To confirm the success of our hepatocellular-specific eNOS KO model, here we show the

eNOS gene that is floxed in both our eNOS$^{fl/fl}$ and eNOS$^{hep-/-}$ mice, along with the

presence of the albumin-cre in only our eNOS$^{hep-/-}$ mice (**Fig. 2.1A**). eNOS$^{hetero+/-}$ mice

have only one allele of eNOS floxed, and were not used in any experiments (**Fig. 2.1A**).

Gene expression from isolated primary hepatocytes demonstrate the reduction of eNOS

in eNOS$^{hep-/-}$ versus eNOS$^{fl/fl}$ mice on a CD (**Fig. 2.1B**). For further confirmation,

fluorescence microscopy of isolated primary hepatocytes, show the deletion of

hepatocellular eNOS in eNOS$^{hep-/-}$ versus eNOS$^{fl/fl}$ mice (**Fig. 2.1C**). Isolated hepatocytes

from eNOS$^{hep-/-}$ versus eNOS$^{fl/fl}$ mice also tend to show a reduction in nitrate and nitrite

concentration (P=0.16), a surrogate marker for NO production (**Fig. 2.1D**).

Animal characteristics

To determine whether loss of hepatocellular eNOS results in a compromised metabolic

phenotype. A vital component of determining whether it is the specific loss of

hepatocellular eNOS that results in detrimental metabolic consequences is

that it is not driven by changes in body composition. There were no differences in body

weight, body fat percentage (%), or liver weight between eNOS$^{fl/fl}$ and eNOS$^{hep-/-}$ mice,

despite clear effects of WD feeding (**Fig. 2.2A-C**). Similarly, WD feeding increased

41

serum ALT, insulin, and decreased serum triglycerides (**Fig. 2.2D-E**). Genotype did not affect serum measurements, although CD fed eNOS[hep-/-] mice displayed elevated serum insulin compared to CD fed eNOS^{fl/fl} mice when examined by a paired t-test. Glucose, insulin, and pyruvate tolerance tests were performed to determine the effect of hepatocellular eNOS on whole body glucose homeostasis. WD feeding increased glucose area under the cover (AUC) for GTTs and ITTs, with no effect of diet on glucose AUC for PTT (**Fig. 2.2F-I**). Hepatocellular eNOS deficiency had no effect on glucose, insulin, or pyruvate tolerance tests (**Fig. 2.2F-I**). However, in CD fed mice only, eNOS[hep-/-] mice displayed elevated glucose AUC during PTT compared to eNOS^{fl/fl} mice, with the main effect of genotype lost when WD animals were added. Interestingly, eNOS[hep-/-] mice displayed elevated markers of hepatic gluconeogenesis (*g6pase* and *ppeck* gene expression) compared to eNOS^{fl/fl} mice, regardless of diet (data not shown).

Liver histology

As expected, WD feeding increased lipid droplet number and size, as well as elevated inflammatory cells, and fibrotic legions, as demonstrated by the representative histology (**Fig. 2.3A-B**). Histological scoring confirmed that 16 weeks of WD feeding significantly increased histological steatosis, ballooning, inflammation, overall NAS score, and fibrosis (**Fig. 2.3C-D**), and eNOS[hep-/-] mice displayed elevated histological hepatic steatosis, inflammation, and NAS score compared to eNOS^{fl/fl} mice (**Fig. 2.3C-D**). WD feeding also markedly increased mRNA expression for markers of inflammation and fibrosis but there was no further exacerbation in the eNOS[hep-/-] mice (**Fig. 2.3D**). As further proof-of-concept, in addition to germline ablation of hepatocellular eNOS, also

hepatic eNOS was knocked down via AAV-Cre and AAV-shRNA in adult mice. After 6 weeks of CD feeding, eNOS^{fl/fl} mice injected with AAV8-TBG-Cre presented with elevated hepatic steatosis and inflammation compared to GFP injected eNOS^{fl/fl} mice (**Fig. 2.6A**). Further, AAV8-TTR-GFP-mNOS3-shRNA knockdown of hepatocellular eNOS resulted in exacerbated histological hepatic steatosis and inflammation compared to scramble control after 2 weeks of WD feeding (**Fig. 2.6C**).

Hepatic mitochondrial function

Based on what we have shown previously both *in vitro* and *in vivo* (1, 21, 34), it was suspected that an impairment in hepatic mitochondrial function may be driving the exacerbated NAFLD development as seen in the eNOS[hep-/-] mice compared to eNOS^{fl/fl} mice. Indeed, complete $1\text{-}^{14}C$-palmitate oxidation to CO_2 was reduced by 50% in whole liver homogenate in eNOS[hep-/-] mice compared to eNOS^{fl/fl} mice, as well as trends for reduced incomplete and total palmitate oxidation (P=0.1 and P=0.08, respectively) (**Fig. 2.4A-C**). Similarly, isolated hepatic mitochondria complete, incomplete, and total ^{14}C-palmitate oxidation were all significantly reduced with WD feeding, and were significantly reduced in eNOS[hep-/-] mice compared to eNOS^{fl/fl} mice (**Fig. 2.4D-F**). This impairment in hepatic mitochondrial fatty acid oxidation was coupled with a reduction in state 3 - complex I and FCCP-stimulated maximal uncoupled mitochondrial respiration in eNOS[hep-/-] mice versus eNOS^{fl/fl} mice (**Fig. 2.4G**). Further, H_2O_2 emission was ~50% higher in CD fed eNOS[hep-/-] mice compared to eNOS^{fl/fl} mice (**Fig. 2.4H**). Similar impairments in hepatic fatty acid oxidation and mitochondrial respiration were also seen in female eNOS[hep-/-] mice, indicating this phenomenon was not sex dependent (**Fig. 2.10**).

These reductions in mitochondrial function in eNOS[hep-/-] mice do not appear to be explained simply be a reduction in hepatic mitochondrial content. Citrate synthase activity, a surrogate marker of mitochondrial content in whole liver homogenate, was slightly elevated in the eNOS[hep-/-] mice (**Fig. 2.11A**). Additionally, while electron transport chain complexes protein content was slightly decreased with WD feeding in CI, CII, and CV, there was no effect of genotype on these markers of mitochondrial content (**Fig. 2.11C-D**).

Hepatic mitochondrial quality/turnover

With the apparent decrease in hepatic mitochondrial function despite no change in mitochondrial content in the eNOS[hep-/-] mice, we posited that the quality of the mitochondria was reduced in eNOS[hep-/-] mice. To assess this, the morphology of the mitochondria were examined, as well as markers of mitochondrial dynamics, including biogenesis, fission and fusion, and examined mitophagic flux. Mitochondrial morphology and structure was determined by TEM, and revealed that mitochondria from eNOS[hep-/-] mice were more elongated (**Fig. 2.5A**). Enlarged mitochondria may be indicative of fat accumulation in the liver and impaired hepatic mitophagy (86). This was associated with slightly reduced protein content of $pDRP1_{s616}$/DRP1 in eNOS[hep-/-] mice (P=0.16), with no change in markers of fusion (OPA1) (**Fig. 2.11D**). Similarly, liver-specific DRP1 KO animals who are deficient in mitochondrial fission, also present with enlarged mitochondrial morphology (86). Despite multiple observations in of the requirement of eNOS and NO for the induction of markers of mitochondrial biogenesis (51, 52), here

there was no genotype effect on pAMPK/AMPK, PGC1α, or TFAM in whole liver

homogenate, and only a slight WD-induced reduction of PGC1α (P=0.06) (**Fig. 2.11D**).

However, certain markers of hepatic mitophagy were decreased in eNOS^hep-/- mice versus

eNOS^fl/fl mice. The mitophagy cascade is initiated by the phosphorylation of ULK1 for

autophagosome formation, then during mitochondrial membrane injury/loss of potential,

PINK1 and BNIP3 are stabilized on the surface to eventually serve as a signal for the

mitochondria to be targeted by autophagy proteins. In isolated liver mitochondria, BNIP3

was significantly reduced in eNOS^hep-/- mice, while PINK1 was increased with WD, and

no clear effect of diet or genotype on LC3-II (**Fig. 2.5B**). In whole liver from eNOS^hep-/-

mice, pULK1/ULK1 protein expression was markedly reduced in CD-fed animals

(~60%), with no change in WD-fed animals versus eNOS^fl/fl mice (**Fig. 2.5C**), while both

PINK1 and BNIP3 protein was also reduced in eNOS^hep-/- mice versus eNOS^fl/fl mice

(P=0.07 and P=0.13, respectively), regardless of diet (**Fig. 2.5C**). Additionally, WD

feeding reduced protein expression of BNIP3, while increasing Parkin, LC3II/I, and

PINK1 (**Fig. 2.5C**). However, such static measurements of mitophagy do not give an

accurate indication of mitophagic flux. To address this, mice were injected with

leupeptin, a lysosomal protease inhibitor, to block autophagic flux and measure the

accumulation of proteins involved in mitophagy after stimulation (16 hr fast). Leupeptin

injection significantly increased protein accumulation of BNIP3 and LC3II in both whole

and isolated mitochondria compared to saline injected animals in all groups

(representative images shown in **Fig. 2.5G**). In whole liver, eNOS^hep-/- mice failed to

mount WD-induced increase in BNIP3 accumulation as seen in eNOS^fl/fl mice (**Fig.**

2.5E). In isolated hepatic mitochondria, LC3-II accumulation tended to be reduced in

eNOS$^{hep-/-}$ mice versus eNOS$^{fl/fl}$ mice (P=0.15), (**Fig. 2.5F**). To further validate the role of

hepatocellular eNOS in mitophagy, *in vivo* AAV-shRNA knockdown of hepatocellular

eNOS significantly blunted accumulation of hepatic isolated mitochondrial LC3-II after

leupeptin injections compared to scramble controls after 2 weeks of WD feeding (**Fig.

2.6D**). Collectively, these findings are in support of previous work from our group (1)

and demonstrate that hepatocyte specific deletion of eNOS impairs mitophagic flux.

Short-term hepatocyte eNOS overexpression

With the clear decline in mitochondrial function in mice lacking eNOS in hepatocytes,

gain-of-function analyses were performed to determine whether overexpression of eNOS

would prevent and/or rescue susceptible to NAFLD and mitochondrial dysfunction.

Protein expression of eNOS in isolated primary hepatocytes exposed to Adv-β-Gal or

varying viral loads of eNOS Adv confirmed successful overexpression of eNOS in

hepatocytes (**Fig. 2.7A**). Adenoviral overexpression of eNOS resulted in the increase in

FCCP-stimulated maximal uncoupled oxygen consumption rate as measured by Seahorse

Analyzer, and increased *nqo1* mRNA expression, as well as increased BNIP3 protein and

mRNA expression compared to β-Gal controls (**Fig. 2.7C-E**). Next, CD-fed 10-week-old

male C57BL/6J mice were injected with either AAV8-TTR-eNOS or AAV8-TTR-GFP

control to determine the effects of *in vivo* hepatocellular eNOS overexpression. At 6

weeks post injection, eNOS mRNA expression was significantly elevated in both whole

liver and isolated primary hepatocytes (**Fig. 2.7F**). Similar to *in vitro* eNOS

overexpression, *in vivo* hepatocellular eNOS overexpression increased basal and maximal

uncoupled respiration in isolated primary hepatocytes from AAV8-TTR-eNOS mice (**Fig. 2.7G**). Collectively, these data suggest that overexpressing hepatocellular eNOS both *in vitro* and *in vivo* increases hepatocyte respiration and increases markers of mitophagy.

Effects of long term hepatocellular eNOS overexpression on NASH development

As mice lacking hepatocellular eNOS displayed exacerbated NAFLD development and decreased mitochondrial function, we speculated that *in vivo* overexpression of eNOS in hepatocytes would mitigate NAFLD development and potentially reverse NAFLD/NASH and rescue hepatic mitochondrial dysfunction. After either CD or WD feeding for 20 weeks, C57BL/6J mice were injected with either an AAV8-TTR-eNOS overexpression virus (AAV-eNOS OE) or AAV8-TTR-GFP (AAV-GFP) control and maintained on their respective diets for an additional 10 weeks. The success was the viral transfection was confirmed via the elevated eNOS expression in whole livers of AAV-eNOS OE CD and WD fed animals, compared to their AAV-GFP-Scr controls (**Fig. 2.8C-D**). Despite an expected WD effect, there was no effect of eNOS overexpression on body weight or body fat at 30 weeks of age (**Fig. 2.8A-B**). Histologically, WD feeding caused marked increases in hepatic steatosis, ballooning, inflammation, overall NAS score and fibrosis (**Fig. 2.8E-H**). However, histological inflammation, NAS score, and fibrosis were attenuated in AAV-eNOS OE animals on both CD and WD (**Fig. 2.8E-H**), indicating that overexpressing hepatocellular eNOS may exert some anti-inflammatory and anti-fibrotic effects in the liver. This attenuation in hepatic inflammation and fibrosis was associated with elevations in NRF2 (nfe2l2) mRNA expression, a known master regulator of the antioxidant response and implicated in our previous studies as being regulated by eNOS

(1). This was not accompanied by alterations in other gene expression markers of inflammation or collagen deposition (**Fig. 2.8I-J**). In addition, unlike the increases in cellular respiration witnessed with short-term eNOS overexpression (**Fig. 2.7H**), we did not see increases with long-term AAV induced overexpression of eNOS on whole liver or isolated mitochondria fatty acid oxidation nor did it prevent WD-induced decreases in ETC protein complexes or BNIP3 and PGC1 hepatic protein content (**Fig. 2.13A-F; H-I; I, J**). Interestingly, AAV-eNOS OE slightly reduced maximal uncoupled mitochondrial respiration regardless of diet (**Fig. 2.13G**).

BNIP3 and NO rescue

Mice with hepatocellular eNOS deficiency present with decreased BNIP3 protein in both whole liver and isolated mitochondria (**Fig. 2.5B-C**), as well as impaired ability to mount a whole liver BNIP3 response to WD with leupeptin injections in eNOS$^{hep-/-}$ mice (**Fig. 2.5F**). Based on these observations, we posited that the beneficial role hepatocellular eNOS during NAFLD development may be BNIP3 dependent. As such, overexpressing BNIP3 in hepatocytes lacking eNOS may attenuate any detrimental effects. In isolated primary hepatocytes from eNOS$^{fl/fl}$ mice, Adv BNIP3 overexpression at 10^5 PFU/ml increased baseline and maximal uncoupled respiration compared to β-Gal controls. In isolated hepatocytes from eNOS$^{hep-/-}$ mice, Adv BNIP3 overexpression at any concentration (10^3 - 10^6 PFU/ml) had no effect on cellular oxygen consumption compared to β-Gal treated cells (**Fig 2.9A-B**). Notably, maximal uncoupled respiration was significantly higher in eNOS$^{fl/fl}$ vs eNOS$^{hep-/-}$ hepatocytes, regardless of treatment (**Fig. 2.9A-B**). Further, Adv BNIP3 overexpression at 10^3 PFU/ml increased total 1-^{14}C-

palmitate oxidation to CO_2 compared to β-Gal treated cells, with no effect of higher concentrations (**Fig. 2.9C**). This was not observed in hepatocytes isolated from eNOS$^{hep-/-}$ mice, as Adv BNIP3 overexpression at 10^3 PFU/ml did not statistically increase total palmitate oxidation vs β-Gal controls (**Fig. 2.9C**). Similar to respiration data, hepatocytes from eNOS$^{hep-/-}$ mice had lower total palmitate oxidation compared to eNOS$^{fl/fl}$, regardless of treatment (main effect for genotype). These data suggest that eNOS may be required for the BNIP3-induced increase in hepatocyte respiration and fatty acid oxidation, with a lower threshold for BNIP3-induced fatty acid oxidation compared to respiration (10^3 vs 10^5 PFU/ml).

To determine if administering exogenous NO would rescue the decreased respiration observed in eNOS$^{hep-/-}$ vs eNOS$^{fl/fl}$ hepatocytes, isolated primary hepatocytes were exposed to varying concentrations (50uM, 100uM) of the NO donor – DETA NONOate. As demonstrated previously, maximal uncoupled respiration was significantly higher in eNOS$^{fl/fl}$ vs eNOS$^{hep-/-}$ hepatocytes, regardless of NO treatment (**Fig. 2.9D**). Interestingly, this was not rescued by NO donor, as this had no effect on respiration in either eNOS$^{hep-/-}$ or eNOS$^{fl/fl}$ hepatocytes (**Fig. 2.9D**). Further, cGMP activity, a surrogate marker of NO production, was no different between eNOS$^{fl/fl}$ vs eNOS$^{hep-/-}$ hepatocytes, while NO donors (250-1000uM) doubled cGMP activity (**Fig. 2.9E**). These data strongly suggest that the reduced respiration seen in eNOS$^{hep-/-}$ hepatocytes is independent of NO production.

Metabolomics

Metabolomic analysis on whole liver from eNOS$^{fl/fl}$ versus eNOS$^{hep-/-}$ mice on either a CD or WD for 16 weeks revealed a number of clear WD effects on metabolites such as itaconic acid, guanosine diphosphate and malic acid (**Fig. 2.12A-B**). Interestingly, the analysis also indicated significant upregulation in lactic acid and kynurenine in eNOS$^{hep-/-}$ mice regardless of diet (**Fig. 2.12B**). An impairment in TCA and/or ETC flux may cause more pyruvate to lactate conversion, and accumulation of kynurenine (a TCA cycle substrate). This would lend support to the idea of mitochondrial impairment in eNOS$^{hep-/-}$ mice. Elevations in these metabolites might also suggest an increased immune response to hepatocellular eNOS deficiency (87, 88). Further, the metabolite myoinositol has been associated with autophagy inhibition, and was elevated in eNOS$^{hep-/-}$ mice (**Fig. 2.12B**).

DISCUSSION

The mechanisms behind the decline in hepatic mitochondrial function with NAFLD development are not fully elucidated. Our group has shown that reduced hepatic eNOS activity is linked with hepatic mitochondrial dysfunction and progression to NASH (47), while NOS inhibition causes hepatic mitochondrial dysfunction and hastens NAFLD development (46). Moreover, we have demonstrated hepatic mitochondria from eNOS null mice displayed decreased markers of mitochondrial turnover, while *in vitro* siRNA-induced knockdown of eNOS in primary hepatocytes reduced fatty acid oxidation and blunts the BNIP3 response to mitophagic stimulation (1). However, the role of hepatocellular-specific eNOS in NAFLD development and maintaining healthy mitochondria in the liver is unresolved. Here, genetic, adenoviral, and AAV approaches were used to provide evidence for its novel effect on hepatic steatosis and inflammation

and its modulation of fatty acid oxidation and mitochondrial respiration in the liver. Interestingly, these detrimental effects of hepatocellular eNOS deficiency are not rescued by BNIP3 overexpression or NO donors. Corroborating previous work from our group (1), hepatocellular eNOS is required for fully functioning mitophagic capacity in the liver to maintain a healthy mitochondrial pool. Moreover, overexpressing hepatocellular eNOS attenuates NASH progression. Taken together, there is compelling evidence for a protective and vital role of hepatocellular eNOS in NAFLD development.

Initial reports suggested that eNOS distribution in the liver was localized to sinusoidal endothelial cells (44, 89-91), but more recent and robust investigations indicated that the distribution of eNOS in the liver is more ubiquitous (92-94). Similar to previous work by our group and others (1, 77), *MACS* was used to achieve highly purified hepatocytes allowing us to confirm the presence of eNOS in hepatocytes.

With multiple approaches used in the current study, we demonstrate that lack of hepatocellular eNOS worsens liver histology. Both AAV-Cre and AAV-shRNA knockdown of eNOS in hepatocytes exacerbate liver steatosis and inflammation on short-term CD and WD feeding, respectively (**Fig. 2.6**). Similarly, after 16 weeks on either CD or WD, eNOS^hep-/- mice present with elevated hepatic steatosis and inflammation compared with eNOS^fl/fl mice (**Fig. 2.3**). This is similar to findings from whole body eNOS null mice, with increased hepatic steatosis and inflammation compared to congenic wild-type mice after 12 weeks of high-fat diet feeding (45). The authors attribute this to alterations in hepatic blood flow due to loss of eNOS in the vasculature – a confounding

factor with whole body eNOS KO models, making it difficult to delineate the role of hepatocellular-specific eNOS in hepatic fat accumulation. Here, lack of hepatocellular eNOS *per se* was identified as a contributing factor in exacerbated NAFLD development.

Mitochondria in skeletal muscle from whole body eNOS null mice have impaired β-oxidation and reduced mitochondrial content (73). The decrease in mitochondrial function is likely driven by the reduction in content, as eNOS and NO are known to promote mitochondrial biogenesis (50-52). Similarly, a robust decrease in palmitate oxidation was seen in both whole liver and isolated hepatic mitochondria in eNOS[hep-/-] versus eNOS^{fl/fl} mice (**Fig. 2.4**). Unlike the whole-body eNOS KO models, this decrease in mitochondrial function cannot be explained by reduced mitochondrial content in eNOS[hep-/-] mice, indicating that eNOS in the hepatocyte plays a fundamental role in hepatic mitochondrial function, beyond a regulator of content or mass.

NO inhibits cytochrome C oxidase (CIV) of the electron transport chain via both competitive and non-competitive sites (95), and also attenuates respiration in complex I and III, which are known sites for ROS production through S-nitrosylation (96, 97). This protective role of NO-throttling of respiration to prevent excess ROS production is apparent in the hepatocellular eNOS deficient mice, who present with a ~50% increase in H_2O_2 emissions compared to eNOS^{fl/fl} mice on a CD. Despite increased ROS production, eNOS[hep-/-] mice presented with reduced state 3 and maximal uncoupled respiration, indicating an increase in coupled and uncoupled mitochondrial respiration. Similarly, primary hepatocytes from eNOS[hep-/-] mice display reduced maximal uncoupled

respiration compared to eNOS$^{fl/fl}$ hepatocytes (**Fig. 2.9**). Interestingly, NO donors did not

rescue the reduced hepatocyte respiration to the level of eNOS$^{fl/fl}$ hepatocytes, indicating

the impaired respiration is not likely mediated by NO. Further studies are warranted to

determine the mechanism behind the NO-independent reduction of mitochondrial

function with hepatocellular eNOS deficiency.

It is well established that eNOS-derived NO is a regulator of mitochondrial biogenesis in

other tissues. Whole body eNOS null mice have attenuated cold-exposure and calorie

restricted-induced mitochondrial biogenesis and present with reduced mitochondrial

content in liver, brain, and heart tissue (50-52), while eNOS is essential for exercised-

induced improvements in mitochondrial function in adipose and cardiac tissue (53, 54).

Conversely, overexpression of eNOS promotes mitochondrial biogenesis in adipose

tissue (55). However, much less is known about the role of eNOS and NO in mitophagy –

a form of quality control where dysfunctional mitochondrial are selected for degradation.

Here we demonstrate that leupeptin injected hepatocyte eNOS deficient mice fail to

mount a WD-induced elevation in whole liver BNIP3 and show reduced isolated

mitochondrial LC3-II, along with decreased static markers of mitophagy (pULK1/ULK1,

PINK1), and elongated mitochondrial morphology (**Fig. 2.5**). Similarly, AAV-shRNA

knockdown of eNOS blunt the leupeptin-induced accumulation of mitochondrial LC3-II

(**Fig. 2.6**). These results are supported by previous work by our group, where eNOS KO

hepatocytes present with reduced markers of mitochondrial biogenesis (PGC1α, TFAM)

and mitophagy (BNIP3, LC3-II/LC3-I), while *in vitro* siRNA-induced knockdown of

eNOS in primary hepatocytes attenuated the induction of BNIP3 in response to

mitophagic stimulation (1). We posit that eNOS deficient hepatocytes fail to remove

poorly functioning mitochondria within the hepatocyte, and these damaged mitochondria

are contributing to elevated oxidative stress and the marked reduction in hepatic

mitochondrial function. Ultimately, this potentially led to the observed elevated

histological steatosis and inflammation.

Our group has shown that hepatic eNOS activity is markedly reduced during progression

from hepatic steatosis to NASH in obese OLETF rats (47), while 4-weeks of L-NAME

administration induced a more NASH-like phenotype versus untreated obese controls

(46). Conversely, others have shown that administering an NO donor can mitigate NASH

progression via reducing M1 macrophage polarization (98) and increasing hepatic stellate

cell apoptosis (99). Given our ability to increase hepatocyte respiration with both Adv

and AAV overexpression of eNOS (**Fig. 2.7**), with concurrent increases in *nqo1* and

BNIP3, these data indicate that increasing hepatocyte eNOS activity may mitigate NASH

development. After 20-week WD-induced NASH phenotype, overexpressing

hepatocellular eNOS attenuated further NASH progression via reductions in histological

inflammation and fibrosis versus GFP controls (**Fig. 2.8**). Despite clear histological

improvement, this was not associated with improvements in inflammatory or macrophage

polarization markers (only elevated *nfe2l2,* **Fig. 2.8I**), nor improvements in

mitochondrial function (**Fig. 2.13**). As eNOS overexpression increased gene expression

of the NRF-2 pathway *in vitro* and *in vivo* (*nqo1* and *nfe2l2*, respectively), the observed

histological benefits may be mediated through the antioxidant effects of NRF-2. This

supports previous work of ours showing the link between eNOS and NRF-2 activation

(1). Given our ability to increase respiration in hepatocytes of CD fed animals at 6 weeks

of eNOS overexpression, we may have missed the window to observe the full effects of

eNOS overexpression in hepatocytes by examining functional outcomes at 10 weeks post

injection. As such, the observed histological improvements at 10 weeks post injection and

30 weeks of their respective diets may be resultant of the earlier benefits of elevated

eNOS expression. Moreover, respiration was assessed in whole liver and isolated

mitochondria from whole liver, which would have included other cell types with intact

eNOS (Kupffer cells, liver sinusoidal endothelial cells) (77). This may have masked the

effects of hepatocellular eNOS overexpression on respiration, and future studies should

also examine these outcomes in isolated hepatocytes. Despite the issue of cell

contamination and determining the ideal time for functional assessment, these data

clearly demonstrate a beneficial role for hepatocellular eNOS overexpression, possibly

via NRF-2 activation. When taken together with aforementioned studies, it is evident that

hepatic eNOS is involved in curbing the development and progression of NASH.

BNIP3 is known to play a role in both cell death and autophagy/mitophagy, and its action

may depend on the type of stress induced (100). BNIP3 null mice present with

exacerbated NAFLD, and reduced hepatic mitochondrial β-oxidation, membrane

potential, and oxygen consumption (58). Further, we have previously shown that eNOS

deficient hepatocytes have a blunted BNIP3 response to mitophagic stimulation (1).

Supporting this, reductions of BNIP3 in whole liver and isolated mitochondria of

eNOS[hep-/-] mice were observed here, while these mice also failed to mount a WD-induced

BNIP3 accumulation with leupeptin injections (**Fig. 2.5**). Hence, overexpressing BNIP3

in hepatocellular eNOS deficient animals may abrogate any detrimental effects of eNOS deficiency. Indeed, Adv BNIP3 overexpression increased both respiration and fatty acid oxidation in isolated primary hepatocytes from eNOS$^{fl/fl}$ mice, while BNIP3 overexpression had no effect in eNOS$^{hep-/-}$ hepatocytes (**Fig. 2.9**). Confirming our *in vivo* model, hepatocytes from eNOS$^{hep-/-}$ mice had lower total palmitate oxidation and maximal uncoupled respiration compared to eNOS$^{fl/fl}$, regardless of treatment. BNIP3 overexpression induces mitophagy (101), and this removal of poorly functioning mitochondria may be the reason for the elevated mitochondrial function seen here with BNIP3 overexpression. This may be dose dependent, as overexpression of BNIP3 has also induced its pro-apoptotic effects and caused mitochondrial dysfunction (102), supporting the reduced respiration seen here with the highest concentration of Adv BNIP3 overexpression in eNOS$^{fl/fl}$ hepatocytes (**Fig. 2.9**). Regardless of concentration, it appears BNIP3 overexpression regulates hepatocyte mitochondrial function via an eNOS dependent mechanism. *In vivo* overexpression of BNIP3 in eNOS$^{hep-/-}$ mice would better elucidate the role of hepatocellular eNOS and BNIP3 in hepatic mitochondrial function. Metabolomic analyses support the notion of mitochondrial impairment in hepatocellular eNOS deficient mice. Whole livers from eNOS$^{hep-/-}$ mice presented with elevated lactic acid and kynurenine levels vs eNOS$^{fl/fl}$ mice (**Fig. 2.12**). This could be indicative of impaired TCA cycle or ETC flux - shunting more pyruvate to lactate production, where excess can be used for glycogen synthesis and lipid storage (103). Additionally, as kynurenine is a substrate for the TCA cycle, increased levels as seen in eNOS$^{hep-/-}$ mice further supports the notion that these mice present with impaired TCA cycle or ETC flux. Moreover, elevated kynurenine pathways have been associated with loss of mitochondrial

function (104). These metabolites are also associated with immune function (87, 88), suggesting a heightened immune response to hepatocellular eNOS deficiency Further, the metabolite myoinositol was elevated in eNOS[hep-/-] mice, which has been implicated in the inhibition of autophagy in fibroblast-like COS-7 cells (105), although its role in the liver has not been elucidated.

A limitation to the study is fully determining if all the observed effects of hepatocellular eNOS manipulation are all mediated through eNOS-derived NO production. As the life of a NO molecule is notoriously short lived, surrogate markers are commonly used. Given the markedly lower abundance of eNOS in hepatocytes compared to other cell types in the liver – namely Kupffer cells and liver sinusoidal endothelial cells (77), hepatocytes may produce extremely low physiological levels of NO. Hence, our surrogate methods of NO production may not be sensitive enough to detect very slight differences between hepatocytes from eNOS^{fl/fl} versus eNOS[hep-/-] mice; where in reality, the total sum of all hepatocellular eNOS derived NO production may be physiologically relevant, as hepatocytes make up ~90% of all cell types in the liver (77). As NO donors failed to rescue reduced respiration seen in eNOS[hep-/-] hepatocytes (**Fig. 2.9**), it appears these effects are independent of NO. Further and more thorough examinations into NO production from hepatocytes with and without eNOS are required to fully determine whether the beneficial effects of hepatocellular eNOS are mediated through NO. Additionally, in CD fed animals only, hepatocellular eNOS deficiency seems to alter glucose homeostasis via elevated serum insulin and worsened pyruvate tolerance testing. Moreover, eNOS[hep-/-] mice have elevated *g6pase* and *ppeck* gene expression, indicative of

increased gluconeogenesis. Examining hepatic glucose output in isolated primary hepatocytes from both eNOS$^{fl/fl}$ and eNOS$^{hep-/-}$ mice would help tease out whether eNOS plays a role in hepatocyte glucose metabolism. This concept is supported by previous work, where re-coupling of eNOS via tetrahydrobiopterin (BH4) administration in diabetic mice lowered blood glucose levels, while this effect was ablated in hepatocytes from eNOS null mice (94).

In conclusion, multiple approaches via gain- and loss- of-function studies have allowed us to identify a novel role for hepatocellular eNOS in prevention of NAFLD via maintenance of a healthy hepatic mitochondrial pool and attenuation of hepatic inflammation. Further research is required to elucidate the mechanism behind the beneficial role of hepatocellular eNOS in hepatic mitochondrial function, given that they appear to be independent of BNIP3 and NO. Accordingly, examination of hepatocellular eNOS and its regulatory functions may shed further light on the mechanisms behind NAFLD development and hepatic mitochondrial dysfunction, and provide potential future therapeutic avenues.

Disclosures

No conflicts of interest, financial or otherwise, are declared by the authors.

Author Contributions

R.P.C., J.A.I., J.P.T., and R.S.R. were involved in the study concept and design. T.T.

provided the eNOS floxed mouse model. R.P.C., M.P.M., G.M.M., V.J., L.B., R.D.S.,

and R.S.R. helped with acquisition of data. R.P.C., M.P.M., G.M.M., R.D.S., and R.S.R

analyzed and interpreted results. R.P.C., and R.S.R. provided statistical analysis of the

data. R.P.C. drafted the manuscript, while R.P.C., M.P.M., G.M.M., R.D.S., J.A.I., J.P.T.,

and R.S.R. revised the manuscript and provided important intellectual content. R.P.C.,

M.P.M., G.M.M., V.J., L.B., T.T., R.D.S., J.A.I., J.P.T., and R.S.R. approved final

version of manuscript. R.P.C. and R.S.R. obtained funding.
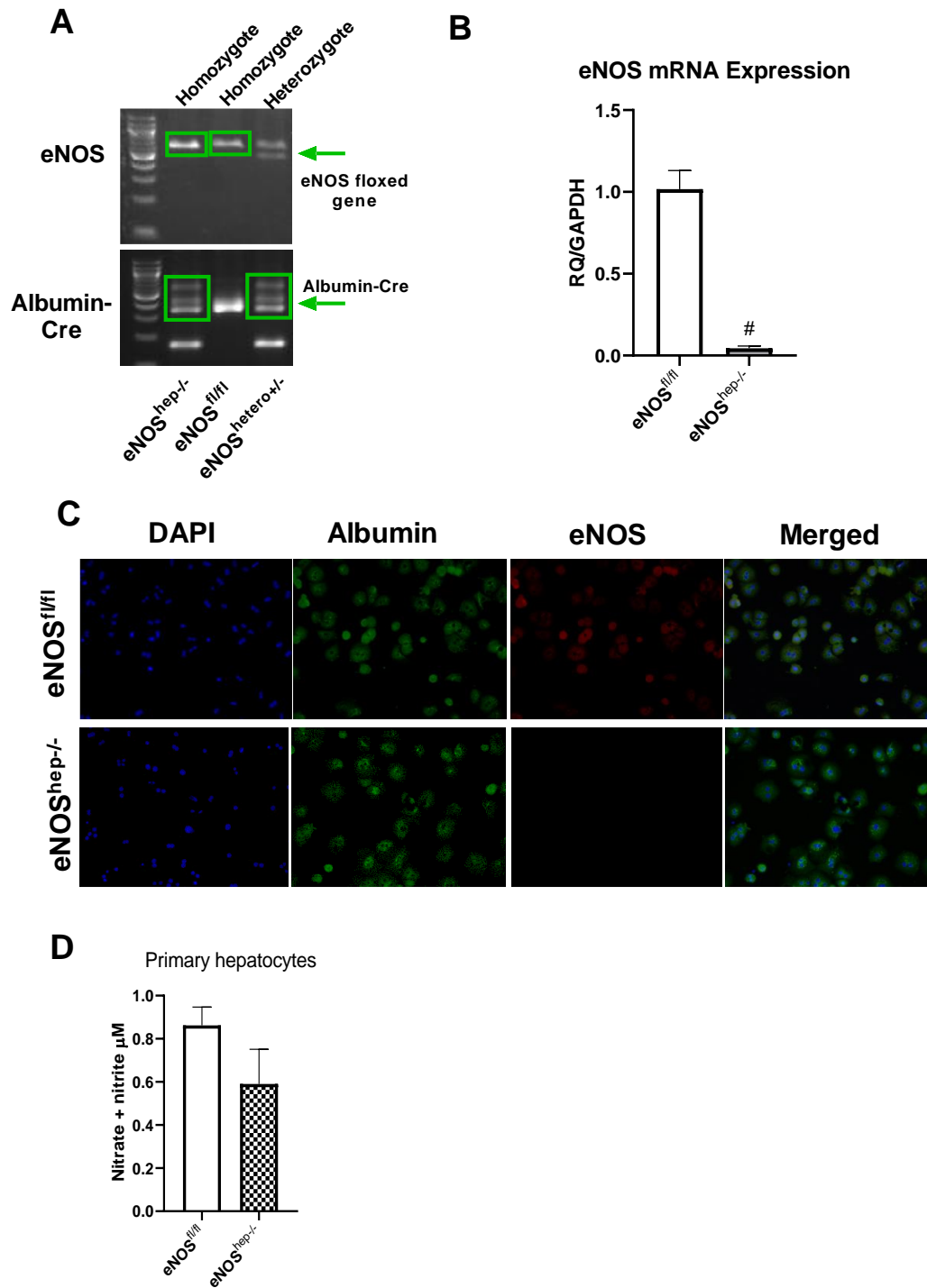
Figures

Figure 2.1: Confirmation of the mouse model and deletion of hepatocellular eNOS in

primary hepatocytes collected from both eNOS$^{fl/fl}$ and eNOS$^{hep-/-}$ mice on a CD.

A) Genotyping images displaying the floxed eNOS gene and the presence of the Albumin-Cre in our eNOS$^{fl/fl}$ and eNOS$^{hep-/-}$ murine line. B) mRNA expression of eNOS in isolated primary hepatocytes from eNOS$^{fl/fl}$ and eNOS$^{hep-/-}$ mice on CD (n=4/group). C) Fluorescence microscopy of isolated primary hepatocytes, confirming the deletion of hepatocellular eNOS. Nuclei were stained with DAPI (blue), hepatocytes stained with albumin (green), and eNOS stained by anti-eNOS antibody (n=4-5 per genotype). D) Nitrate and nitrite concentration in supernatant from isolated primary hepatocytes from eNOS$^{fl/fl}$ and eNOS$^{hep-/-}$ mice on CD (P=0.16) (n=6-8). Data are presented as mean ± SEM. CD, control diet.
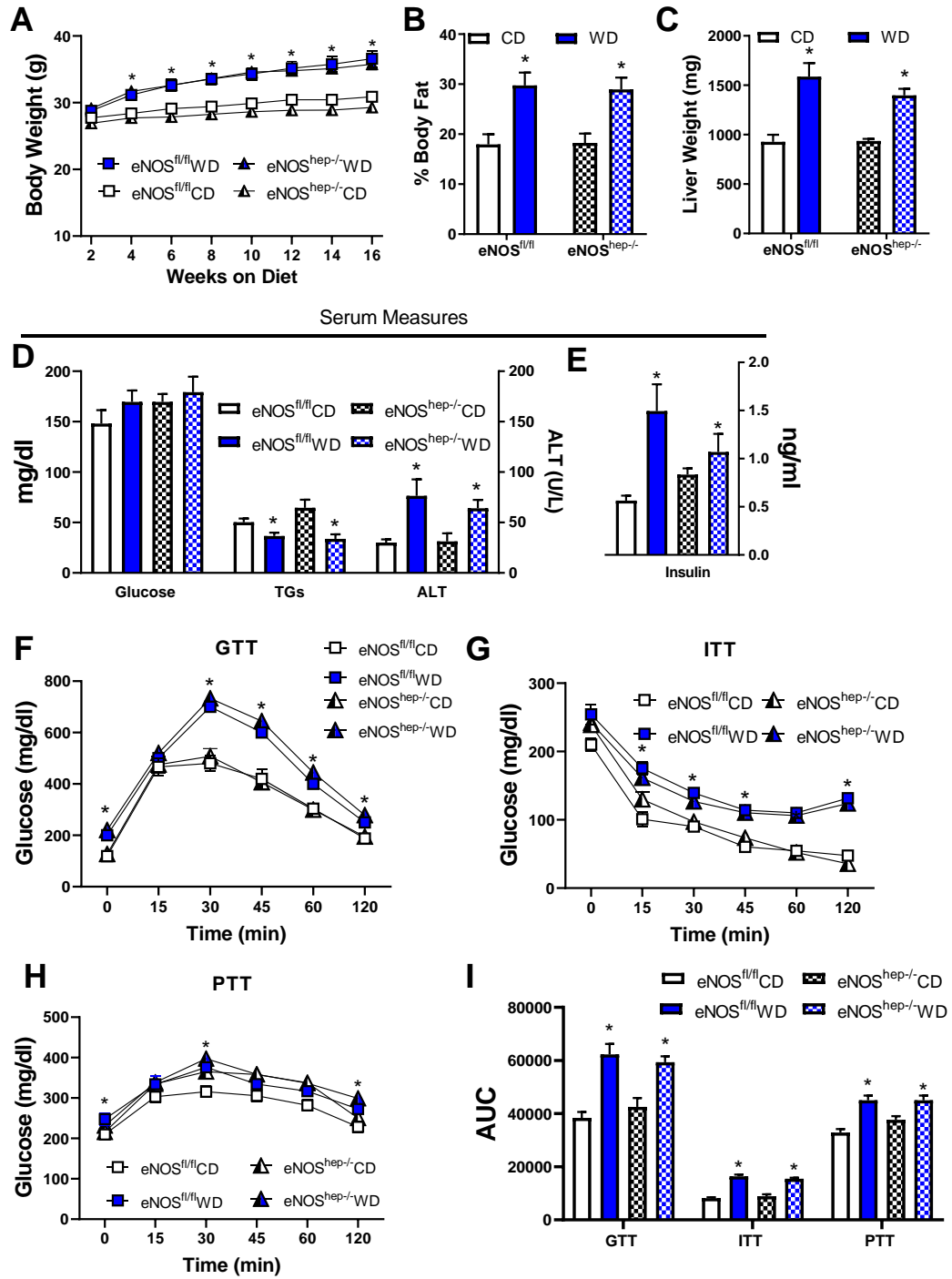
Figure 2.2: Effects of hepatocellular eNOS deficiency on animal characteristics and

glucose tolerance. A) eNOS$^{fl/fl}$ and eNOS$^{hep-/-}$ mice were randomized to either a CD or

WD and body weight was tracked for 16 weeks (n = 13-17/group). B) Final body fat %

and C) liver weight, after 16 weeks on respective diets (n = 13-17/group). D). Serum

glucose, TGs, and ALT and E) insulin concentrations (n = 13-17/group). F-H) GTT, ITT,

and PTTs were performed on a subset of eNOS$^{fl/fl}$ and eNOS$^{hep-/-}$ mice on either a CD or

WD for 10 weeks (n = 4-11/group). I) Total glucose AUC for GTT, ITT, and PTT (n = 4-

11/group). Data are presented as mean ± SEM.* main effect of diet (P<0.05 vs CD). CD,

control diet; WD, western diet; TGs, triglycerides; ALT, alanine aminotransferase; GTT,

glucose tolerance test; ITT, insulin tolerance test; PTT, pyruvate tolerance test; AUC,

area under the curve.
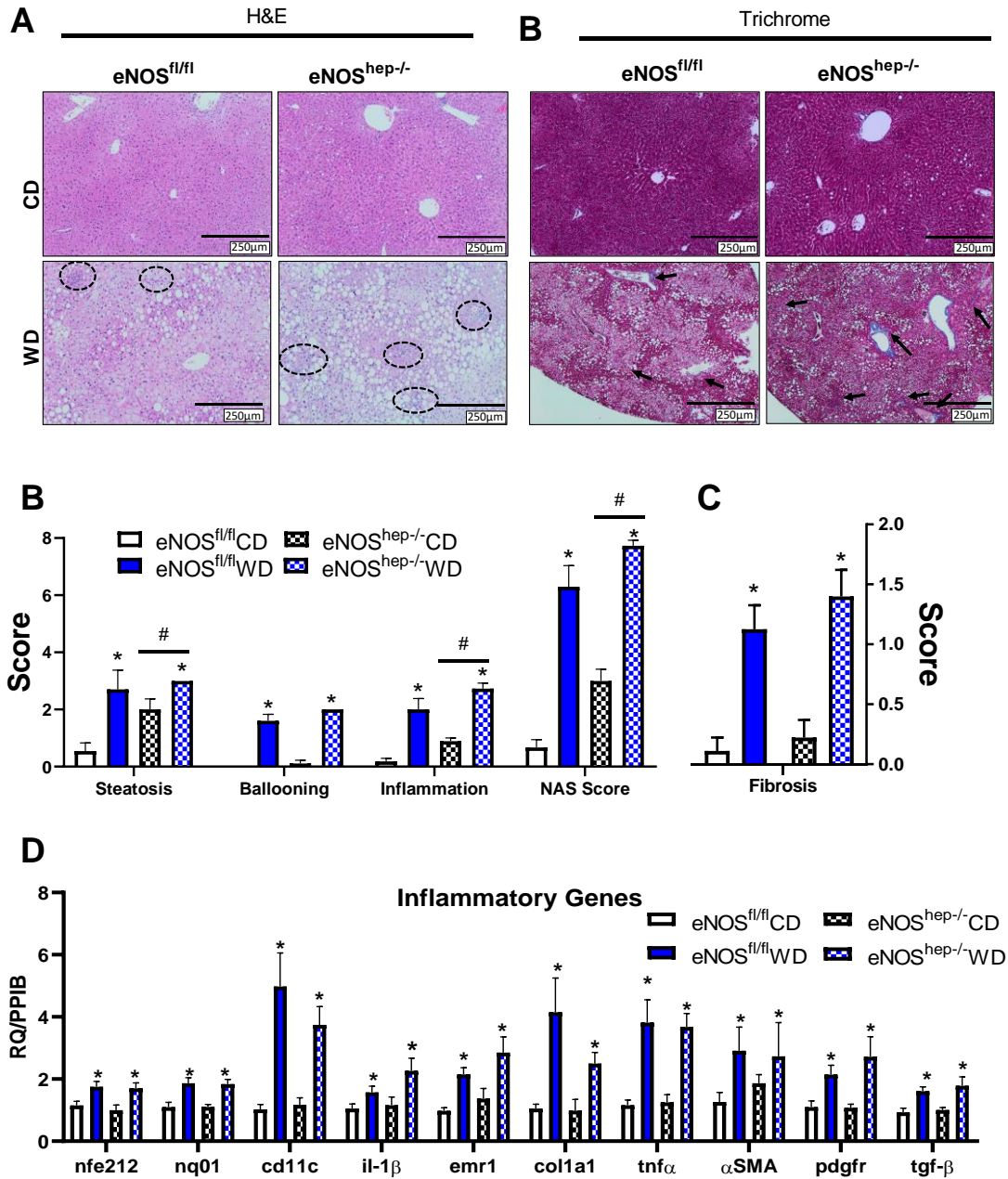
Figure 2.3: Effects of hepatocellular eNOS deficiency on liver histology and inflammation. A) Representative liver H&E and B) trichrome staining from the indicated mice at 16 weeks of age. C) Histological and D) fibrosis scoring based of H&E and trichrome images (n = 10-17/group). E) mRNA expression of markers of hepatic

inflammation (n = 13-17/group). Data are presented as mean ± SEM. *main effect of diet (P<0.05 vs CD), #main effect of genotype (P<0.05 vs eNOS$^{fl/fl}$). CD, control diet; WD, western diet; H&E, haemotoxylin and eosin; NAS, NAFLD activity score.
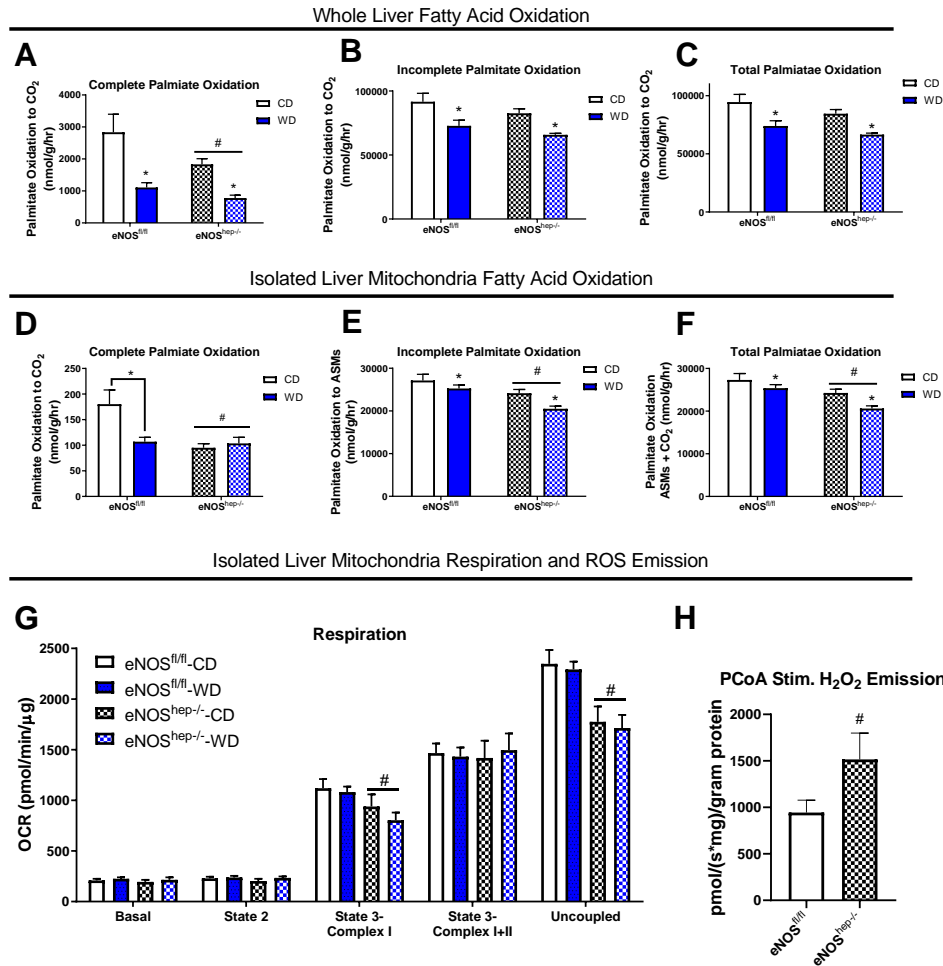
Figure 2.4: Effect of hepatocellular eNOS deficiency on hepatic mitochondrial function.

A) Whole liver complete, B) incomplete, and C) total $[1\text{-}^{14}C]$ pyruvate oxidation to CO_2

(n = 13-17/group). D) Isolated liver mitochondria complete, E) incomplete, and F) total

$[1\text{-}^{14}C]$ pyruvate oxidation to CO_2 (n = 13-17/group). G) Oxygen consumption in isolated

liver mitochondria (n = 6-10/group). H) PCoA stimulated H2O2 emission in isolated liver

mitochondria from male and female (combined) eNOS$^{fl/fl}$ and eNOS$^{hep-/-}$ fed a CD only (n

= 7-9/group). Data are presented as mean ± SEM.*main effect of diet (P<0.05 vs CD),

#main effect of genotype (P<0.05 vs eNOS$^{fl/fl}$). CD, control diet; WD, western diet;

PCoA, palmitoyl-CoA; β-HAD, 3-hydroxyacyl-CoA dehydrogenase.
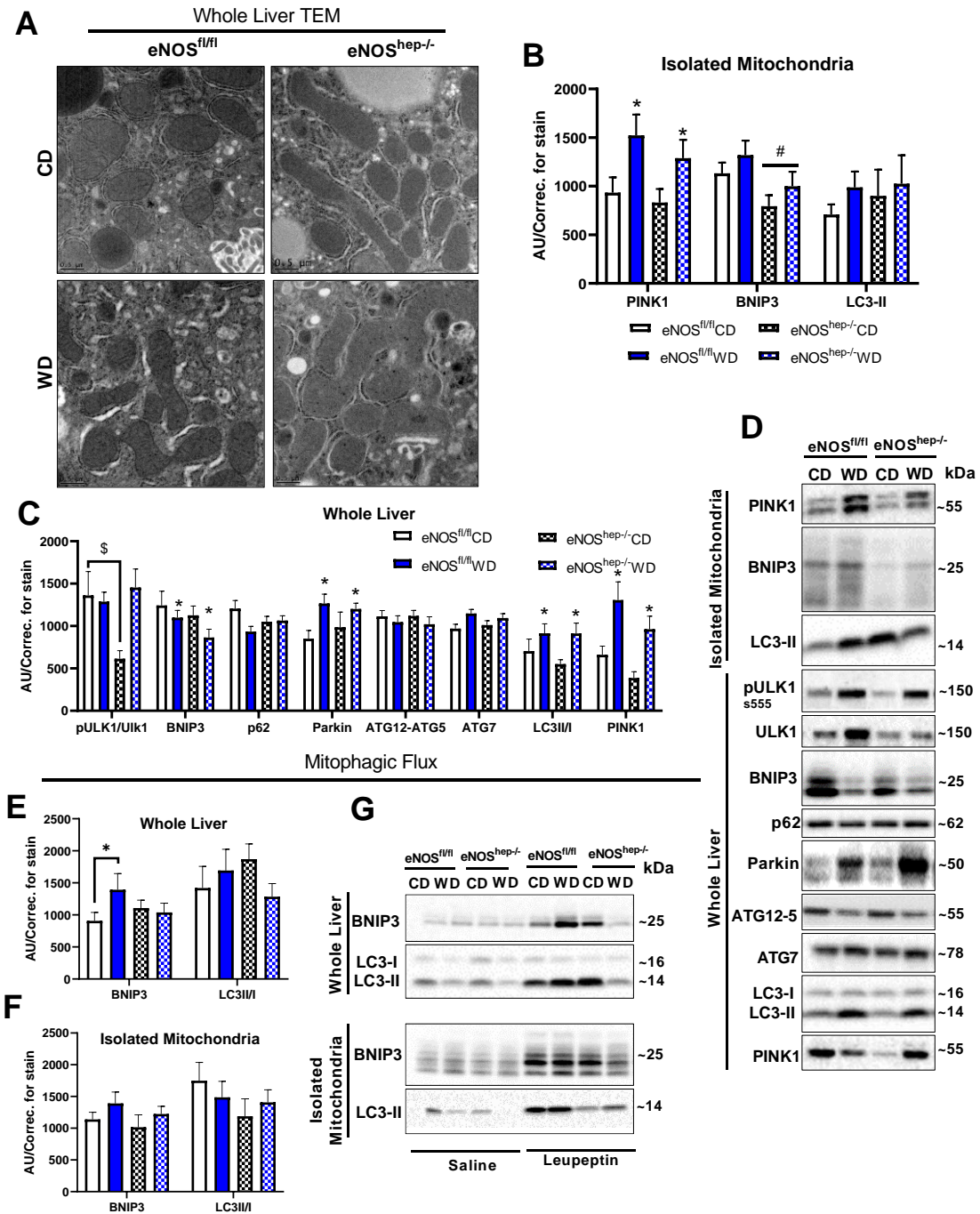
Figure 2.5: Effects of hepatocellular eNOS deficiency on mitochondrial morphology,

quality, and turnover. A) Representative TEM images of whole liver. B) Protein

expression of markers of mitophagy in isolated liver mitochondria and C) whole liver homogenate (n = 13-23/group), and D) their representative Western blot images. Protein expression of the accumulation of mitophagy proteins after in vivo leupeptin injection in E) whole liver and F) isolated liver mitochondria (n = 5-9/group), with G) their representative Western blot images. Data are presented as mean ± SEM.*main effect of diet (P<0.05 vs CD), #main effect of genotype (P<0.05 vs eNOS$^{fl/fl}$), $ significant diet and genotype interaction (P<0.05). CD, control diet; WD, western diet; TEM, transmission electron microscopy.

A

eNOS$^{fl/fl}$-AAV-GFP **eNOS$^{fl/fl}$-AAV-TBG-Cre**

B

eNOS Protein Expression

AU/Correc. for protein

*

eNOS$^{fl/fl}$-AAV-GFP   eNOS$^{fl/fl}$-AAV-TGB-Cre

AAV-eNOS shRNA in C57BL/6J mice

C

WD AAV-Scramble **WD AAV-eNOS shRNA**

D

AAV Leupeptin LC3

$

#

AU

Saline Leup Saline Leup

AAV-Scramble   AAV-eNOS shRNA
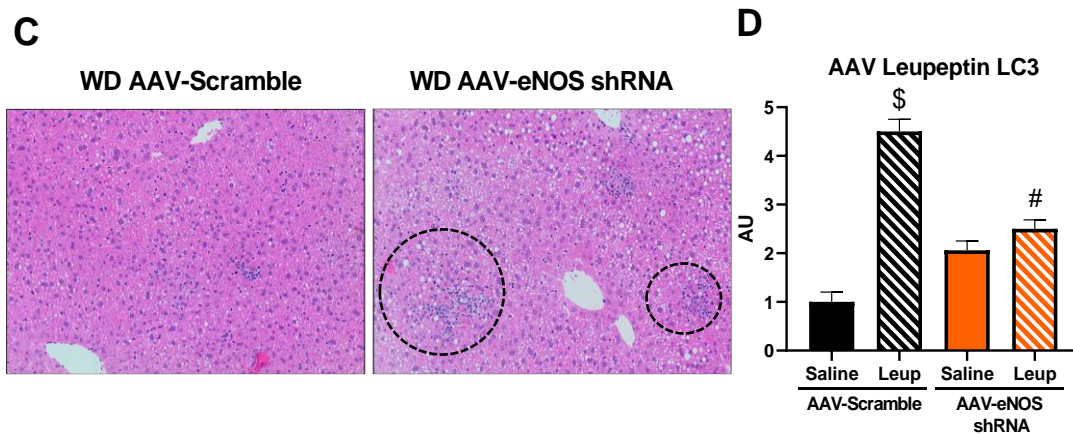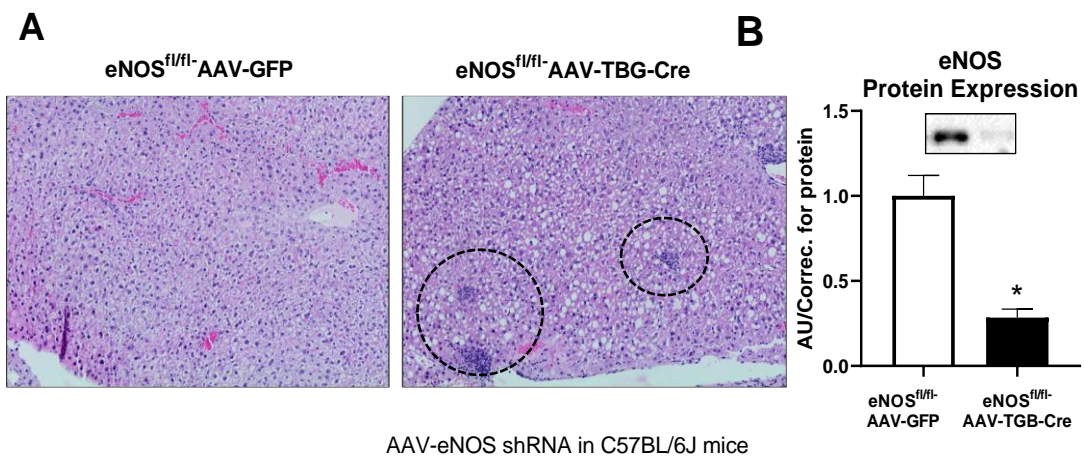
Figure 2.6: Effects of hepatocellular eNOS knockdown via Cre injection in eNOS$^{fl/fl}$ animals and shRNA knockdown in C57BL/6J mice. A) Representative liver H&E staining after 6 weeks of CD feeding from eNOS$^{fl/fl}$ mice injected with AAV-8-TGB-Cre at 10 weeks of age. B) Protein expression of eNOS in isolated primary hepatocytes (n = 3-5/group). C) Representative liver H&E staining after 2 weeks of WD feeding from C5fBL/6J mice injected with AAV-eNOS shRNA at 10 weeks of age. D) Protein expression of the accumulation of LC3-II in isolated mitochondria after in vivo leupeptin

injection (n = 3-4/group). Data are presented as mean ± SEM. * significantly different from GFP (P<0.05), $ significant from saline within AAV-Scramble (P<0.05). # significantly different from AAV-Scramble within leupeptin injected animals (P<0.05). CD, control diet; WD, western diet.
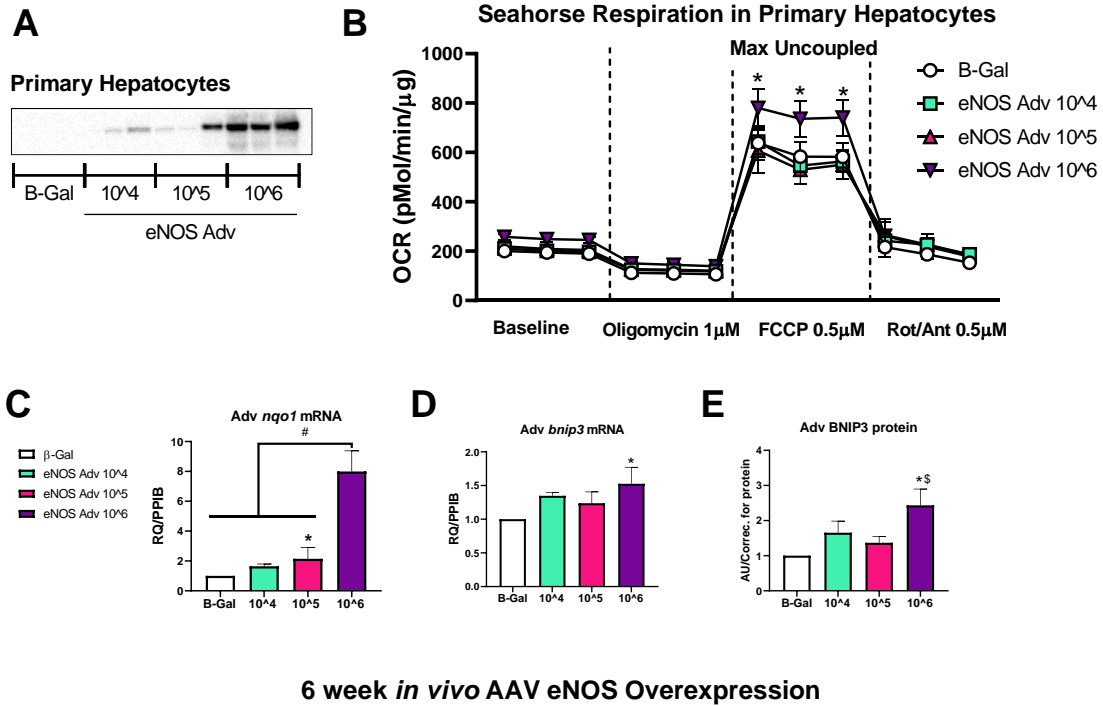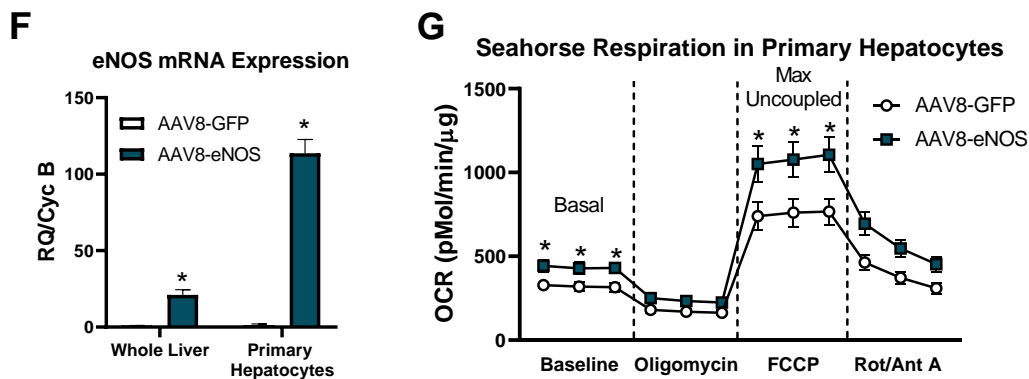
Figure 2.7: Effects of hepatocellular eNOS overexpression on primary hepatocyte

respiration. A) Representative Western blot image of Adv overexpression in primary

hepatocytes. eNOS expression in cells exposed to Adv-β-Gal are under exposed due to

the robust increases in eNOS expression in cells exposed to Adv-eNOS. B) Oxygen

consumption rate in isolated primary hepatocytes (n = 3), C-D) Gene expression and E)

protein expression of BNIP3in isolated primary hepatocytes (n = 3). At 6 weeks post

AAV8-TTR-eNOS overexpression - F) eNOS gene expression in

whole liver and isolated primary hepatocytes, and G) oxygen consumption rate in isolated

primary hepatocytes (n= 7-8/group). Data are presented as mean ± SEM.*significantly

different from B-Gal, #significantly different from B-Gal, 10^4, 10^5, &significantly

different from 10^5 (for all P<0.05). Adv, adenoviral; AAV, adeno associated virus.
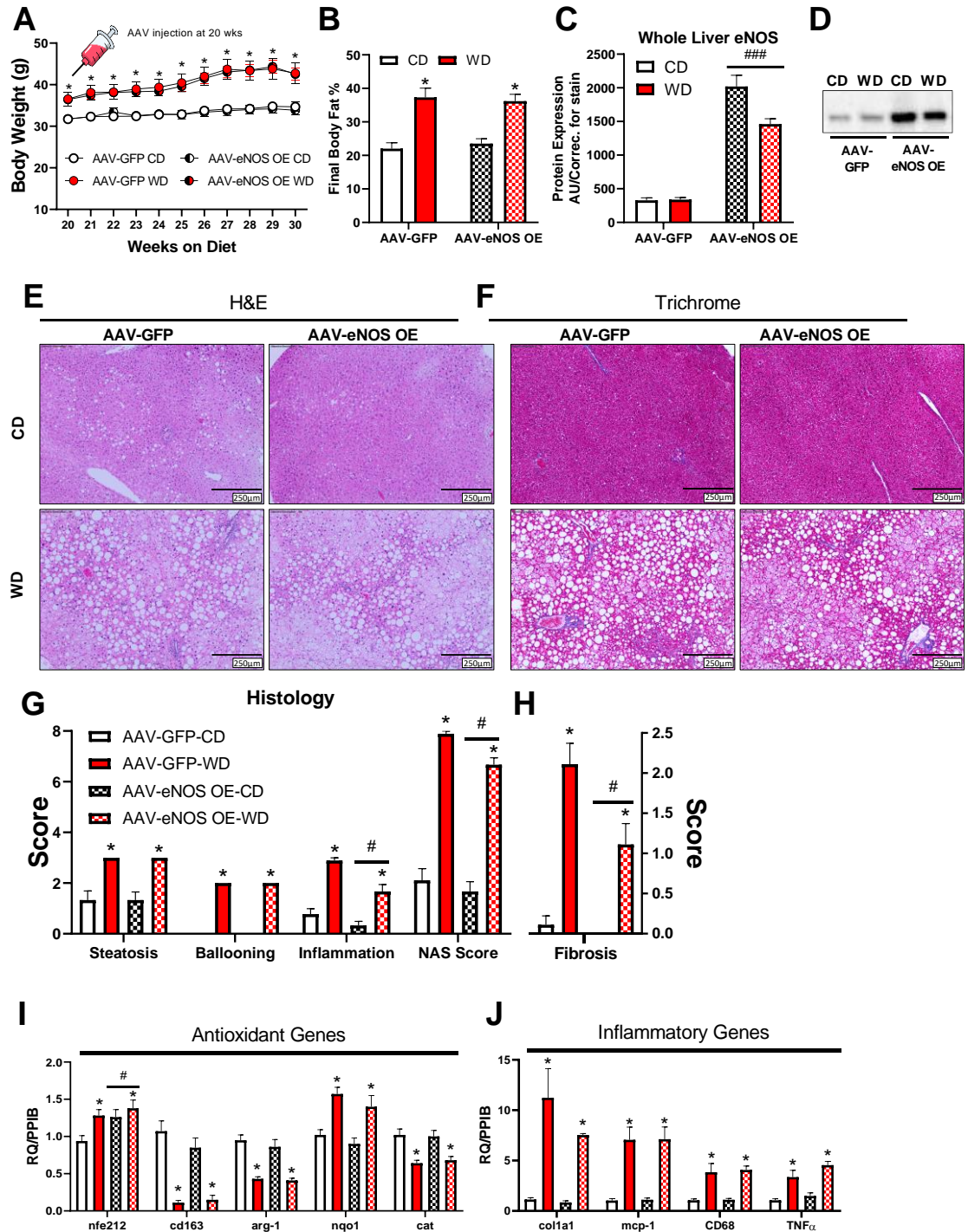
Figure 2.8: Effect of long-term hepatocellular eNOS over expression on liver histology.

A) C57BL/6J mice were randomized to receive either a CD or WD for 20 weeks, then

further randomized to receive either an AAV8-TTR-eNOS overexpression virus or

AAV8-TTR-GFP at the 20 week mark, while the body weights were recorded until 30

weeks of age (n = 10/group). B) Final body fat % (n = 10/group). C) Whole liver protein

expression of eNOS confirming the viral overexpression (n = 10/group), and D) the

representative Western blot image. E) Representative liver H&E and F) trichrome

staining from the indicated mice at 30 weeks of age. G) Histological and H) fibrosis

scoring based of H&E and trichrome images (n = 8/group). I) mRNA expression of

markers of hepatic anti-oxidant genes and J) inflammatory genes (n = 9-10/group). Data

are presented as mean ± SEM.*main effect of diet (P<0.05 vs CD), #main effect of

overexpression (P<0.05 vs AAV-GFP). CD, control diet; WD, western diet; H&E,

haemotoxylin and eosin; NAS, NAFLD activity score.
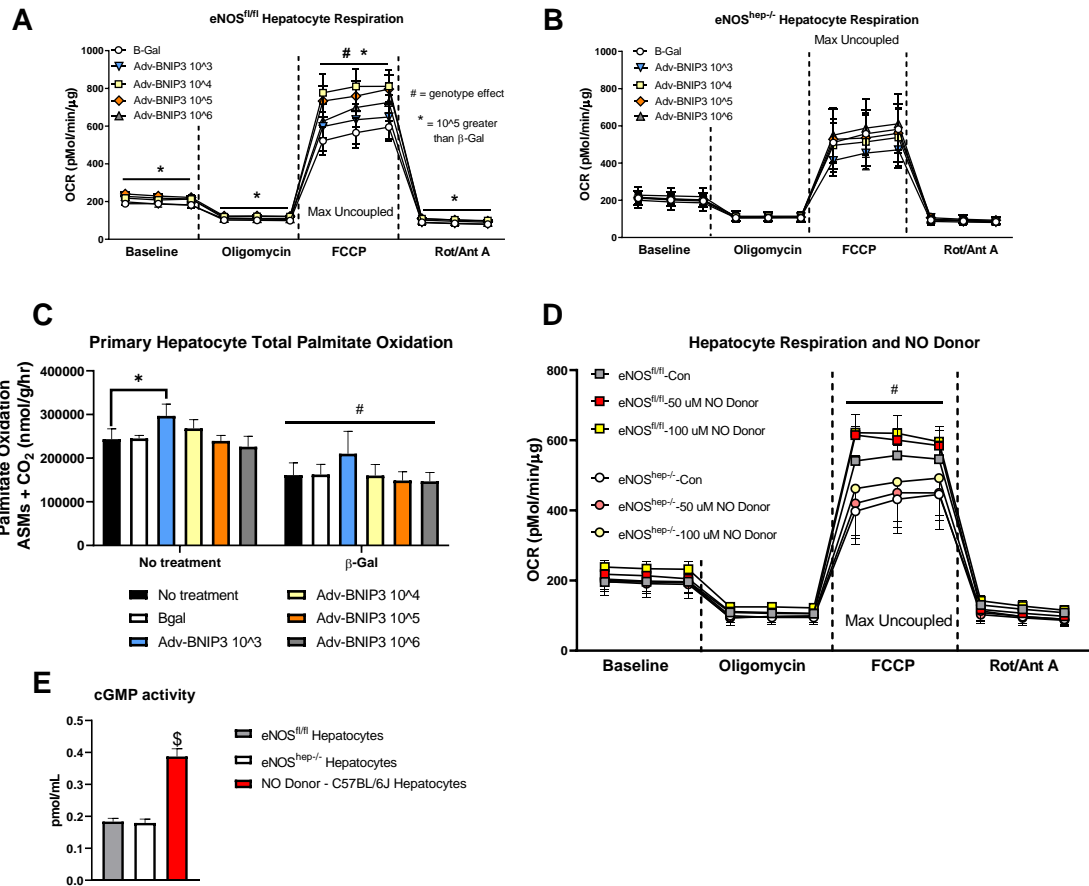
Figure 2.9: Effects of Adv BNIP3 overexpression in primary isolated hepatocytes from CD fed mice. A) Confirmation of BNIP3 overexpression. Effects of either no treatment, β-Gal, or BNIP3 overexpression (Adv BNIP3 10^3 – 10^6 PFU/ml) on B) respiration in isolated hepatocytes from eNOS^{fl/fl} mice and C) eNOS[hep-/-] mice, and D) total palmitate oxidation in hepatocytes from both eNOS^{fl/fl} and eNOS[hep-/-] mice (n = 3-6/group). E) Effect of NO donor (50-100uM) on respiration in isolated hepatocytes from eNOS^{fl/fl} mice and F) cGMP activity in hepatocytes isolated from eNOS^{fl/fl}, eNOS[hep-/-] mice, and hepatocytes from C57BL/6J mice treated with NO donors (250-1000uM).

Data are presented as mean $\pm$ SEM. *significantly different from β-Gal (P<0.05),

#significantly different from eNOS^{fl/fl} (P<0.05), $significantly different from eNOS^{fl/fl}

and eNOS[hep-/-] (P<0.05). Adv, adenoviral; CD, control diet; Con, control non treated cells.
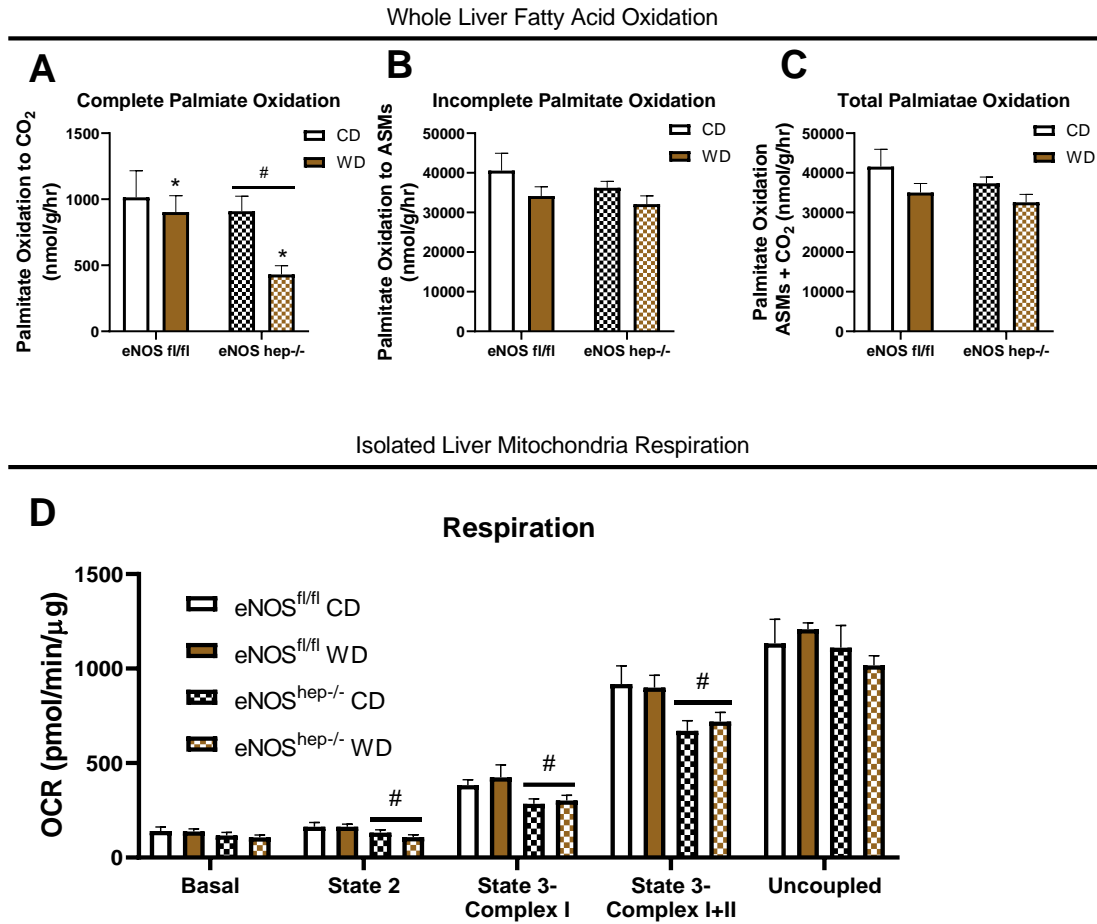
Figure 2.10: Effect of hepatocellular eNOS deficiency on hepatic mitochondrial function in female eNOS^{fl/fl} and eNOS[hep-/-] mice. A) Whole liver complete, B) incomplete, and C) total [1-^{14}C] pyruvate oxidation to CO_2 (n = 7-8/group). D) Oxygen consumption in isolated liver mitochondria (n = 7-8/group). Data are presented as mean ± SEM. *main effect of diet (P<0.05 vs CD), #main effect of genotype (P<0.05 vs eNOS^{fl/fl}).
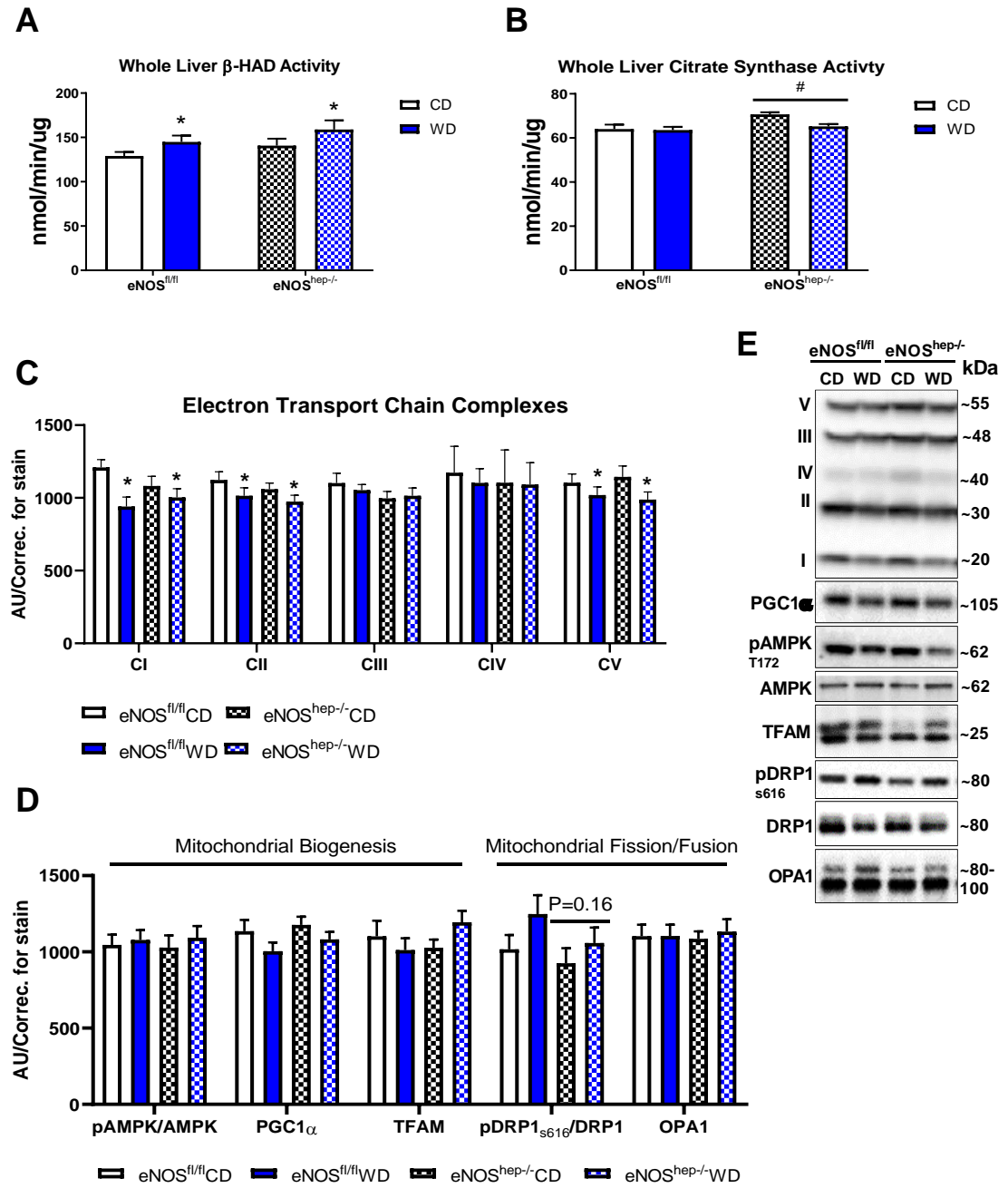
Figure 2.11: Effects of hepatocellular eNOS deficiency on markers of mitochondrial content, biogenesis, and fission/fusion. A) Whole liver β-HAD activity and B) whole liver citrate synthase activity (n = 13-17/group). Protein expression of C) electron

transport chain complexes and D) markers of mitochondrial biogenesis and

fission/fusion (n = 13-17/group), and E) their Western blot representative images. Data

are presented as mean ± SEM.*main effect of diet (P<0.05 vs CD), #main effect of

genotype (P<0.05 vs eNOS$^{fl/fl}$). CD, control diet; WD, western diet.

A

B
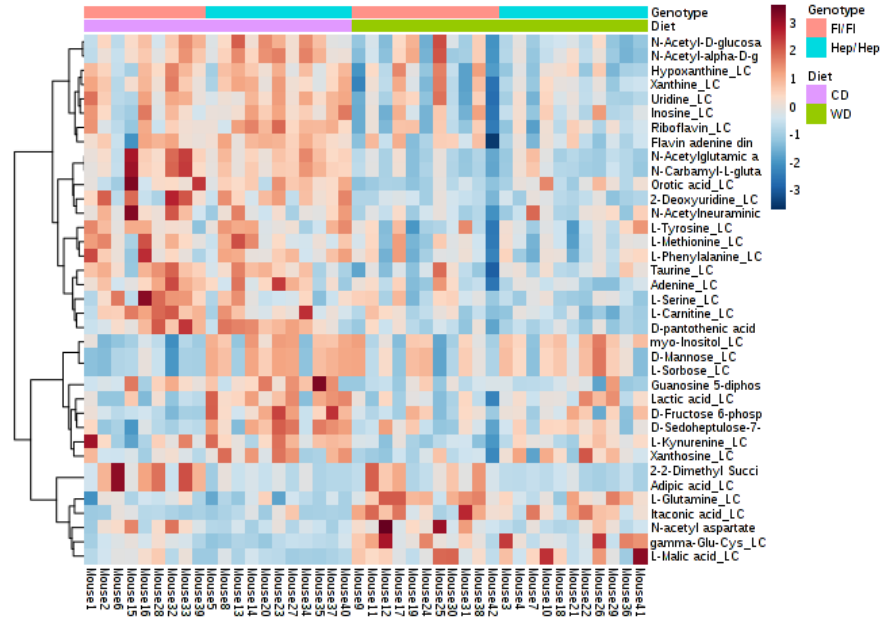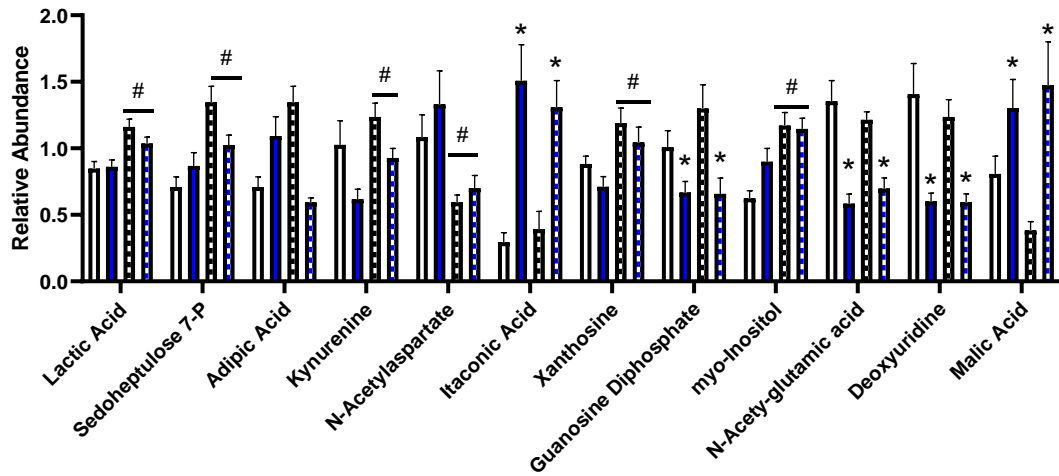
Figure 2.12: Metabolomic analysis was carried out via ion-paired liquid

chromatography/mass spectrometry (LC/MS) metabolite profiling on frozen whole liver

from eNOS$^{fl/fl}$ and eNOS$^{hep-/-}$ mice. A) Heat map of metabolite abundance segregated by genotype and diet. B) Relative abundance of metabolites. Data are presented as mean ± SEM *main effect of diet (P<0.05 vs CD), #main effect of genotype (P<0.05 vs eNOS$^{fl/fl}$). CD, control diet; WD, western diet.
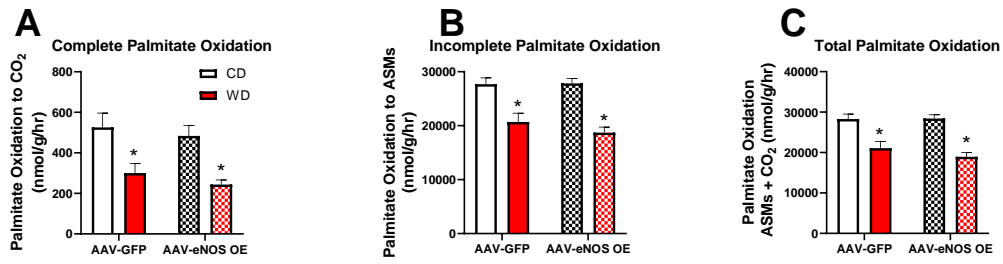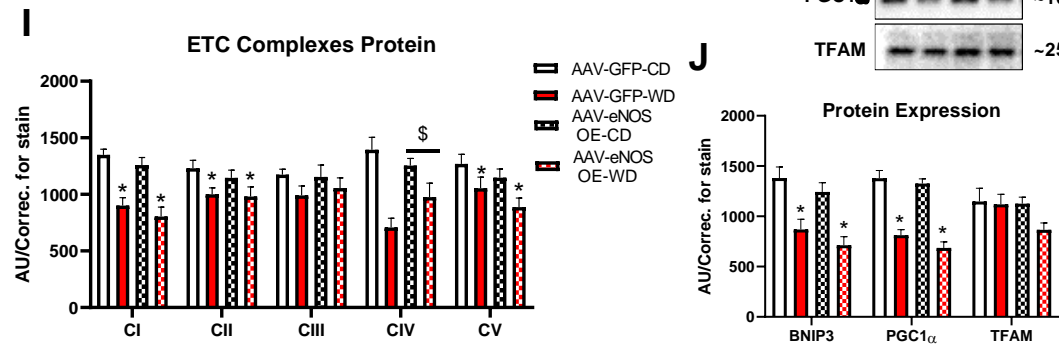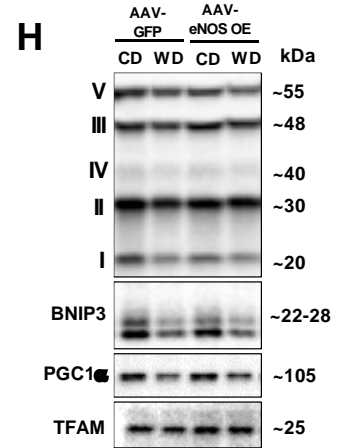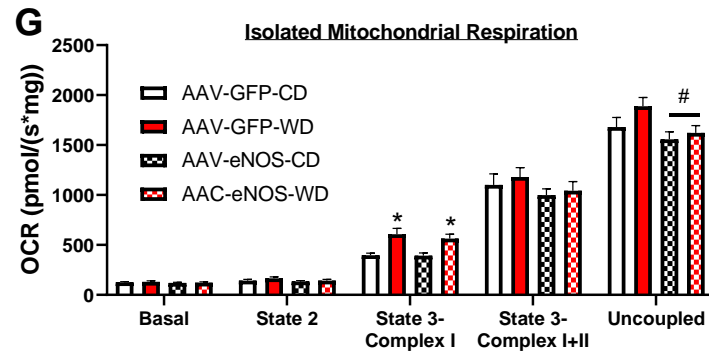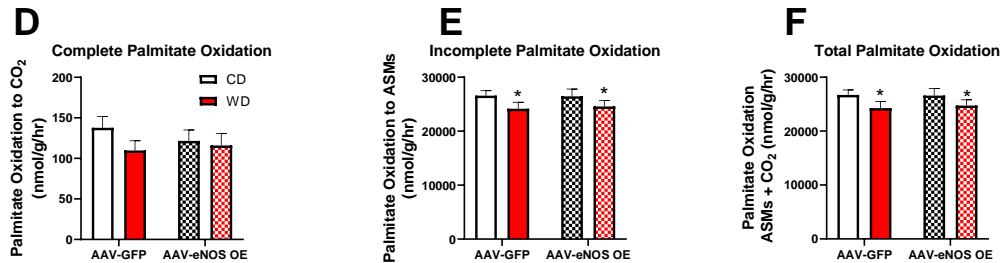
Figure 2.13: Effect of hepatocellular eNOS over expression on hepatic mitochondrial

function and content. A) Whole liver complete, B) incomplete, and C) total

[1-^{14}C] pyruvate oxidation to CO_2 (n = 10/group). D) Isolated liver mitochondria

complete, E) incomplete, and F) total [1-^{14}C] pyruvate oxidation to CO_2 (n = 10/group).

G) Oxygen consumption in isolated liver mitochondria (n = 10/group). H-I) Protein

expression of the electron transport chain (ETC) complexes and their representative

Western blot images, J) markers of mitochondrial turnover (n = 10/group). Data are

presented as mean ± SEM.*main effect of diet (P<0.05 vs CD), #main effect of

overexpression (P<0.05 vs AAV-GFP). $ significant diet and genotype interaction

(P<0.05). CD, control diet; WD, western diet.

Primers	Forward Sequence 5'-3'	Reverse Sequence 5'-3'
arg-1	GATCACATCCCAAAATTCCC	CTTCATCTTTCTTCCCACAC
αsma	AAACAGGAATACGACGAAG	CAGGAATGATTTGGAAAGGA
bnip3	ACCACAAGATACCAACAGAG	AATCTTCCTCAGACAGAGTG
cat	CTCCATCAGGTTTCTTTCTTG	CAACAGGCAAGTTTTTGATG
cd11c	TCACACCTGCAGAGATTT	TACTCAGACGGCCATGGT
cd68	GTGTCTGATCTTGCTAGGACC	GTGCTTTCTGTGGCTGTAG
col1a1	ACGCCATCAAGGTCTACTGC	ACTCGAACGGGAATCCATCG
emr1	TTTCAAATGGATCAGAAGG	CAGAAGGAAGCATAACCAAG
Il-1β	GCTACCTGTGTCTTTCCCGT	CATCTCGGAGCCTGTAGTGC
mcp-1	ACTGAAGCCAGCTCTCTCTTCCTC	TTCCTTCTTGGGGTCAGCACAGAC
nfe212	CATTCCCGAATTACAGTGTC	GGAGATCGATGAGTAAAAATGG
nqo1	CCTTTCCAGAATAAGAAGACC	AATGCTGTAAACCAGTTGAG
pdgrf	GATTGACATCCTGCCTGACC	CATGGAACTCCACCAAATCC
ppib	TGGAGATGAATCTGTAGGAC	CAAATCCTTTCTCTCCTGTAG
tgfβ1	AAGTTGGCATGGTAGCCCTT	GCCCTGGATACCAACTATTGC
tnf-α	GTGACAAGCCTGTAGCCCAC	GCAGCCTTGTCCCTTGAAGA

Table 2.1: Gene primer sequences.

CHAPTER 3 - Deletion of hepatocellular eNOS impairs exercise-induced improvements in hepatic mitochondrial function and autophagy markers

Rory P. Cunningham[1,3], Mary P. Moore[1,3], Ryan J. Dashek[3,5], Grace M. Meers[1,3], Vivien Jepkemoi[1], Luigi Boccardi[1], Takamune Takahashi[6], Vicki J. Vieria-Potter[3], Jill A. Kanaley[3], Frank W. Booth[3,4], R. Scott Rector[1,2,3]

[1]Research Service, Harry S Truman Memorial Veterans Medical Center, Columbia, Missouri 65212, USA; [2]Departments of Medicine-Division of Gastroenterology and Hepatology, [3]Nutrition and Exercise Physiology, [4]Department of Biomedical Sciences, [5]Department of Veterinary Pathobiology, University of Missouri, Columbia, MO 65211, USA; [6]Division of Nephrology and Hypertension, Vanderbilt University School of Medicine, Nashville, Tennessee 37232, USA.

Address of Correspondence:

R. Scott Rector, PhD
Research Health Scientist and Associate Professor
Harry S Truman Memorial VA Hospital
Departments of Medicine - Division of Gastroenterology
and Hepatology and Nutrition and Exercise Physiology
University of Missouri-Columbia
Columbia, MO 65212
Tel: 573-884-0979
Fax: 573-884-4595
Email: rectors@health.missouri.edu

ABSTRACT

Exercise has been shown to improve hepatic mitochondrial function while attenuating NAFLD, yet the mechanisms are unresolved. Endothelial nitric oxide synthase (eNOS) is a potential mediator of these hepatic mitochondrial adaptations due to its role in exercise-induced mitochondrial improvements in other tissues. Here, male and female hepatocyte-specific eNOS knockout (eNOS$^{hep-/-}$) and intact hepatic eNOS (eNOS$^{fl/fl}$) mice performed voluntary wheel running exercise (EX) or remained in sedentary cage conditions for 10 weeks. EX resolved the exacerbated hepatic steatosis in eNOS$^{hep-/-}$ mice (P<0.05), driven by the males. In addition, elevated H_2O_2 emission (~50% higher in eNOS$^{hep-/-}$ vs eNOS$^{fl/fl}$ mice, P<0.05), was completely ablated with EX. Interestingly, EX increased [1-^{14}C] palmitate oxidation in male eNOS$^{fl/fl}$ (P<0.05), but this response was blunted in the eNOS$^{hep-/-}$ male mice. eNOS$^{hep-/-}$ mice also had lower markers of the energy sensors pAMPK/AMPK and mTOR and p-mTOR, and the autophagy initiators ULK1 and pULK1 compared to eNOS$^{fl/fl}$ mice (P<0.05). While mitochondrial respiration and markers of mitochondrial content were not increased with EX, female mice showed elevated ETC protein content and markers of mitochondrial biogenesis (TFAM, *pgc1α*) (P<0.05). Collectively, we demonstrate for the first time the requirement of hepatocellular eNOS for the EX-induced elevation in hepatic fatty acid oxidation in male mice. Deletion of hepatocellular eNOS also impairs the energy sensing ability of the cell and inhibits the activation of the autophagy initiating factor ULK1. Collectively, these data uncover the important and novel role of hepatocellular eNOS in exercise-induced hepatic mitochondrial adaptations, and help to further the understanding behind the mechanisms of NAFLD development.

INTRODUCTION

Nonalcoholic fatty liver disease (NAFLD) is a range of liver disease spanning hepatic

lipid accumulation (steatosis), steatohepatitis (NASH) and fibrosis, to its end stage of

cirrhosis and hepatocellular carcinoma. NAFLD is tightly linked with insulin resistance

and type 2 diabetes and is considered an independent risk factor for cardiovascular, liver-

related, and all-cause mortality (9, 10). Hepatic mitochondrial dysfunction is strongly

associated with NAFLD progression, including increased reactive oxygen species and

decreased oxidative capacity (18, 20, 24). With no FDA-approved pharmacological

treatments, diet and exercise remain the cornerstone of treatment for NAFLD. Studies

from our lab have consistently demonstrated that exercise is a powerful tool for reducing

hepatic steatosis and NAFLD, while improving hepatic mitochondrial function (29, 30,

33, 34), but the precise mechanisms causing mitochondrial dysfunction as well as

exercise-induced improvements in mitochondrial function in NAFLD remain unresolved.

Given its well established role in regulating mitochondrial biogenesis (49-52), endothelial

nitric oxide synthase (eNOS) may be playing a significant role in hepatic mitochondrial

adaptations to exercise. Whole body eNOS null mice display blunted exercised-induced

improvements in mitochondrial biogenesis and content in both adipose and cardiac tissue

(53, 54). These data strongly indicate the requirement for eNOS in exercise-induced

mitochondrial adaptations. Unfortunately, whole body eNOS null models do not allow us

to determine the specific contributions of hepatic eNOS to exercise-induced

mitochondrial benefits.

Our group has demonstrated via multiple approaches a beneficial role for eNOS in NAFLD prevention. Reduced hepatic eNOS activity is linked with NAFLD progression to NASH, a reduction that is prevented with chronic voluntary wheel running exercise (47). Moreover, systemic NOS inhibition causes hepatic mitochondrial dysfunction and accelerates NAFLD development (46), while hepatocellular eNOS deficiency impairs hepatic mitochondrial biogenesis and turnover (1). Moreover, our group has recently generated a hepatocyte-specific eNOS knockout mouse (eNOS[hep-/-]) that exhibits exacerbated NAFLD development and reduced hepatic mitochondrial function. Importantly, it is unknown if exercise can rescue this phenotype.

Exercise is also a potent inducer of autophagy – the ability to clear dysfunctional proteins and mitochondria (mitophagy) (35, 106). Exercise-induced autophagy is mediated primarily through AMP-activated protein kinase (AMPK) activation of Unc-51 Like Autophagy Activating Kinase 1 (ULK1) (62), while this is also regulated by the inhibitory effects of mammalian target of rapamycin (61). Indeed, fully functioning autophagy/mitophagy is required for beneficial exercise-induced adaptations in skeletal muscle (107-109), although its role in exercise adaptations in the liver is relatively unknown. While the role of eNOS in mitochondrial biogenesis with exercise is clear, its role in exercise-induced autophagy/mitophagy is relatively unknown, and will be examined in the current study.

Our group has demonstrated that female rodents are not only protected from hepatic steatosis compared to male mice, but also displayed elevated markers of hepatic

88

mitochondrial biogenesis and mitophagy (66, 67). Additionally, female mice possessed elevated hepatic mitochondrial content, respiratory capacity, and lower reactive oxygen species emission compared to male mice, regardless of physical activity status (68-70). The mechanisms conferring benefit to hepatic mitochondria in female rodents has yet to be resolved.

This study examined whether voluntary wheel running exercise (EX) could rescue the exacerbated NAFLD phenotype and reduced hepatic mitochondrial function observed in eNOS[hep-/-] mice. Further, the molecular signals involved in hepatic mitochondrial improvements with exercise, with and without hepatocellular eNOS were examined. Both male and female mice were utilized to determine if sex plays a role in hepatic adaptations to exercise on the backdrop of hepatic eNOS deficiency. Exercising these mice will circumvent the confounding issue with whole body eNOS null animals allowing us to determine if hepatocellular eNOS *per se* is required for the exercise-induced improvements in hepatic mitochondrial function. Based on the requirement of eNOS for exercise-induced mitochondrial adaptations in other tissues, it was hypothesized that eNOS[hep-/-] mice would demonstrate attenuated exercise-induced improvements in hepatic mitochondrial function, regardless of sex.

RESEARCH DESIGN AND METHODS

Animal protocol

Hepatocyte-specific eNOS knockout (KO) (eNOS[hep-/-]) mice have been generated by crossing homozygous eNOS floxed (eNOS^{fl/fl}) mice on a C57BL/6J background (48) with

albumin-Cre recombinase transgenic mice (Jackson Labs no. 002684; Bar Harbor, ME). At 10 weeks of age, male and female eNOS$^{fl/fl}$ and eNOS$^{hep-/-}$ mice were randomized into either sedentary (SED) or voluntary wheel running exercise (EX) conditions. SED mice were group housed and separated by sex with no access to running wheels, while EX mice were individually housed and provided a running wheel. This resulted in a total of 8 groups (n = 10-14/group): Male eNOS$^{fl/fl}$ SED, Male eNOS$^{fl/fl}$ EX, Male eNOS$^{hep-/-}$ SED, Male eNOS$^{hep-/-}$ EX, Female eNOS$^{fl/fl}$ SED, Female eNOS$^{fl/fl}$ EX, Female eNOS$^{hep-/-}$ SED, Female eNOS$^{hep-/-}$ EX. All mice received a semipurified control diet (CON; no. D12110704; Research Diets, New Brunswick, NJ) containing 10% kcal fat, 70% kcal carbohydrate (3.5% kcal sucrose), and 20% kcal protein, and kept in these conditions for 10 weeks. Total distance ran and time spent on the running wheel was measured by daily monitoring of the number of running wheel revolutions continuously throughout the intervention using a Sigma Sport BC 800 bicycle computer (Cherry Creek Cyclery, Foster Falls, VA). The voluntary running wheel approach represents a less stressful model of increasing physical activity versus forced treadmill exercise training.

For all animal experiments, room temperature was kept constant at 21-22°C with a 12:12 light/dark cycle. Food intake and body weight of the animals was recorded weekly, and body composition (4in1-1100 Analyzer; EchoMRI, Houston, TX) measured monthly. Food consumption was measured by taking the difference in grams of food given and grams of food remaining 7 days later and multiplying total grams consumed by energy content per gram of the diet and dividing by 7 to give kilocalories per day. Running wheels were locked 48 hr prior to terminal procedure to avoid the confounding effects of

acute exercise on hepatic physiology. On the day of euthanasia, mice were fasted overnight for 12 hr (2000-0800), before being anesthetized with pentobarbital sodium (80-100 mg/kg). Blood was collected via cardiac puncture, and the animals were euthanized via removal of the heart. Livers were quickly excised from anesthetized mice and prepared for mitochondrial isolation, nuclear extraction, homogenization for palmitate oxidation, and fixed in 10% formalin or snap-frozen in liquid nitrogen for later processing as described in detail in the following sections. All animal protocols were approved by the University of Missouri and the Harry S Truman Animal Care and Use Committees.

Mitochondrial isolation

Hepatic mitochondria were isolated as previously described (30, 34). Briefly, roughly 100 mg of fresh liver tissue was minced and homogenized using a Teflon pestle in mitochondrial isolation buffer (220 mM mannitol, 70 mM sucrose, 10 mM Tris base, 1 mM EDTA, pH 7.4). The sample was centrifuged at 1,500 g for 10 min. The supernatant was retained and underwent a series of three centrifugations (6,000–8,000 g), while the resultant pellet was resuspended with gentle glass-on-glass homogenizations. Sample was maintained at 4°C throughout the isolation protocol. The final pellet was suspended in mitochondrial incubation buffer (110 mM sucrose, 60 mM KMES, 20 mM glucose, 20 mM HEPES, 10 mM KH_2PO_4, 3 mM $MgCl_2$, 0.5 mM EGTA, pH 7.4), and rested for 30 min before being used for determining protein content via BCA, mitochondrial respiration, [1-^{14}C] palmitate oxidation, or stored at −80°C for Western blot analysis.

Mitochondrial respiration

In the both the eNOS$^{fl/fl}$ vs eNOS$^{hep-/-}$ and eNOS overexpression studies, hepatic

mitochondrial respiration and H$_2$O$_2$ production was assessed in isolated hepatic

mitochondria using high-resolution respirometry (Oroboros Oxygraph-2k; Oroboros

Instruments; Innsbruck, Austria), with all values corrected to total mitochondrial protein

loaded. Respiration and H$_2$O$_2$ production, measured via oxygen consumption and

Amplex^{TM} UltraRed reagent, respectively (#A36006, Thermo Fisher Scientific), was

assessed by the addition of isolated mitochondria and various substrates to the Oroboros

as described previously (1, 30, 33, 34). For respiration, isolated mitochondria (100-150

μg mitochondrial protein) were initially placed in respiration chambers in respiration

media (MiR05; sucrose, 100 mM; K-lactobionate, 60 mM; EGTA, 0.5 mM; MgCl$_2$, 3

mM; taurine, 20 mM; KH$_2$PO$_4$, 10 mM; HEPES, 20 mM; adjusted to pH 7.1 with KOH at

37C; and 1 g/L fatty acid free BSA) for assessment of baseline respiration (Basal).

Oxygen flux was measured by addition of glutamate (5mM) and malate (2mM) to the

chambers in the absence of ADP for assessment of State 2 respiration. Once respiration

had stabilized, serial additions of ADP were added (125 μM total) to stimulate and

quantify oxidative phosphorylation (OXPHOS) with electron flux through complex I

(State 3 – Complex I). Complex I and II respiration were assessed by the addition of 7.5

mM of succinate to the chamber (State 3 – Complex I+II). Following this, maximal

uncoupled respiration was achieved by serial additions of 0.125μM FCCP (Carbonyl

cyanide 4-(trifluoromethoxy) phenylhydrazone) (Uncoupled). Increases in maximal

uncoupled respiration >20% following the addition of reduced cytochrome *c* (2 μM) was

used for mitochondrial preparation quality control and samples were removed from

analyses. For H_2O_2 production, Amplex^{TM} UltraRed reagent (4µl) (#A36006, Thermo

Fisher Scientific) and horseradish peroxide (HRP) (8µl) were added to the chamber

before the addition of 100-150µg of isolated mitochondrial protein. In the presence of the

HRP, the Amplex^{TM} UltraRed reagent reacts with H_2O_2 to produce a red-fluorescent

product which can be quantified and used as a surrogate marker for H_2O_2 emission. After

baseline respiration is stabilized, 20µM of palmitoyl-CoA was added to the chamber,

followed by serial additions of 10µM of palmitoyl-CoA until a maximal response was

achieved. For H_2O_2 emission, males and females were combined due to a lower sample

size and not enough statistical power to detect sex differences. Each substrate condition

was tested in a technical replicate from a single mitochondrial preparation per mouse.

Hepatic fatty acid oxidation

Using whole liver homogenate, hepatic fatty acid oxidation capacity was determined by

the addition of [1-^{14}C] palmitate, as previously described (34). Briefly, the amount of

$^{14}CO_2$ produced in 1 hr was trapped in a sodium hydroxide solution. Perchloric acid was

then be added to stop the reaction and incubation continued for another hr. $^{14}CO_2$ (a

measure of complete oxidation), and the 1-^{14}C containing acid-soluble metabolites (a

measure of incomplete oxidation) was measured with a liquid scintillation counter.

Western blots

Western blot analyses were completed in whole liver homogenate, isolated hepatic

mitochondria, and hepatocyte lysates. In preparation, sample protein concentrations were

determined by Pierce BCA protein assay (no. 23225, ThermoFisher Scientific). Primary

antibodies used are as follows: oxidative phosphorylation (OXPHOS) mitochondrial

profile (ab110413; Abcam, Cambridge, MA), peroxisome proliferator-activated receptor

gamma coactivator 1-α (PGC1α, no. WH0010891M3, Millipore-Sigma, Burlington,

MA), mitochondrial transcription factor A (TFAM; Santa Cruz Biotechnology, Dallas,

TX), BNIP3 (no. 3769; Cell Signaling Technology, Danvers, MA), 1A/1B light chain 3B

(LC3; no. 4108S, Cell Signaling), mammalian target of rapamycin (mTOR, no. 2972S;

Cell Signaling Technology), p-mTOR Ser2488 (no. 2971S; Cell Signaling technology),

Unc-51 Like Autophagy Activating Kinase 1 (D8H5) (ULK1, no. 8054S; Cell Signaling

Technology), pULK1 Ser555 (D1H4) (no. 5869S, Cell Signaling Technology), Parkin

(no. 4211; Cell Signaling Technology), AMP-activated protein kinase (AMPK, no.

2532S; Cell Signaling Technology), pAMPK (Thr172) (no. 2351; Cell Signaling

Technology), Primary antibodies were used at 1:1,000 dilution, and secondary antibody

at 1:5,000 dilution. Blots were analyzed via densometric analysis (Image Laboratory Beta

3, Bio-Rad Laboratories, Hercules, CA). Total protein was assessed with Amido black

(0.1%, Sigma) to control for differences in protein loading and transfer as previously

described (34, 67).

Quantitative real-time PCR

Initially, RNA was extracted from frozen liver tissue or hepatocyte cultures with a

commercially available kit (no. 74104, Qiagen), and a cDNA library was synthesized

(Promega). A Nanodrop spectrometer was used to assess purity and quality of RNA and

cDNA (model ND-1000, NanoDrop, Thermo Scientific, Wilmington, DE). Quantitative

real-time PCR (qPCR) was conducted using Sybr Green reagents (172–5121, BioRad)

and primer pairs listed in **Table 3.1** (Sigma). PCR product melt curves were used to

assess primer specificity. Data are represented relative to *18S* using the $2^{-\Delta\Delta CT}$ method.

Liver histology

To histologically determine hepatic steatosis development, the fresh liver placed in 10% formalin for 24 hr was then imbedded in paraffin, sectioned and stained with haematoxylin and eosin (H&E) by IDEXX RADIL (Columbia, MO). NAFLD activity score (NAS) – the aggregate of hepatic steatosis, ballooning, and inflammation histology scores (3) of liver sections were conducted by a trained and blinded observer. NAS refers to the aggregate of hepatic steatosis, ballooning, and inflammation histology scores, to give an overall indication of histological NAFLD development.

Enzymatic and serum assays

Further examination of mitochondrial content was assessed in whole liver homogenate with enzymatic assays. Citrate synthase activity, a well-established surrogate marker of mitochondrial content, was measured as previously described in whole liver homogenate (34).

Statistical analysis

Statistical analyses were completed in SPSS (IBM SPSS Statistics for Windows, Version 24.0. Armonk, NY) with an alpha level of $P<0.05$ used to determine statistical significance of all comparisons. Comparison across all three variables (sex, EX, and genotype) were analyzed via three-way (3×2) ANOVA. When comparing just two variables, i.e. removing sex as a variable for males and females combined, or EX when comparing within EX groups only, a two-way (2x2) ANOVA was used. A Fisher's least significant difference post hoc test was used when a three-way or two-way ANOVA

detected a significant interaction term (P<0.05). Figures were made using GraphPad

Prism 8.3. All data are presented as means ± standard error SEM.

RESULTS

Animal Characteristics

It is important to determine that the effects of hepatocellular eNOS deficiency on liver-

specific outcomes are not driven simply by changes in body composition. Male mice

weighed significantly more than female mice (~20%) and had higher RP fat mass, and

significantly higher food intake than female mice regardless of genotype (**Table 3.2**).

Interestingly, EX did not reduce body weight, although this is likely due to the increase in

the average weekly food intake with EX (**Table 3.2**). As expected, EX increased heart to

body weight ratio, as well as decreasing final body fat, delta body fat change, and

retroperitoneal (RP) fat mass (**Table 3.2**). Whole body eNOS null mice have limited

exercise capacity for treadmill training (110). Importantly, both eNOS$^{hep-/-}$ and eNOS$^{fl/fl}$

ran the same distance, with no effect of sex (**Table 3.2**). Hence, our hepatocyte-specific

eNOS null mice allow us to tease out the role of hepatocellular eNOS in hepatic

mitochondrial adaptations to wheel running exercise.

Liver histology

Similar to our previous results, eNOS$^{hep-/-}$ mice displayed elevated histological hepatic

inflammation, and NAS score compared to eNOS$^{fl/fl}$ mice, regardless of sex or EX (**Fig

3.1A-B**). As we have published previously (66, 67), male mice had elevated hepatic

steatosis compared to female mice regardless of other conditions, with no effect of sex on

inflammation and NAS (**Fig. 3.1A-B**). Histological ballooning score was zero for all

groups, likely due to the low-fat diet and relatively young age of the animals (**Fig. 3.1B**).

EX was able to reduce hepatic steatosis in all groups, as well as reducing total NAS,

regardless of sex or genotype (**Fig. 3.1A-B**). The EX-induced reduction in NAS was

driven by the males (**Fig. 3.1B**). This is likely due to the low NAS score in all female

groups, possibly due to the increased gene expression of antioxidant genes (*cat, gpx1,*

nqo1, nfe212) compared to males (**Table 3.3**).

Mitochondrial function

Our group have previously shown EX to increase whole liver fatty acid oxidation (30,

34). As expected, EX significantly increased complete, incomplete, and total palmitate

oxidation in eNOS$^{fl/fl}$ males (**Fig. 3.2A-C**). This EX-induced increase in fatty acid

oxidation was completely absent in eNOS$^{hep-/-}$ males, who had significantly reduced

complete, incomplete, and total palmitate oxidation compared to eNOS$^{fl/fl}$ regardless of

EX (**Fig. 3.2A-C**). EX increased complete palmitate oxidation in females (genotype

effect driven by males), but EX had no effect on incomplete or total palmitate oxidation

in females, regardless of genotype (**Fig. 3.2A-C**). Further, females had lower complete

and total palmitate oxidation compared to males, regardless of EX or genotype (**Fig.

3.2A, C**).

In isolated hepatic mitochondria, eNOS$^{hep-/-}$ mice had lower state 3 – complex I+II

respiration compared to eNOS$^{fl/fl}$ mice (**Fig. 3.3D**). Notably, eNOS$^{hep-/-}$ mice had a ~50%

increase in H_2O_2 emission compared to eNOS$^{fl/fl}$ mice, and this was completely ablated

with EX (**Fig. 3.3F**). There was a sex by genotype interaction for all respiration states

apart from state 3 – complex I+II, with female eNOS$^{hep-/-}$ mice showing decreases respiration compared to eNOS$^{fl/fl}$ mice, which was not observed in male mice (**Fig. 3.3A-C, D**). Interestingly, EX slightly reduced basal, state 3 – complex I, and maximal uncoupled respiration, regardless of genotype or sex (**Fig. 3.3A, C, E**).

Mitochondrial content

As eNOS is a known regulator of mitochondrial content (50-52), we examined whether the observed reductions in mitochondrial function in hepatocellular eNOS deficient mice was explained by reduced hepatic mitochondrial content. In concurrence with our previous reports, there no effect of genotype on protein expression of electron transport chain (ETC) complexes (**Fig. 3.4A-F**). EX increased protein content of CI, while decreasing CIV (**Fig, 3.4 A, D**). Interestingly, females displayed elevated protein content of all complexes apart from CIV compared to males, regardless of EX or genotype (**Fig. 3.4A-F**). This is supported by previous studies, where females have higher markers of mitochondrial content compared to their male counterparts (68, 69). Here, there was no effect of EX, sex, or genotype on whole liver citrate synthase activity, a classical marker of mitochondrial mass (**Fig. 3.4G**).

Markers of mitochondrial biogenesis

Whole body eNOS null mice show a blunted increase in exercise-induced markers of mitochondrial biogenesis, including PGC1α and TFAM (53, 54). Here, there was no effect of genotype on protein expression of PGC1α or TFAM (**Fig. 3.5B-C; Table 3.3**). There was a sex by genotype interaction for PGC1α protein, such that PGC1 was slightly

decreased in eNOS$^{hep-/-}$ vs eNOS$^{fl/fl}$ males, but this reduction was not observed in

eNOS$^{hep-/-}$ females (**Fig. 3.5B**). EX increased *pgc1α* and *tfam* mRNA expression in all

groups, but not protein content (**Fig. 3.5B, C; Table 3.3**). Interestingly, eNOS$^{hep-/-}$ mice

showed reduced activation of AMPK (pAMPK to total AMPK ratio), regardless of EX or

sex (**Fig. 3.5A**), suggesting that hepatocytes from these mice have an impaired energy

sensing ability compared to eNOS$^{fl/fl}$ mice. Similar to our previous work (66, 67), females

exhibited marked elevation in TFAM protein compared to males, regardless of EX or

genotype (**Fig. 3.5C**). Further, females have increased mRNA expression of

mitochondrial biogenesis markers (*pgc1α, tfam,* and *sirt1*), compared to males (**Table

3.3**).

Markers of mitochondrial turnover

Our group has previously demonstrated that hepatocellular eNOS is required for the

maintenance of hepatic mitophagy (1). Further, AMPK and mTOR activity are well-

established regulators of the autophagy initiator – ULK1 (59, 61), while AMPK is

required for the exercise-induced activation of ULK1 (62). Given these previous reports,

coupled with the reduction in AMPK activity in eNOS$^{hep-/-}$ mice, we suspected that

exercise-induced hepatic mitophagy might be altered in eNOS$^{hep-/-}$ mice. Both total and

phosphorylated mTOR were reduced in eNOS$^{hep-/-}$ mice compared to eNOS$^{fl/fl}$ mice,

regardless of EX or sex (**Fig. 3.6A-B**), with no effect of any variable on p-mTOR/mTOR

ratio (data not shown). Additionally, both total and phosphorylated ULK1 were

significantly reduced in eNOS$^{hep-/-}$ mice, and the robust EX-induced elevation in these

markers as seen in male eNOS$^{fl/fl}$ mice was completely absent in eNOS$^{hep-/-}$ mice (**Fig.**

3.6C-D). Surprisingly, this reduction in the autophagy initiator ULK1 did not affect the selected downstream markers of autophagy/mitophagy – whole liver Parkin, BNIP3, and mitochondrial LC3-II were not affected by genotype (**Fig. 3.6E-G**). Similar to what we have previously reported (66), female mice exhibit increased markers of autophagy/mitophagy compared to males (elevated Parkin and BNIP3 protein expression, **Fig. 3.6E-F**). Although females also showed a higher pULK/ULK1 ratio compared to males (data not shown), when examining the individual proteins, female mice had markedly lower phosphorylated and total ULK1 compared to males (**Fig. 3.6C-D**), indicating a lower total abundance of ULK1 in female livers. The lower pULK1 content may be explained by the increase in *mtor* gene expression in females, a potent inhibitor of ULK1 (61, 62), but there was no effect of sex on mTOR and p-mTOR protein content or p-mTOR/mTOR (**Fig. 3.6A-B**), suggesting sex differences in ULK1 may not be regulated by mTOR activity.

DISCUSSION

There is an established role for eNOS in the regulation of mitochondrial biogenesis and in exercise-induced adaptations in heart, skeletal muscle and adipose tissue (49-54). Here, we demonstrate for the first time that while wheel running exercise attenuated hepatic steatosis and ROS emission regardless of genotype, exercise-induced increases in hepatic fatty acid oxidation in eNOS$^{fl/fl}$ mice were completely absent in eNOS$^{hep-/-}$ males. Coupling this with reduced AMPK activation in eNOS$^{hep-/-}$ mice resulted in a blunted induction of the autophagy initiator ULK1 with exercise. Interestingly, while female mice displayed elevated markers of mitochondrial biogenesis and altered autophagy markers

compared to male mice, they demonstrated little response to exercise. These novel data collectively suggest a requirement of hepatocellular eNOS for the full beneficial effects of exercise on hepatic mitochondrial function and turnover.

Whole body eNOS knockout mice have increased hepatic steatosis and inflammation compared to their wild-type counterparts (45), while we have shown mice lacking eNOS are more susceptible to western diet-induced NASH (1). Additionally, we previously reported that hepatocellular eNOS deficient eNOS[hep -/-] mice displayed exacerbated histological NAFLD compared to eNOS^{fl/fl} mice. Our current findings are in support of this, as eNOS[hep-/-] mice have greater histological inflammation and overall NAS score compared to eNOS^{fl/fl} mice (**Fig. 3.1**). However, this appears to be driven by the males, with female mice showing similar histological scoring across genotypes, and not surprising lower steatosis compared to males. This is consistent with previous findings, as female rodents are protected against hepatic steatosis and NAFLD development versus their male counterparts (66-70). Importantly, EX resolved inflammation and NAS score in eNOS[hep-/-] mice, suggesting hepatocellular eNOS is dispensable for EX-induced histological improvements in the liver, at least on a low-fat diet.

We have shown previously that exercise robustly increases hepatic mitochondrial fatty acid oxidation (29, 30, 33, 34). Similarly, this study shows that EX increased fatty acid oxidation in eNOS^{fl/fl} mice, but this increase was completely ablated in male eNOS[hep-/-] mice (**Fig. 3.2**). This is in accordance with previous studies, where whole body eNOS null mice have a blunted response to swim training-induced elevations in mitochondrial

101

biogenesis and content in cardiac and adipose tissue (53, 54). Surprisingly, females had lower complete and total fatty acid oxidation compared to males and did not respond to EX. This may be due to increased mitochondrial coupling control in females, as shown previously (68, 69) where females utilize fatty acids more efficiently, requiring less oxidation. The lack of response to EX in females is supported by previous work, unlike males, who required EX to achieve the elevated mitochondrial function observed in females (69). This novel data indicates the requirement of hepatocellular eNOS *per se*, for the induction of fatty acid oxidation with EX, at least in male mice. Despite this blunted induction of fatty acid oxidation with EX, eNOS[hep-/-] mice still reduced hepatic steatosis in response to EX. While this might suggest that increasing fatty acid oxidation is not essential to resolve hepatic steatosis, it is important to note that all mice had relatively low steatosis given their low-fat diet and young age, and increased fatty acid oxidation may be required for larger, absolute reductions in histological steatosis. Further, it is also possible that peroxisomal (non-mitochondrial) fatty acid oxidation increased with EX, or other alterations in pathways related to hepatic lipid accumulation – *de novo* lipogenesis or triglyceride exporters. These pathways should be examined for potential exercise-induced upregulation in response to hepatocellular eNOS deficiency.

Our group and others have shown mitochondrial oxidative capacity to increase with EX in order to cope with the extra demands placed on the mitochondria (33, 68, 69). In the current study, wheel running EX may not have elicited enough perturbation on the system to increase mitochondrial respiratory capacity or content (**Fig. 3.2, 3.3**), given the young age of the animals and low-fat control diet feeding. Another possibility is the slightly

lower average daily running distance in eNOS$^{fl/fl}$ and $^{hep-/-}$ mice compared to other studies (~6 km/day vs ~9-10 km/day (69)). Whether hepatocellular eNOS is required for the induction of mitochondrial respiration and content with exercise of different modalities, volume or intensities will require future studies.

A hallmark of NAFLD/NASH progression is the increase in ROS emission and oxidative stress. Previous reports have shown that EX attenuates HFD-induced elevated H_2O_2 emission (68, 69). As seen here and previously stated by our group, hepatic mitochondrial H_2O_2 emission in eNOS$^{hep-/-}$ mice was ~50% higher compared to eNOS$^{fl/fl}$ mice (**Fig. 3.3**). This effect was completely abrogated with EX, accompanied by inductions of a number of genes involved in mitigating H_2O_2 production (*arg1, cat, gpx1*); indicating eNOS is not required for the EX-induced reduction of ROS emission or anti-oxidant defense in the liver. Previous studies found females to possess lower H_2O_2 emission than males, and lends support to the notion of higher quality mitochondria in females (68-70). Unfortunately, our samples size was insufficient for statistical power to separate H_2O_2 production by sex; but, the genes associated with attenuating H_2O_2 (*arg1, cat, gpx1*), were significantly elevated in females compared to males (**Table 3.3**).

Mitochondrial quality is built upon the tightly linked processes of biogenesis and mitochondrial autophagy, termed mitophagy. There is well-established evidence for exercise as a potent inducer of autophagy and mitophagy in skeletal muscle, with initial reports indicating this also occurs in the liver (35, 106, 108). Indeed, fully functional autophagy/mitophagy is required for exercise training-induced improvements in skeletal

muscle mitochondrial adaptations and physical performance (107, 109) . The energy

sensing abilities of the cell are crucial in the autophagy initiation with exercise; regulated

primarily by the interplay between the activating and inhibitory effects of AMPK and

mTOR on the autophagy initiator ULK1, respectively (61, 62). Exercise increases AMPK

activity and is known to promote autophagy by directly activating Ulk1 (62) – a vital

protein for autophagy initiation in hepatocytes (111). Here, eNOS[hep-/-] mice presented

with dysregulated markers of energy sensing proteins – with reduced AMPK and mTOR

regardless of sex or EX (**Fig. 3.5, 3.6**). Decreased AMPK activity may explain the

marked attenuation of exercise-induced increases in both total and Ser555 phosphorylated

ULK1 in male mice, given that it is directly phosphorylated by AMPK during exercise

(62). However, this cannot be explained by an increased inhibitory effect of mTOR, as

both total and phosphorylated mTOR were reduced in eNOS[hep-/-] mice. mTOR activates

eNOS in endothelial cells (112), and the lack of eNOS in the hepatocytes may be

negatively feeding back to reduce total mTOR in the liver. Despite dysregulated markers

of energy sensing ability in eNOS[hep-/-] mice, this did not affect mitochondrial LC3-II

content (**Fig. 3.6**), a marker of end stage autophagy/mitophagy. Thus the reduction in

AMPK activity may not be sufficient to then reduce mitophagy. This is supported by

previous work, as AMPK activation alone was not sufficient to regulate autophagy in

human skeletal muscle during exercise (113). Collectively, these novel data indicate that

hepatocellular eNOS may regulate exercise-induced autophagy/mitophagy in the liver, at

least in males, although more robust and dynamic measurements of

autophagic/mitophagic flux are required to confirm this.

Our group and others have previously shown marked sex differences in NAFLD development in rodents, with females conferring some protection for hepatic steatosis development (66-70). This is thought to be due, in part, to increased mitochondrial function (68-70) and markers of mitophagy and biogenesis (66, 67). Here, females showed elevated markers of mitochondrial content (ETC) and biogenesis (TFAM protein, *pgc1α* mRNA) compared to males. This is likely due to increased hepatic *esr1* mRNA expression (**Table 3.3**), the gene encoding estrogen receptor α – known to induce mitochondrial biogenesis and content (114, 115). This may also explain how the reduction in PGC1α in eNOS[hep-/-] males was prevented in eNOS[hep-/-] females (**Fig. 3.5**). Additionally, decreased BNIP3 in eNOS[hep-/-] males was not observed in eNOS[hep-/-] females (**Fig. 3.5**). This interesting interaction may suggest that possible regulation of BNIP3 by hepatocellular eNOS is sex dependent. Notably, females had markedly lower total and phosphorylated ULK1, possibly due to increased *mtor* gene expression, an inhibitor of ULK1 (62), although mTOR protein content was not affected by sex. This suggests decreased autophagic initiation compared to males despite having elevated downstream autophagy/mitophagy markers (Parkin, BNIP3) (**Fig. 3.6**), and may not be regulated by mTOR. This is consistent with previous literature, with females presenting with reduced mitophagy flux despite elevated Parkin and BNIP3 (69). The authors suggested that females have increased mitochondrial coupling efficiency, and therefore less need for mitophagy. This increased efficiency may also explain why EX markedly reduced ETC Complex IV (cytochrome C oxidase) in females, complex of the ETC. We have previously demonstrated EX to decrease Complex IV in male WT mice (116), and it may be related to the increased efficiency of the mitochondria. Although females are

likely displaying similar mitophagic capacity here, more thorough methods of mitophagic flux are required to confirm this.

Collectively, this study demonstrates for the first time the requirement of hepatocellular eNOS for the full hepatic mitochondrial adaptations to exercise. While exercise improved liver histology and reduced mitochondrial H_2O_2 emission in both groups of mice, hepatocellular eNOS deficient male mice failed to exhibit exercise-induced increases in hepatic fatty acid oxidation. Further, we uncover a role for hepatocellular eNOS in EX-induced autophagy/mitophagy where hepatocellular eNOS is required for normal hepatic AMPK activation and exercise-induced increases in activation in the autophagy initiator ULK1. These novel data help to further uncover the important role of hepatocellular eNOS in NAFLD development and the molecular mechanisms behind exercise-induced hepatic mitochondrial adaptations.

Acknowledgements

Disclosures

No conflicts of interest, financial or otherwise, are declared by the authors.

Author Contributions

R.P.C. and R.S.R. were involved in the study concept and design. T.T. provided the eNOS floxed mouse model. R.P.C., M.P.M., R.J.D., G.M.M., V.J., L.B., and R.S.R. helped with acquisition of data. R.P.C., M.P.M., R.J.D., G.M.M., and R.S.R analyzed and interpreted results. R.P.C., and R.S.R. provided statistical analysis of the data. R.P.C. drafted the manuscript, while R.P.C., M.P.M., G.M.M., R.J.D., V.J.V., J.A.K, F.W.B., and R.S.R. revised the manuscript and provided important intellectual content. R.P.C., M.P.M., R.J.D., G.M.M., V.J., L.B., T.T., V.J.V., J.A.K, F.W.B., and R.S.R. approved final version of manuscript. R.P.C., R.J.D., and R.S.R. obtained funding.
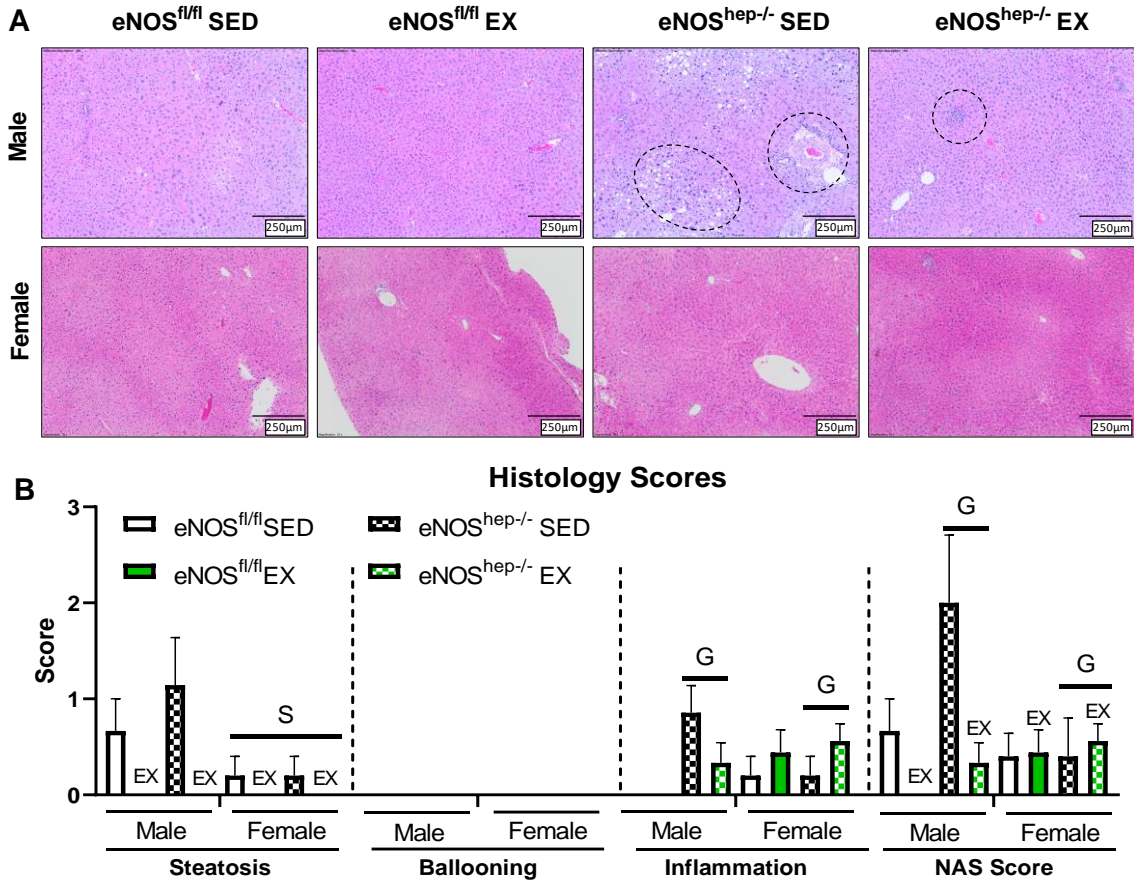
Figures

Figure 3.1: Effects of hepatocellular eNOS deficiency, sex, and EX on liver histology and inflammation. A) Representative liver H&E slides from the indicated mice at 20-24 weeks of age. B) Histological steatosis scoring, C) inflammation scoring, and D) total NAS for all groups (n = 10-14/group). Ballooning scores were included in total NAS but no represented as the score was zero for all groups. Data are presented as mean ± SEM. S, main effect of sex (P<0.05); EX, main effect of exercise (P<0.05); G, main effect of genotype. EX, voluntary wheel running exercise; H&E, haemotoxylin and eosin; NAS, NAFLD activity score.
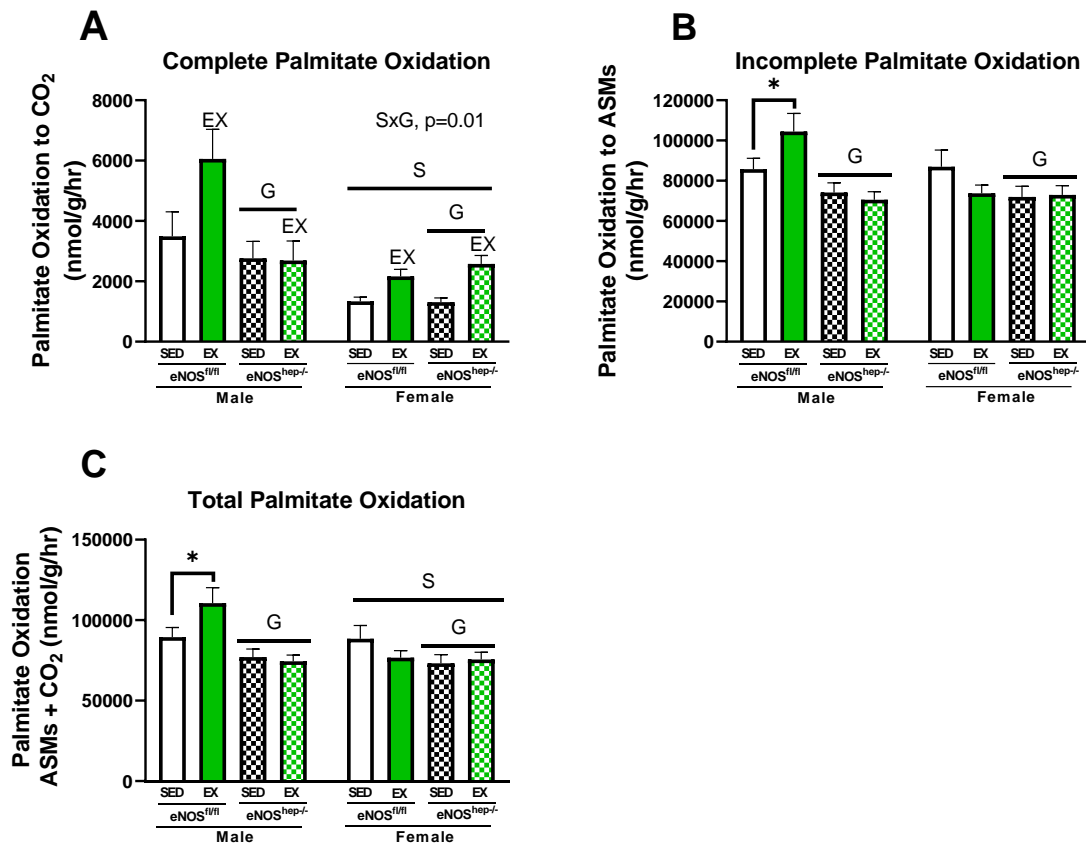
Figure 3.2: Effects of hepatocellular eNOS deficiency, sex, and EX on whole liver homogenate fatty acid oxidation. A) Whole liver complete, B) incomplete, and C) total [1-^{14}C] pyruvate oxidation to CO_2 (n = 10-14/group). Data are presented as mean ± SEM. S, main effect of sex (P<0.05); EX, main effect of exercise (P<0.05); G, main effect of genotype (P<0.05). EX, voluntary wheel running exercise; ASMs, acid soluble metabolites.
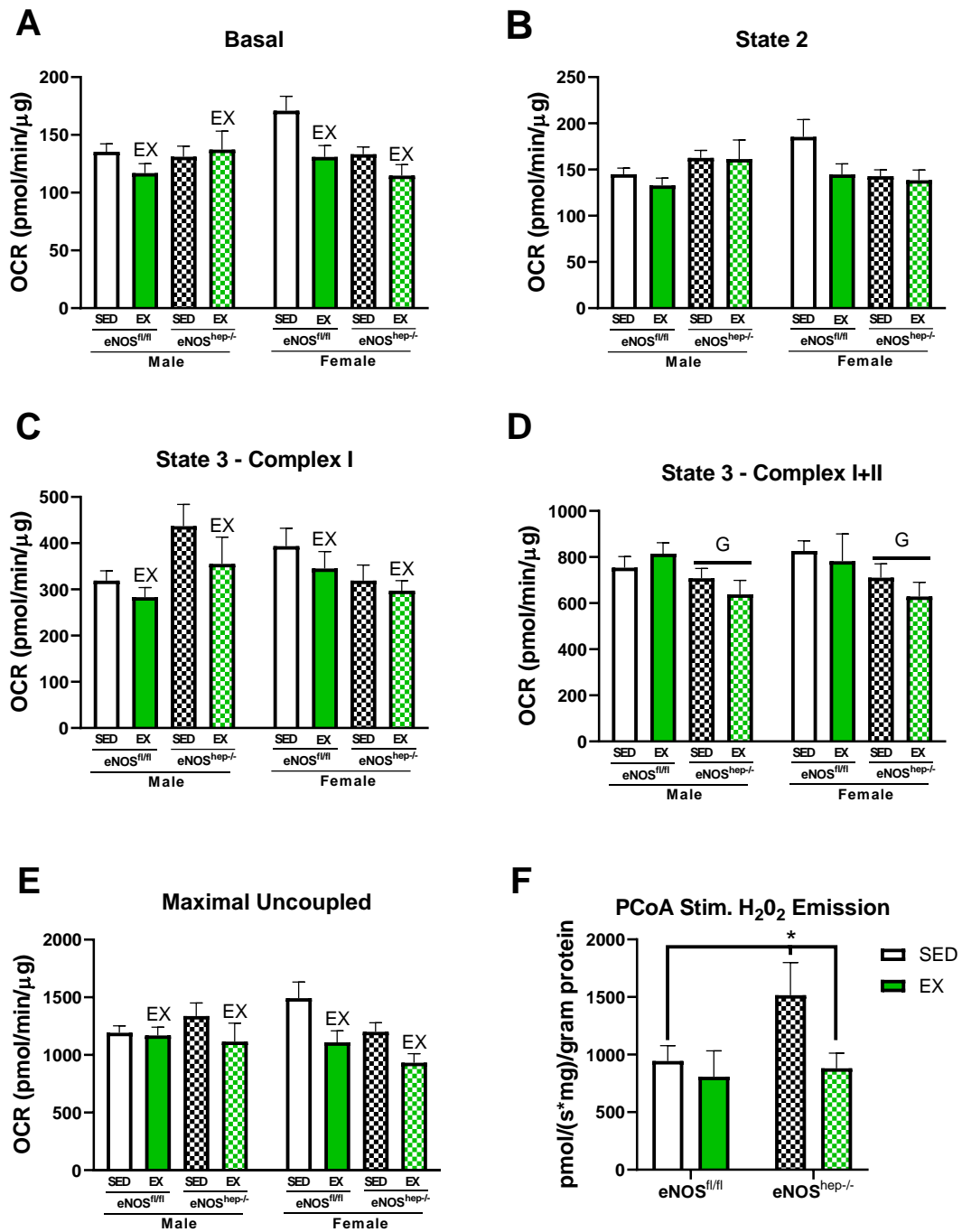
Figure 3.3: Effects of hepatocellular eNOS deficiency, sex, and EX on isolated hepatic

mitochondrial respiration. A) Basal oxygen consumption rate (OCR), B) state 2 OCR, C)

state 3 complex I OCR D) state 3 complex I+II OCR, E) maximal uncoupled OCR.

F) PCoA stimulated H_2O_2 emission in isolated liver mitochondria from male and female combined (n = 7-9/group). Data are presented as mean $\pm$ SEM. S, main effect of sex (P<0.05); EX, main effect of exercise (P<0.05); G, main effect of genotype (P<0.05). EX, voluntary wheel running exercise; OCR, oxygen consumption rate; PCoA, palmitoyl-CoA.
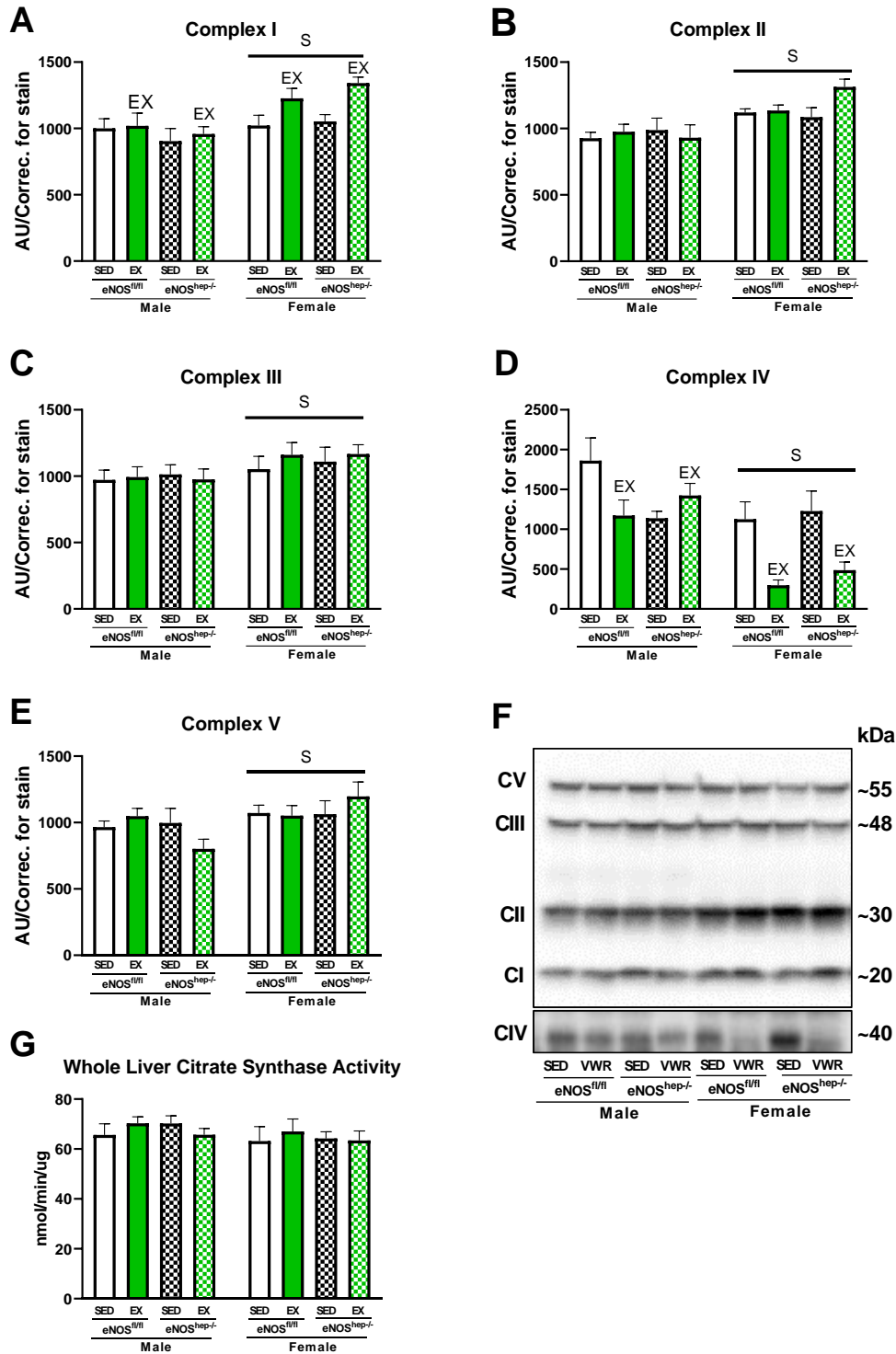
Figure 3.4: Effects of hepatocellular eNOS deficiency, sex, and EX on markers of

hepatic mitochondrial content in whole liver homogenate. A-E) Protein abundance of the

electron transport chain complexes I-V (n = 10-14/group), and F) their representative

Western blot images. G) Citrate synthase activity (n = 9-10/group). Data are presented as

mean ± SEM. S, main effect of sex (P<0.05); EX, main effect of exercise (P<0.05); EX,

voluntary wheel running exercise; C, complex.
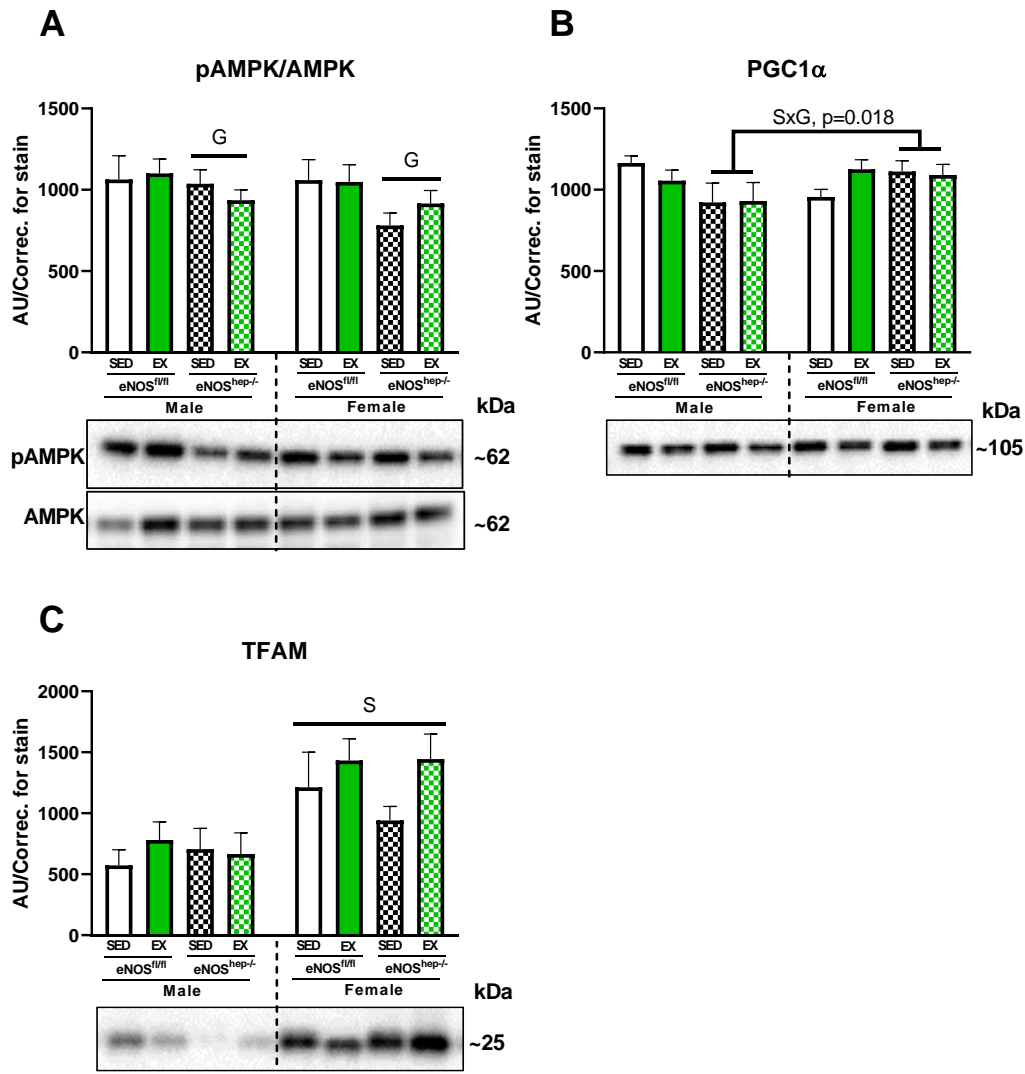
Figure 3.5: Effects of hepatocellular eNOS deficiency, sex, and EX on markers of

hepatic mitochondrial biogenesis in whole liver homogenate. Protein abundance and their

representative Western blot images of; A) the ratio of phosphorylated AMPK to total

AMPK, B) PGC1α, C) TFAM (n = 10-14/group). Data are presented as mean ± SEM. S,

main effect of sex (P<0.05); EX, main effect of exercise (P<0.05); G, main effect of

genotype (P<0.05); SxG, sex and genotype interaction (P<0.05). EX, voluntary wheel

running exercise.

A mTOR

B p-mTOR

C ULK1

D pULK1

E Parkin

F BNIP3

G Isolated Mitochondria LC3-II
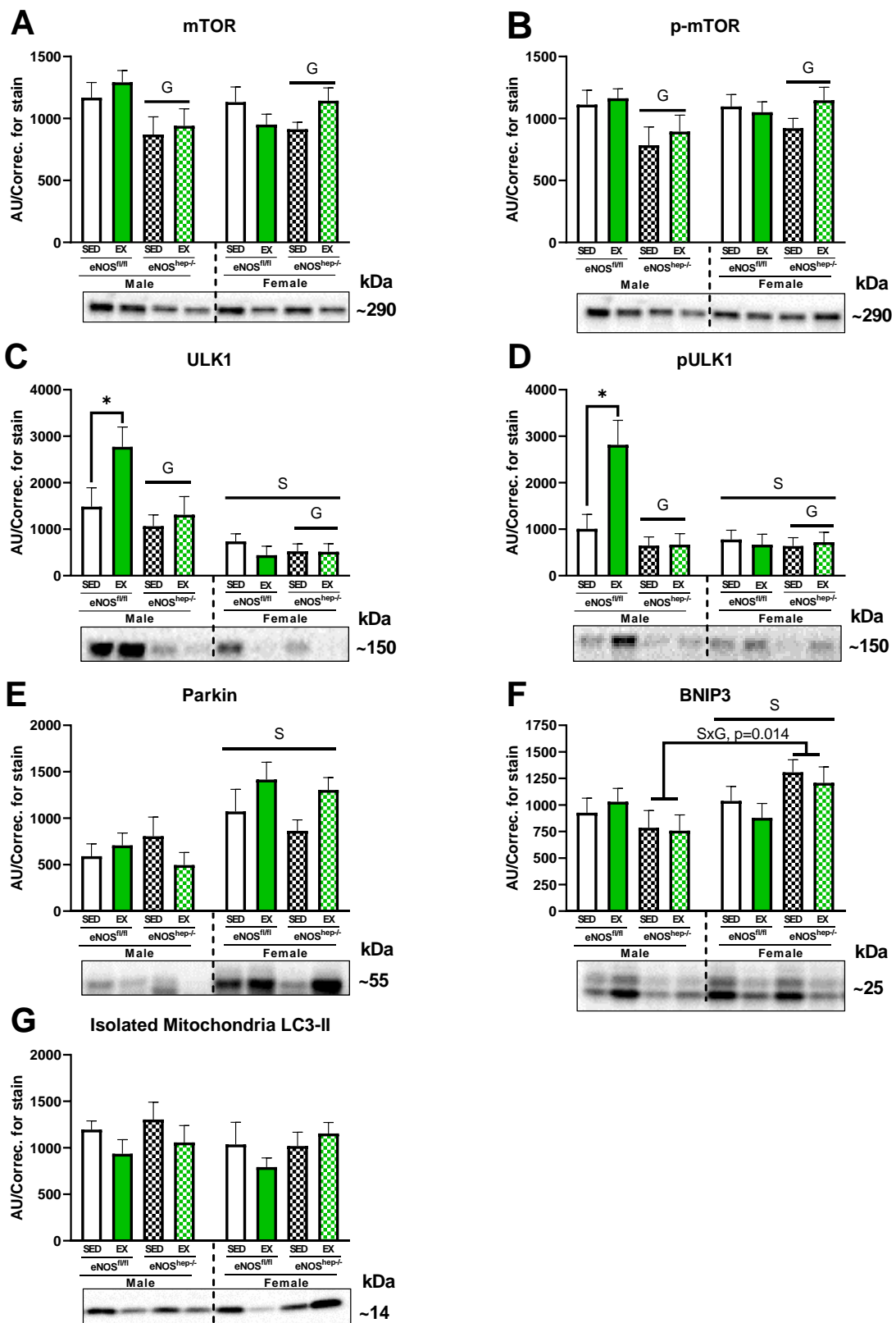
Figure 3.6 (previous page): Effects of hepatocellular eNOS deficiency, sex, and EX on markers of hepatic mitochondrial turnover. Protein abundance of markers of mitochondrial turnover and their representative Western blot images in whole liver homogenate; A) mTOR, B) p-mTOR, C) ULK1, D) pULK1, E) Parkin F) BNIP3, and G) isolated hepatic mitochondria LC3-II (n = 10-14/group). Data are presented as mean $\pm$ SEM. S, main effect of sex (P<0.05); EX, main effect of exercise (P<0.05); G, main effect of genotype (P<0.05); SxG, sex and genotype interaction (P<0.05). EX, voluntary wheel running exercise.

Primers	Forward Sequence 5'-3'	Reverse Sequence 5'-3'
nqo1	CCTTTCCAGAATAAGAAGACC	AATGCTGTAAACCAGTTGAG
nfe212	CATTCCCGAATTACAGTGTC	GGAGATCGATGAGTAAAAATGG
esr1	CAAGGTAAATGTGTGGAAGG	GTGTACACTCCGGAATTAAG
pgc1α	AAAGGATGCGCTCTCGTTCA	AAGGGAGAATTGCGGGGTGTGT
tfam	TCCAAGCCTCATTTCACAAGC	CCAAAAAGACCTCGTTCAGC
sirt1	AAACAGTGAGAAAATGCTGG	GGTATTGATTACCCTCAAGC
mtor	CTTCACAGATACCCAGTACC	AGTAGACCTTAAACTCCGAC
arg-1	GATCACATCCCAAAATTCCC	CTTCATCTTTCTTCCCACAC
cat	CTCCATCAGGTTTCTTTCTTG	CAACAGGCAAGTTTTTGATG
gpx1	GGAGAATGGCAAGAATGAAG	TTCGCACTTCTCAAACAATG
18S	GTAAAACTGCCAGAGAGAAAC	GGGAATATAGTTGGCTAAGTG

Table 3.1: SYBER RT-PCR primer list.

117

	eNOS$^{fl/fl}$ SED	eNOS$^{fl/fl}$ EX	eNOS$^{hep-/-}$ SED	eNOS$^{hep-/-}$ EX	eNOS$^{fl/fl}$ SED	eNOS$^{fl/fl}$ EX	eNOS$^{hep-/-}$ SED	eNOS$^{hep-/-}$ EX
Final Body weight (g)	27.93 ± 0.46	26.23 ± 0.89	27.31 ± 0.81	26.68 ± 1.03	21.67 ± 0.61^S	21.86 ± 0.44^S	22.02 ± 0.7^S	23.23 ± 0.6^S
Body fat (%)	15 ± 0.014	11 ± 0.014^{EX}	17 ± 0.011	11 ± 0.015^{EX}	19 ± 0.01^S	13 ± 0.012^{S,EX}	20 ± 0.025^S	14 ± 0.01^{S,EX}
Delta change body fat (%)	3 ± 0.009	-1 ± 0.015^{EX}	5 ± 0.016	-2 ± 0.019^{EX}	5 ± 0.01	-3 ± 0.015^{EX}	5 ± 0.02	-2 ± 0.011^{EX}
Liver (mg)	898.84 ± 38.2	863.37 ± 24.8	877.5 ± 51.8	868.24 ± 54.2	905.67 ± 52.9	851.22 ± 20.6	856.86 ± 27	817.07 ± 51.5
RP fat (mg)	729.83 ± 63.6	579.16 ± 96.3^{EX}	753.9 ± 79.7	608.29 ± 102.8^{EX}	480.4 ± 58.5^S	316.8 ± 47.8^{S,EX}	434.2 ± 48^S	405.7 ± 51.6^{S,EX}
Heart:body weight (mg/g)	4.5 ± 0.16	5.15 ± 0.15^{EX}	3.95 ± 0.37	5.14 ± 0.19^{EX}	4.54 ± 0.15	4.97 ± 0.13^{EX}	4.3 ± 0.08	5.15 ± 0.15^{EX}
Average weekly food intake (g)	18.6 ± 0.12	24.67 ± 0.49^{EX}	18.44 ± 0.76	24.62 ± 0.56^{EX}	15.52 ± 0.4^S	22.99 ± 0.5^{S,EX}	14.95 ± 0.51^S	22.78 ± 0.5^{S,EX}
Average Daily Running Distance (km/day)	-	6.38 ± 0.46	-	6.31 ± 0.54	-	6.4 ± 0.42	-	6.09 ± 0.34

Table 3.2: Animal characteristic following 10 weeks of SED or EX on a control diet. Data are presented as mean ± SEM (n = 10-14/group). S, main effect of sex (P<0.05); EX, main effect of exercise (P<0.05). EX, voluntary wheel running exercise;

118

	eNOS$^{fl/fl}$ SED	eNOS$^{fl/fl}$ EX	eNOS$^{hep-/-}$ SED	eNOS$^{hep-/-}$ EX	eNOS$^{fl/fl}$ SED	eNOS$^{fl/fl}$ EX	eNOS$^{hep-/-}$ SED	eNOS$^{hep-/-}$ EX
nqo1	1.08 ± 0.16	1.19 ± 0.13^{EX}	1.02 ± 0.21	1.51 ± 0.22^{EX}	3.36 ± 0.66^{S}	5.31 ± 0.55^{S,EX}	4.32 ± 0.85^{S}	5.35 ± 0.58^{S,EX}
nfe2l2	1.01 ± 0.19	1.47 ± 0.2^{EX}	1.22 ± 0.31	1.76 ± 0.25^{EX}	2.56 ± 0.57^{S}	3.44 ± 0.35^{S,EX}	2.64 ± 0.6^{S}	3.4 ± 0.4^{S,EX}
esr1	1.03 ± 0.19	1.05 ± 0.15^{EX}	0.77 ± 0.15	1.2 ± 0.22^{EX}	1.74 ± 0.52^{S}	2.03 ± 0.16^{S,EX}	1.48 ± 0.4^{S}	2.6 ± 0.39^{S,EX}
pgc1α	1.05 ± 0.12	1.29 ± 0.22^{EX}	1.03 ± 0.2	1.34 ± 0.23^{EX}	1.43 ± 0.27^{S}	2.04 ± 0.28^{S,EX}	1.57 ± 0.29^{S}	2.8 ± 0.38^{S,EX}
tfam	1.08 ± 0.16	1.24 ± 0.11^{EX}	0.92 ± 0.18	1.19 ± 0.1^{EX}	1.82 ± 0.37^{S}	2.4 ± 0.16^{S,EX}	1.65 ± 0.31^{S}	2.22 ± 0.18^{S,EX}
sirt1	1.1 ± 0.16	1.13 ± 0.1^{EX}	0.82 ± 0.14	1.2 ± 0.15^{EX}	1.75 ± 0.28^{S}	2.02 ± 0.15^{S,EX}	1.5 ± 0.23^{S}	2.14 ± 0.25^{S,EX}
mtor	1.09 ± 0.15	0.97 ± 0.12	0.95 ± 0.16	1.24 ± 0.1	1.71 ± 0.29^{S}	1.8 ± 0.09^{S}	1.59 ± 0.27^{S}	1.63 ± 0.18^{S}
arg1	1.07 ± 0.14	1.13 ± 0.17	0.83 ± 0.19	1.05 ± 0.15	1.48 ± 0.28^{S}	1.74 ± 0.18^{S}	1.2 ± 0.23^{S}	1.89 ± 0.23^{S}
cat	1.33 ± 0.34	1.98 ± 0.34^{EX}	0.88 ± 0.22	1.57 ± 0.28^{EX}	1.65 ± 0.42^{S}	2.77 ± 0.23^{S,EX}	1.76 ± 0.46^{S}	2.76 ± 0.23^{S,EX}
gpx1	1.04 ± 0.1	1.45 ± 0.17^{EX}	1.06 ± 0.22	1.51 ± 0.19^{EX}	1.28 ± 0.2^{S}	2.3 ± 0.21^{S,EX}	1.72 ± 0.3^{S}	2.35 ± 0.18^{S,EX}

Table 3.3: Gene expression was determined using RT-PCR. Relative expression of all hepatic mitochondrial biogenesis, turnover, and oxidative stress genes were normalized to *18S*, and presented as mean ± SEM (n=8-10/group). S, main effect of sex (P<0.05); EX, main effect of exercise (P<0.05). EX, voluntary wheel running exercise.

CHAPTER 4 – Summary, Limitations, and Future Directions

SUMMARY

The spectrum of liver disease that comprises nonalcoholic fatty liver disease (NAFLD) ranges from steatosis, to steatohepatitis and fibrosis (NASH), to cirrhosis and hepatocellular carcinoma. This condition affects >75% of people with overweight or obesity (72), and its rapidly increasing prevalence comes at great cost to both the affected individual and the medical system. Due to its association with many other life threatening diseases and lack of approved pharmacological treatments (9, 10), studies investigating the molecular mechanisms of NAFLD are vital.

Hepatic mitochondrial dysfunction is a striking feature of NAFLD/NASH development; to such an extent that NAFLD/NASH has been considered a mitochondrial disease (18). To date, the mechanisms behind the decline in hepatic mitochondria during disease progression remain unresolved. Our group have previously demonstrated that endothelial nitric oxide synthase (eNOS) is associated with reduced hepatic mitochondrial function and NAFLD development (47), while NOS inhibition exacerbates NASH progression and reduces hepatic mitochondrial function (46). Further, eNOS null animals display elevated hepatic steatosis (45), and eNOS has been shown to be an important regulator of mitochondrial health and function in other tissues (4, 49-53). Taken together, these data indicate that eNOS may be a potential mediator of hepatic mitochondrial function in the liver.

Accordingly, this dissertation focused on manipulating hepatocellular eNOS via multiple approaches to fully elucidate its role in NAFLD/NASH development. These studies

extend previous work by our group showing *in vitro* deletion of eNOS impairs fatty acid oxidation and mitophagic capacity in hepatocytes (1). Generating this tissue-specific eNOS KO murine model was paramount in removing the confounding variables of whole-body KO models, and allowed determination of whether hepatocellular eNOS *per se* is playing a role of NAFLD development. Here, the utilization of gain and loss of function approaches, including genetic, adeno-associated virus, and adenoviral manipulations both *in vitro* and *in vivo*, helped to establish the role of hepatocellular eNOS in hepatic mitochondrial dysfunction with NAFLD. Further, lifestyle interventions were employed, such as western diets of varying lengths and physical activity, to comprehensibly test the idea that eNOS plays a beneficial and important role in the liver.

The first study characterized our hepatocyte-specific eNOS KO mice (eNOS$^{hep-/-}$) versus intact hepatocellular eNOS mice (eNOS$^{fl/fl}$) on either a control diet (CD) or western diet (WD). Several lines of evidence reveal that ablation of hepatocellular eNOS exacerbates NAFLD development; i) eNOS$^{hep-/-}$ mice displayed elevated histological hepatic steatosis and inflammation compared to eNOS$^{fl/fl}$ mice, particularly on a control diet (CD); ii) eNOS$^{hep-/-}$ mice had reduced fatty acid oxidation in whole liver and isolated liver mitochondria, and reduced mitochondrial respiration compared to eNOS$^{fl/fl}$ mice; iii) eNOS$^{hep-/-}$ mice had reduced static markers of mitophagy, and an impaired mitophagic response when autophagy was blocked compared to eNOS$^{fl/fl}$ mice; iv) Knockdown of hepatocellular eNOS via AAV-Cre and AAV-shRNA approaches further exacerbated hepatic steatosis and inflammation, and impaired the WD-induced increase in mitophagic flux.

121

Further Adenoviral and AAVdriven overexpression models of eNOS were utilized both *in vitro* and *in vivo* to increase isolated hepatocyte respiration and markers of mitophagy. Additionally, long-term eNOS overexpression mitigated WD-induced histological NASH, without alterations in mitochondrial function (**Aim 1**). Hepatocellular eNOS appeared to exert its beneficial effects on mitochondrial function via BNIP3, as BNIP3 overexpression increased respiration and fatty acid oxidation in hepatocytes isolated from eNOS^{fl/fl} mice but had no effect on hepatocytes from eNOS[hep-/-] mice. This study showed for first time that hepatocyte-specific deletion of eNOS impaired hepatic mitochondrial function and exacerbated NAFLD development. Further, an additional role of hepatocellular eNOS was identified in mitochondrial quality control and attenuating inflammation during NASH development and progression.

These data support previous work showing whole body eNOS null mice have exacerbated hepatic steatosis (45), and reduced mitochondrial function (73). The whole body eNOS KO models made it difficult to delineate the role of hepatocellular-specific eNOS in hepatic fat accumulation and mitochondrial function. This novel mouse model identified the lack of hepatocellular eNOS *per se* as a contributing factor in exacerbated NAFLD development and reducing hepatic mitochondrial function.

It has been repeatedly shown that exercise improves hepatic mitochondrial function (29, 30, 33, 34). Using the hepatocyte-specific eNOS null model, the second study established if hepatocellular eNOS was required for the voluntary wheel running exercise-induced improvements in hepatic mitochondrial function. Voluntary wheel running exercise attenuated NAFLD development and H_2O_2 emission in eNOS[hep-/-] mice. Exercise increased fatty acid oxidation in eNOS^{fl/fl} mice, although this effect was completely

ablated in male eNOS$^{hep-/-}$. Further, eNOS$^{hep-/-}$ mice displayed dysregulated markers of energy sensing proteins, with mTOR and AMPK activation reduced in eNOS$^{hep-/-}$ mice, with the exercise-induced induction of the autophagy initiator ULK1 blunted in eNOS$^{hep-/-}$ mice. Interestingly, while female mice displayed elevated markers of mitochondrial biogenesis and altered autophagy markers compared to male mice, they showed little response to exercise. Collectively, this study demonstrated the requirement of hepatocellular eNOS for the full beneficial effects of exercise on hepatic mitochondrial function and markers of turnover.

When taken together, both studies helped to confirm the exacerbated NAFLD development in eNOS$^{hep-/-}$ mice, with results in the second study analogous to our first study. In the second study, eNOS$^{hep-/-}$ mice also displayed exacerbated histological hepatic steatosis, , which was ameliorated with exercise. The blunted mitochondrial improvements in response to exercise in eNOS$^{hep-/-}$ mice is in accordance with previous work confirming the requirement of eNOS in mitochondrial adaptations to exercise (53, 54), and support the hypothesis that hepatocellular eNOS is essential for the maintenance of healthy mitochondrial function in the liver. The blunted response to exercise in the absence of hepatocellular eNOS may be due to an impaired ability to sense energy changes within the liver, as eNOS$^{hep-/-}$ mice presented with reduced mTOR and AMPK. This likely resulted in the blunted exercise-induced response of the autophagy initiator ULK1, as AMPK activation is required for the induction of ULK1 with exercise (62). This supports our finding of reduced ULK1 in CD fed eNOS$^{hep-/-}$ mice from the first study – suggesting eNOS maybe be regulating autophagy initiation in the liver. Similarly, BNIP3 was reduced in the male eNOS$^{hep-/-}$ mice but not in the female mice regardless of

exercise (sex by genotype interaction), supporting the observed reduction of BNIP3 from the first study. This further solidifies the link between hepatic eNOS and BNIP3, at least in male mice.

In the first paper, females eNOS[hep-/-] mice responded similar to males - with reduced hepatic fatty acid oxidation and mitochondrial respiration. In particular, WD-fed eNOS[hep-/-] females had ~50% reduction in complete palmitate oxidation compared to their eNOS^{fl/fl} WD-fed counterparts. In the second paper, the differences between eNOS[hep-/-] and eNOS^{fl/fl} females fatty acid oxidation was not as striking, and it is likely that females needed a WD challenge to see this difference. Further, a sex by genotype interaction was observed for BNIP3; BNIP3 was reduced in male eNOS[hep-/-] mice but not in eNOS[hep-/-] females. This interesting interaction may suggest that possible regulation of BNIP3 by hepatocellular eNOS is sex dependent. Additionally, sex effects occurred regardless of genotype, as females presented with increased markers of mitochondrial biogenesis and autophagy/mitophagy (BNIP3, Parkin) compared to males, supporting previous work (66, 67). Surprisingly, females displayed marked reductions in ULK1 compared to males, and may be indicative of reduced autophagy initiation despite elevated downstream markers. This is consistent with previous literature, with females presenting with reduced mitophagy flux despite elevated Parkin and BNIP3 (69), and may be related to the improved efficiency of the mitochondria requiring less need for mitophagy.

Collectively, both of these studies categorically uncover the vital role of hepatocellular eNOS in NAFLD development and mitochondrial function in the liver (**Figure 4.1**). This premise has been comprehensibly tested with multiple gain and loss of function approaches, while challenged with physical activity and western diet. Taken together,

these studies have identified a novel role for eNOS in the maintenance of hepatic

mitophagy, and the requirement of hepatocellular eNOS for the full hepatic mitochondrial

adaptations to exercise. These novel data help to further uncover the role of

hepatocellular eNOS in NAFLD development, and the molecular mechanisms behind

exercise-induced hepatic mitochondrial adaptations.
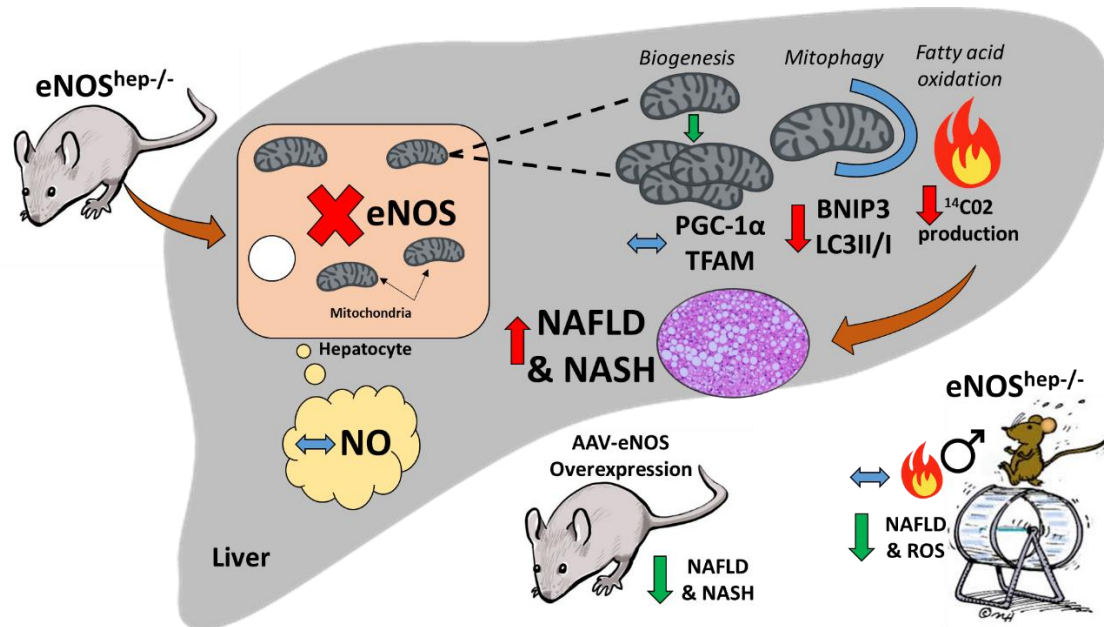
Figure 4.1. Schematic illustration of the uncovered role that hepatocellular endothelial nitric oxide synthase (eNOS) plays in nonalcoholic fatty liver disease/steatohepatitis (NAFLD/NASH) development. Genetic and viral ablation of hepatocellular eNOS *in vivo* results in no change in markers of mitochondrial biogenesis, but impairs hepatic mitophagy capacity and hepatic mitochondrial function, which leads to increased NAFLD/NASH. Overexpressing hepatocellular eNOS attenuates NAFLD/NASH development without observed changes in mitochondrial function. Exercising eNOS[hep-/-] mice reduces hepatic steatosis and reactive oxygen species (ROS) emission, but does not increases fatty acid oxidation in male mice.

LIMITATIONS AND FUTURE DIRECTIONS

Are the effects of hepatocellular eNOS mediated by NO?

Nitric oxide (NO) is notoriously difficult to accurately measure due to its rapid diffusion

once produced (<1 sec). As such, surrogate markers are commonly used. Here, nitrate

and nitrite concentrations and cGMP activity were used, byproducts of NO production, to determine differences in NO production between isolated primary hepatocytes from eNOS$^{fl/fl}$ and eNOS$^{hep-/-}$ mice. Modest reductions of nitrate and nitrite were observed in eNOS$^{hep-/-}$ hepatocytes ($\sim$30%), which did not reach statistical significance (P=0.16), and no difference between cGMP activity between genotypes. These equivocal results make it difficult to determine whether eNOS$^{hep-/-}$ hepatocytes produce less NO. With these data in mind, there are a number of issues to be considered. Given the markedly lower abundance of eNOS and subsequent NO production in hepatocytes compared to other cell types in the liver – namely Kupffer cells and liver sinusoidal endothelial cells, surrogate methods of NO production used here may not be sensitive enough to detect very slight differences between hepatocytes from eNOS$^{fl/fl}$ versus eNOS$^{hep-/-}$ mice. Despite this low NO production on a cell to cell level, the total sum of all hepatocellular eNOS derived NO production may be physiologically relevant, as hepatocytes make up $\sim$90% of all cell types in the liver. These slight differences in NO production between hepatocytes from eNOS$^{fl/fl}$ versus eNOS$^{hep-/-}$ mice make cell contamination a significant issue. Our rigorous *MACS* purification process aims to remove cells in a whole liver homogenate where eNOS is highly expressed (Kupffer and endothelial cells). Given that only a certain number of isolated primary hepatocytes are collected per cell culture plate well, and from

that sample a smaller amount is used for the nitrate and nitrite assay, a small percentage of contamination from high eNOS expressing cells may cause marked differences in NO production and wash out the small effect that might be seen with just hepatocytes.

To further tease out whether eNOS is exerting its effects through NO-dependent mechanisms or via the eNOS protein itself, future studies should overexpress

126

hepatocellular eNOS both *in vitro* and *in vivo* while treating either the cells or animals with L-NAME, a global NOS inhibitor. This would simultaneously increase eNOS activity while reducing any NO production. If our prior results of increased respiration in hepatocytes with eNOS overexpression are unable to be repeated in the presence of L-NAME, this would support the notion that the benefits of eNOS are mediated through NO. If benefits of eNOS overexpression are still observed with L-NAME administration, this would indicate that the functional protein of eNOS itself is regulating beneficial changes that are independent of NO. This would open other avenues of research into the mechanisms behind this phenomenon.

Elucidating mechanisms of protection with long-term eNOS overexpression
Observations of attenuated histological NASH with long-term hepatocellular eNOS overexpression despite no increases in mitochondrial function and markers of mitochondrial dynamics requires attention. Given the ability to increase respiration in hepatocytes of CD fed animals at 6 weeks of eNOS overexpression, the window to observe the full effects of eNOS overexpression in hepatocytes by examining functional outcomes at 10 weeks post injection may have been missed. As such, the observed histological improvements at 10 weeks post injection and 30 weeks of their respective diets may be resultant of the earlier benefits of elevated eNOS expression. Moreover, fatty acid oxidation and respiration was assessed in whole liver and mitochondria isolated from whole liver using a crude isolation technique, which would have included other hepatic cell types with intact eNOS (Kupffer cells, hepatic stellate cells, liver sinusoidal endothelial cells, etc). This may have masked the effects of hepatocellular eNOS overexpression on respiration, and future studies should examine these outcomes in

127

isolated hepatocytes also. Additionally, more exaggerated differences between eNOS overexpression and scramble treated animals may have been seen if a more severe NASH phenotype was induced. Future studies should consider adding 10-15% high fructose corn syrup to the drinking water to exacerbate NASH development (117), and examine outcomes in hepatocytes from these animals in addition to whole liver and isolated mitochondria.

More robust mitophagy measurements

Impaired mitophagy in hepatocellular eNOS deficient animals is a major contributing factor to the exacerbated hepatic mitochondrial function seen in these animals. To overcome the issue with just measuring static markers of autophagy/mitophagy, mitophagic flux was measured via leupeptin injections. This allows autophagy proteins to accumulate to give an indication of active mitophagy. Again, this is a surrogate marker of mitophagy, as it does not allow determination of whether the mitochondria are being degraded in the lysosome. Gold standard mitophagy measurements, such as duel fluorescence reporters whose signal is quenched in the acidic environment of the lysosome, are reviewed in more detail in the extended literature review. We attempted using the dual mCherry and GFP reporter *in vivo* in preliminary studies, but due to methodological issues and time constraints with the COVID-19 pandemic we were unable to generate data on this mitophagy measurement. Future studies should employ these techniques to confirm mitophagic capacity in eNOS$^{hep-/-}$ vs eNOS$^{fl/fl}$ mice.

Additionally, isolated mitochondrial LC3-II was our marker of end stage autophagy/mitophagy in the second study with voluntary wheel running. Examining mitophagic flux via leupeptin injections (at least) was needed before confirmation that; 1)

exercise induced autophagy/mitophagy, 2) this induction was blunted in eNOS[hep-/-] mice, and 3) that females have lower need for mitophagic flux based on their marked reductions in ULK1 vs males. Future studies should employ these more robust measures of mitophagy to confirm the effect of exercise on hepatic mitophagy and potential sex differences.

Restoring/inducing mitophagy in eNOS[hep-/-] mice would allow for full determination that impaired mitophagy is playing a major role in reducing mitochondrial function and exacerbating NAFLD in mice lacking hepatocellular eNOS. Based on our data, it was suspected that mitophagy is impaired via reductions in BNIP3. As such, overexpressing BNIP3 *in vivo* in eNOS[hep-/-] mice with robust mitophagy measurements would determine whether eNOS is mediating hepatic mitophagy via BNIP3. Further, if this resulted in improved hepatic mitochondrial function and alleviated hepatic steatosis and inflammation, this would indicate that impaired hepatic mitophagy *per se* was a significant contributing factor in the exacerbated NAFLD observed in eNOS[hep-/-] mice.

To explore the interplay between eNOS and BNIP3, affinity chromatography 'pull-down assays' should be employed to identify any physical association between eNOS and BNIP3 in hepatocytes upon mitophagic stimulation.

Impaired glucose control with hepatocellular eNOS deficiency
A potential avenue of further research that was outside the scope of the current studies was the indication of impaired glucose control in eNOS[hep-/-] mice. These mice displayed elevated serum insulin levels in CD only, and this may have maintained serum glucose levels which were not affected by genotype. Further, eNOS[hep-/-] mice on a CD had

significantly elevated glucose response to a pyruvate tolerance test compared to eNOS$^{fl/fl}$

mice. These data, coupled with increased gene expression for markers of hepatic

gluconeogenesis (*g6pase* and *ppeck*), indicate that eNOS$^{hep-/-}$ mice have exacerbated

hepatic glucose output. This idea is supported by previous work, where re-coupling of

eNOS via tetrahydrobiopterin (BH4) administration in diabetic mice lowered blood

glucose levels, while this effect was ablated in hepatocytes from eNOS null mice (94). To

rigorously test hepatic glucose output differences in eNOS$^{fl/fl}$ and eNOS$^{hep-/-}$ mice,

hyperinsulinemic-euglycemic clamps with radio-labelled tracers should be performed, in

addition to examining hepatic glucose output in isolated primary hepatocytes from both

eNOS$^{fl/fl}$ and eNOS$^{hep-/-}$ mice. This would confirm whether eNOS plays a role in

hepatocyte glucose metabolism, and may be a fruitful avenue of future research.

Sex dependent responses to voluntary wheel running

In the current study, females had very little to no response to exercise compared to males.

In addition, no change in mitochondrial content or respiration was observed. These

results may be due to voluntary wheel running not eliciting enough perturbation on the

system to increase mitochondrial respiratory capacity or content given the young age of

the animals and low-fat diet feeding. Further, the slightly lower average daily running

distance in eNOS$^{fl/fl}$ and $^{hep-/-}$ mice compared to other studies (~6 km/day vs ~9-10

km/day (69)), likely contributing to the lack of an exercise response. As such, higher

exercise intensity and or volume may be required to confirm whether hepatocellular

eNOS is required for the induction of mitochondrial respiration and content in the current

study, especially with female mice. As wheel running is voluntary, future studies should

apply treadmill training to induce increased exercise intensities/volume and induce more physiological stress and adaptations to elicit the required response in female mice.

A potential reason why exercise was able to reduce H_2O_2 emission but not increase fatty acid oxidation in eNOS$^{hep-/-}$ mice may be due to the lack of statistical power to separate H_2O_2 emission by sex. As the blunted exercise response in eNOS$^{hep-/-}$ mice was driven largely by the males, this improvement in H_2O_2 emission may have been seen in females only. Future studies should have the appropriate number of males and females to fully determine whether the ability for exercise to reduce H_2O_2 emission is sex dependent.

CHAPTER 5 – Extended Literature Review

Introduction

Nonalcoholic fatty liver disease (NAFLD) is a progressive disease of the liver that ranges on a wide pathological spectrum from hepatic steatosis to a more severe nonalcoholic steatohepatitis (NASH) phenotype, which can progress to fibrosis and cirrhosis (2). Numerous factors are involved in the progression of NAFLD, including changes in lipid metabolism, insulin resistance, inflammatory cytokines, and oxidative stress (3). NAFLD has a high incidence rate, with reports in the general population ranging from 10-30% and as high as 80-100% in obesity and morbid obesity (4, 5). NAFLD progression is the most rapidly increasing indication for liver transplantation in the United States (8), and now can be considered a multisystem disease affecting many extra-hepatic organs. Indeed, NAFLD is an independent risk factor for cardiovascular, liver-related, and all-cause mortality (9, 10), and doubles the risk of development of type 2 diabetes (11). Currently, there are no FDA-approved pharmacological treatments for NAFLD.

Hepatic mitochondrial dysfunction and NAFLD

While the mechanisms behind NAFLD development have not been fully elucidated, mounting evidence suggests that hepatic mitochondrial dysfunction is tightly linked to disease progression (17-19). Characteristics of hepatic mitochondrial dysfunction in the setting of NAFLD/NASH progression include decreased electron transport chain (ETC) content, abnormal mitochondrial morphology, and reduced respiration and β-oxidation (20). However, there is some controversy surrounding this timing of hepatic mitochondrial dysfunction during NAFLD development. In rodent models, a decline in

hepatic mitochondrial function is observed early in fatty liver development; our group has shown that mitochondrial dysfunction in the liver even precedes hepatic steatosis development (21). In human NAFLD/NASH development it is not as clear. Previous studies have reported either a compensatory increase or no change in hepatic mitochondrial function and TCA cycle flux during fatty liver development in humans (22, 23), but this is lost during NASH progression (24, 25). Moreover, NASH patients present with porous mitochondria and elevated hepatic oxidative stress, along with impaired mitochondrial biogenesis and decreased ETC complexes (24). NAFLD is also associated with increased mitochondrial membrane potential, electron leak, and elevated ROS production (118). In fact, NASH patients have lower maximal hepatic mitochondrial respiration and increased proton leakage, despite having higher mitochondrial mass. This is associated with elevated hepatic oxidative stress, greater H_2O_2 emission, and reduced anti-oxidant capacity (24). Despite the debate over its timing during NAFLD/NASH development, mitochondrial dysfunction is clearly implicated in exacerbating disease progression, and therapies that target hepatic mitochondria may provide novel avenues for NAFLD/NASH treatment. Yet, the mechanisms behind hepatic mitochondrial function, and ultimately NAFLD development are unresolved. In this extended literature review, it is posited that one potential mediator of hepatic mitochondrial dysfunction and NAFLD progression is the loss of endothelial nitric oxide synthase (eNOS), and its product nitric oxide (NO), due to this enzyme's well-established role in metabolic health and mitochondrial dynamics (discussed later). This review will focus on the roles of hepatocellular eNOS and NO in maintaining a healthy mitochondrial pool within the liver and how this may pertain to NAFLD pathogenesis.

Nitric Oxide

Since the discovery of a role for NO in maintaining cardiovascular homeostasis by Furchcott, Ignarro, and Murad, for which they shared a Nobel Prize in Physiology or Medicine in 1998, numerous physiological and pathophysiological functions of NO have been described. NO is an autocrine and paracrine signaling gas that has many diverse functions and molecular targets, such as regulating neurotransmission, vascular tone, gene transcription, mRNA translation, and post-translational modification [reviewed in detail (37, 38)]. NO is produced by the nitric oxide synthase (NOS) enzyme, which consists of three isoforms; neuronal NOS (nNOS), inducible NOS (iNOS), and endothelial NOS (eNOS). All three isoforms catalyze the production of NO by converting L-arginine to L-citrulline, with oxygen, reduced nicotinamide-adenine-dinucleotide phosphate (NADPH), and tetrahydrobiopterin (BH4) used as essential substrates and cofactors (39). The biological role of NO is often concentration dependent; pathological levels (μM) are typically produced by iNOS as an immune defense mechanism when macrophages are induced leading to cytotoxicity. Alternatively, physiological levels of NO (nM) are constitutively produced by nNOS and eNOS. The effects of NO are largely concentration dependent, and as the concentration of a gas reduces by a decay constant as the distance from its point of origin, the enzymes that produce NO are poised to be a robust cellular tool in tailoring subcellular responses as needed. This is most notably apparent in the well characterized role of eNOS in vascular endothelial cells, where it is located at the luminal plasma membrane in order to rapidly increase its production of NO and cause vasodilation in response to increases in shear stress. Since its initial discovery

as a potent vasodilator in endothelial cells, eNOS has been shown to provide important regulatory functions in a variety of tissues.

eNOS activation

Activity of eNOS is largely controlled by phosphorylation at multiple sites that can positively or negatively influence its activity. Seven phosphorylation sites have been characterized, including two stimulatory sites (S615, S1177), three inhibitory sites (S114, T495, Y657), and two sites for which the influence on eNOS activity is undetermined (Y81, S633) (119, 120). Of particular interest is that eNOS is activated via S1177 and S615 phosphorylation by AMP-activated protein kinase (AMPK) (121), serine/threonine protein kinase (Akt) (122) and protein kinase A (PKA) (123). These data highlight the ability for eNOS activity to be modulated both by external stimuli (Akt, PKA), as well as the internal metabolic state (AMPK) of the cell. Many NAFLD therapeutics target AMPK activation due its purported benefits on *de novo* lipogenesis inhibition, increased fatty acid oxidation, and stimulation of mitochondrial biogenesis (124). Interestingly, activation of AMPK by exercise (125) or metformin (126) does not occur in eNOS knockout (KO) mice; whereas, NO donors can stimulate AMPK phosphorylation (127). This lends support to the notion that eNOS may exert its metabolic benefits in an AMPK-dependent manner and play an important role in scenarios where metabolism and/or the energy state is perturbed, i.e. obesity/NAFLD.

The link between eNOS and NAFLD

Mounting evidence from whole body eNOS KO rodent models demonstrate its importance for metabolic health. Mice lacking eNOS have elevated FFAs and triglycerides, as well as reduced mitochondrial content and beta-oxidation in skeletal muscle (73). Additionally, eNOS KO mice develop insulin resistance at the level of the liver and other peripheral tissues (128), and accumulate more liver fat compared to WT mice on a high-fat diet (45). Taken together, these data clearly outline an important role for eNOS in metabolic health. In the context of NAFLD development, the vast majority of studies examining eNOS have focused on its role in regulation of hepatic blood flow and vascular resistance. Portal hypertension is a major complication in liver disease caused by increased intrahepatic vascular resistance mediated in part by eNOS derived NO (42); cirrhotic livers also present with significantly reduced whole eNOS activity (43, 44), while NAFLD patients across varying degrees of severity show marked hepatic eNOS dysfunction (129).

There is also limited evidence indicating that loss of eNOS is associated with increased hepatic steatosis. Double KO mice obtained from crossing obese leptin receptor deficient (*Leprdb/db*) mice crossed with eNOS KO mice exhibit elevated hepatic steatosis compared with *Leprdb/db* (130). Similarly, eNOS KO mice fed a 60% high fat diet for 12-weeks accumulate ~25% more TAG than WT counterparts; a finding which the authors attributed to attenuated microsomal triglyceride transfer protein (TAG export) activity in eNOS KO mice (45). Finally, hepatic TAG accumulation was increased with four weeks of NOS inhibition with the non-selective NOS inhibitor (N^{ω}-nitro-L-arginine methyl ester; L-NAME), in hyperphagic OLETF rats (46). Moreover, we also have

shown that reduced eNOS activation is associated with NAFLD progression (1, 47).

Importantly, loss of eNOS activation, as well as NAFLD development, were prevented with chronic voluntary wheel running exercise, indicating a potential role for exercise-induced elevations in eNOS activity in liver health [41]. The whole body eNOS null model coupled with evidence of reduced eNOS activation with NAFLD development demonstrates a potential protective role for eNOS in the pathogenesis of NAFLD, but these studies fail to define the role of hepatocyte-specific eNOS in this pathogenesis, as this enzyme is present in other cell types within the liver.

Hepatocellular eNOS

Considerable discrepancy exists in the literature regarding the distribution of eNOS in the liver. In a seminal report, Shah et al. demonstrated in rats that eNOS regulates sinusoidal perfusion and immunohistochemistry demonstrated its expression was restricted to liver endothelial cells (89). Based largely on this report, numerous subsequent studies on hepatic eNOS presume a mere endothelial localization of eNOS yet offer little, if any, supporting evidence (44, 89-91). Further, mounting evidence identifies a more ubiquitous eNOS distribution in the liver; McNaughton et al. used immunohistochemistry and in situ hybridization to demonstrate widespread eNOS expression in human liver samples (92). In addition, Mei and Thevananther (93) demonstrated an increase in eNOS S1177 phosphorylation in isolated primary hepatocytes following epidermal growth factor stimulation. Interestingly, eNOS was localized in the cytosol in a pattern consistent with hepatocyte mitochondrial distribution. Similarly, increased eNOS activation in isolated primary wild-type hepatocytes was observed with BH4 administration (94).

137

In one of the most comprehensive proteomic analysis of any organ to date, Azimifar and

colleagues used density gradient centrifugation and magnetic affinity cell sorting

techniques to obtain highly purified murine hepatic cell types; hepatocytes, Kupffer cells,

liver sinusoidal endothelial cells, hepatic stellate cells,

andintrahepatic cholangiocytes (77). Using an advanced liquid chromatography tandem

mass spectrometry approach, they clearly identified eNOS in their purified hepatocytes,

with its highest expression in Kupffer cells and liver sinusoidal endothelial cells. Using

the same methodology, our group has confirmed these findings by identifying eNOS

expression in isolated primary hepatocytes from WT mice using magnetic-activated cell

sorting and immunofluorescence (1). Taken together, these more recent and

methodologically robust data strongly imply the presence of eNOS in hepatocytes.

Mitochondrial NOS

Further confounding the role of NOS enzymes in hepatocytes, a body of evidence

supporting the existence of mitochondrial NOS (mtNOS) that is present on the inner

mitochondrial membrane. As there is no fourth NOS gene in mammalian genomes,

mtNOS is thought to be a variant of one of the three known NOS isoforms. Initial reports

identified eNOS as the mtNOS in skeletal muscle, brain, and liver (131, 132). Later it

was demonstrated that eNOS physically associates with the outer leaflet of the outer

mitochondrial membrane (133) and as such is not believed to be the "bona fide" mtNOS

on the inner membrane (134). Instead, evidence exists to support both nNOS and iNOS as

mtNOS. Persichini et al. demonstrated that the PDZ domain nNOS physically interacts

with cytochrome c oxidase (COX) and used immunogold to identify nNOS in the inner

mitochondrial membrane (135). Alternatively, Totoyan and Giulivi identified mtNOS as iNOS in purified rat liver mitochondria (136). Regardless of isoform or sub-mitochondrial localization, it is apparent that a NOS isoform is present in hepatic mitochondria and, given the current discussion, this may have significant implications in hepatic mitochondrial physiology. While the influence and significance of "mtNOS" as it relates to NAFLD has not previously been addressed, it is outside the scope of this extended literature review

eNOS and mitochondrial respiration

How eNOS plays a role in NAFLD pathogenesis may be its function as a mediator of mitochondrial function. A key physiological role of eNOS (and other NOS enzymes) derived NO is its well-characterized interaction with COX in the mitochondrial electron transport chain. NO inhibits COX via both competitive and non-competitive sites (95). Importantly, these inhibitory actions of NO on COX were demonstrated across both pathological and physiological spectrum of both NO and O_2 concentrations. These data indicate that the rate of O_2 consumption at a given [O_2] is inversely proportional to [NO]. In addition, NO may influence other aspects of mitochondrial bioenergetics, including attenuation of complex I and III, which are known sites for ROS production through S-nitrosylation (96, 97), and NO-dependent throttling of the TCA cycle in rat hepatocytes (137). Thus, constitutive NO production may act to adjust mitochondrial respiration, in a manner similar to metformin – which exerts its hepatic benefits by throttling mitochondrial respiration to increase hepatic AMPK activation (138). Taking hypoxia, a known activator of eNOS, as an example, such respiratory inhibition by NO would

139

prevent excess O_2 consumption by mitochondria closest to the O_2 source and allow for more ubiquitous tissue O_2 distribution. Similarly, in a fed condition, which activates eNOS via insulin mediated Akt activation, this NO throttle could reduce substrate oxidation in the most proximal mitochondria thus limiting the extent of ROS production in this microdomain. This function may be particularly relevant to the attenuation of mitochondrial derived ROS in NAFLD by attenuating electron transport flux and membrane potential in the face of increased electron transport chain pressure from nutrient excess.

eNOS and mitochondrial dynamics

A healthy mitochondrial pool is dependent on adequate turnover of mitochondria within the cell. This turnover hinges on the intimately linked processes of biogenesis and autophagy - where dysfunctional, aberrant mitochondria are removed via selected autophagy (mitophagy), and replaced in an effort to maintain mitochondrial homeostasis within the cell (56). The role of eNOS and NO in the regulation of autophagy and mitophagy is discussed later in that section of the review, whereas this section will focus on eNOS and eNOS derived NO on mitochondrial biogenesis.

The link between eNOS derived NO and its regulation of mitochondrial function in other tissues is well established. In a seminal paper by Nisoli et al, the addition of an NO donor to cultured brown adipocytes induced markers of mitochondrial biogenesis and content in a cyclic GMP and peroxisome proliferator receptor γ coactivator α (PGC1α) dependent manner (50). In the same study, cold exposure-induced mitochondrial biogenesis in brown adipose tissue was significantly attenuated in whole body eNOS null mice, while

eNOS null mice also presented with reduced markers of mitochondrial content in brain, heart, and liver tissue (50). Furthermore, calorie restricted-induced mitochondrial biogenesis is severely attenuated in eNOS null mice (52). The reverse is also true – global eNOS overexpression prevented diet induced obesity while increasing markers of mitochondrial biogenesis and activity in adipose tissue (55). Additionally, TNFα-induced downregulation of eNOS expression impairs mitochondrial biogenesis and function in different tissues of obese rodents (139), further solidifying the link between eNOS and mitochondrial biogenesis. Interestingly, exercise-induced adaptations in mitochondrial health may be dependent on eNOS. In fact, six weeks of swim training increased mitochondrial biogenesis, mitochondrial DNA content, and glucose uptake in subcutaneous adipose tissue of wild-type but not eNOS KO mice (53). Similarly, genetic ablation of eNOS attenuated exercise-induced increases in mitochondrial biogenesis and function in cardiomyocytes (54). Collectively, these studies demonstrate a strong tie between eNOS and mitochondrial biogenesis, and that exercise promotes eNOS dependent improvements in mitochondrial biogenesis and function.

eNOS and advanced liver disease

Our lab has recently demonstrated that normal hepatic eNOS activation is dramatically reduced in the obese OLETF rat during the transition from hepatic steatosis to NASH (47), implicating the loss of normal eNOS function in the advancement of liver disease. In a subsequent study, treating obese OLETF rats with L-NAME for 4 weeks reduced hepatic mitochondrial respiration, increased hepatic TAG accumulation, and induced a more NASH-like phenotype (increased stellate cell and Kupffer cell activation markers)

141

compared with untreated obese controls (46). These studies support previous work implicating reduced eNOS activity and NO production in the activation of Kupffer cells and hepatic stellate cells (140, 141).

On the other hand, increasing NO bioavailability may provide some hepatoprotection against metabolic insults. Giving a systemic NO donor has been shown to attenuate NASH progression, in part through lowering M1 macrophage polarization (98) and promotion of hepatic stellate cell apoptosis (99). Perhaps more encouraging, initial studies with a liver-selective NO donor, V-PVRRO/NO, which avoids the potential confounding factors of systemic NO delivery, including hypotension, have shown protection against drug induced (142) and bile duct ligation induced liver injury (143) and also reduced high fat diet induced hepatic steatosis by >50% (144). Targeting eNOS may also be a strategy for attenuating NASH development; mice treated with relaxin-2 increased hepatic eNOS activation and attenuated Kupffer cell and stellate cell activation in methionine–choline-deficient (MCD) diet-induced NASH (145). Collectively, these data demonstrate an association between loss of hepatic eNOS function and NASH. Importantly, increasing hepatic eNOS and NO shows promise as a potential therapeutic to curb advanced liver disease progression, possibly by attenuating hepatic inflammation. Future studies overexpressing hepatocellular eNOS in the face of a liver insult would help identify its role in mitigating NASH development.

Autophagy – An overview

Autophagy is a highly conserved process across all eukaryotic organisms involving the self-degradation of damaged and/or superfluous cellular components. The word originates from Greek "auto" meaning oneself, and "phagy" meaning to eat. Autophagy is a vital process in order to maintain cellular homeostasis by removing dysfunctional proteins, microbial invaders, or because the components are needed for energy and support cellular metabolism. The study of autophagy has garnered much interest in recent years due to its purported importance in human health and disease. Notably, the 2016 Nobel Prize in Physiology or Medicine was awarded to Dr. Yoshinori Ohsumi for his discovery and elucidation of the autophagy mechanisms in yeast while showing similar mechanisms are involved in mammalian cells. The process of breaking down and recycling of organelles have allowed cells to adapt and respond appropriately to different stressors by providing nutrients, as well as basal autophagy working as a housekeeping process to prevent toxicity from a buildup of damaged proteins. Hence, any deficiency in autophagy can lead to deleterious effects in cellular and systemic health. Impaired autophagy has been linked to a myriad of diseases; neurodegenerative diseases (146), cancer (147), aging (148), and obesity and metabolism related disorders (149), including NAFLD, NASH, and liver cancer (150, 151).

Autophagy forms and mechanisms

The current study of autophagy identifies three different form: macroautophagy, microautophagy, and chaperone-mediated autophagy. Macroautophagy, hereafter simply called autophagy, involves the sequestration of cytosolic proteins into a doubled-walled

membrane termed the autophagosome, which is fused with the lysosome for enzymatic degradation. Microautophagy is the direct engulfment of cytoplasmic content by the lysosome and does not require the autophagosome formation. Chaperone-mediated autophagy involves molecular cytosolic chaperones unfolding targeted proteins before their translocation across the lysosomal membrane chaperones located in the lysosomal lumen.

Two forms of macroautophagy (autophagy) have been identified: selective and non-selective. Non-selective autophagy occurs during times of extreme nutrient depravation to supply the cell of metabolic building blocks and energy until homeostasis is reached (152). Selective autophagy serves as more of a quality control process in the cell, and therefore must be able to distinguish between protein aggregates and selected organelles, or functioning organelles from dysfunctional ones that have been targeted for degradation. The selective autophagic process and target an array of different organelles for degradation such as ribosomes (ribophagy), lipids (lipophagy), glycogen (glycophagy), and mitochondria (mitophagy), among others. Mitophagy is a vital process in cells to remover aberrant and dysfunctional mitochondria in order to maintain a healthy mitochondrial pool within the cell. Deficiency in the mitophagic process can cause a buildup of defective mitochondria, resulting in cell and tissue damage.

Regulation of autophagy

Autophagy occurs at basal levels to serve as a homeostatic function for cells but can be induced in certain physiological scenarios when required. In order to provide

intracellular nutrients and energy, autophagy is rapidly upregulated during periods of high energetic demand such as starvation or cellular structural remodeling. Autophagy can also be upregulated during pathological conditions where damaging organelles/proteins need removal, such as oxidative stress, infection, or protein aggregate accumulation. Further, other regulators of autophagy include temperature, acidity, oxygen concentrations, hormonal factors, and cellular density. These regulators of autophagy and the intricate role they play are outside the scope of this extended literature review, and are discussed in much greater detail elsewhere (149, 153).

Mechanisms of autophagy/mitophagy

When autophagy/mitophagy is upregulated, mTOR is inactivated which activates the autophagy related genes (Atg), specifically atg1 (mammalian homologue being Ulk1/2). The phosphorylation of the Ulk proteins activates further Atg proteins which ultimately result in the formation of the autophagosome (154). In tandem, upon autophagic stimulation, cytosolic LC3 (LC3-I) is conjugated to phosphatidylethanolamine to form LC3-phosphatidylethanolamine conjugate (LC3-II). This lipidated LC3-II is then recruited to autophagosome membranes to act as a 'docking station' for organelles targeted for degradation, including mitochondria. When mitochondria are damaged, their clearance via mitophagy is either through ubiquitin-dependent or independent mechanisms. The phosphatase and tensin homologue (PTEN)-induced putative kinase 1 (PINK1)–Parkin pathway is the regulator for ubiquitin-dependent mitophagy (155). During mitochondrial injury/loss of membrane potential, PINK1 is cleaved from the inner mitochondrial membrane and is stabilized on the outer mitochondrial membrane. Its

auto-phosphorylation results in cytosolic Parkin translocating to the mitochondrial surface, triggering and Parkin's E3 ligase activity and causes poly-ubiquitination. These poly-ubiquinated chains are phosphorylated by PINK1 and serves as a signal for these dysfunctional mitochondria to be targeted by autophagy proteins associated with the autophagosome. These adapter proteins, such as p62, recognize these ubiquitinated mitochondria and facilitate their binding to the autophagosome through LC3. Other mitochondrial receptors outside of the PINK1-Parkin pathway, such as BCL2/adenovirus E1B 19 kDa protein-interacting protein 3 (BNIP3), facilitate the mitochondrial fusion with the autophagosome via LC3, while also promoting fission of damaged organelles (101). There are also examples of crosstalk between these pathways, as BNIP3 helps stabilize PINK1 to the outer mitochondrial membrane during loss of membrane potential (156).

Mitophagy measurement

Traditional measurements of mitophagy consist of electron microscopy, where the mitochondria can be detected in autophagic and lysosomal membranes and provide a relatively sound measure of mitophagy. However, only a small section of cell/tissue can be examined at any one time by a trained eye, making this time consuming and difficult to quantify on a larger scale. Other markedly less robust but easier to measure indicators of mitophagy include the gene or protein expression of mitophagic genes/proteins such as BNIP3, Pink1, Parkin, p62, LC3, etc., but these are static measurements of the abundance of these markers at an arbitrary time point or time of animal sacrifice and do not give an accurate indication of mitophagic flux. The protein p62 can be used as a marker of

146

mitophagy, as it binds to LC3 and is degraded during lysosomal degradation, with decreased levels suggestive of increases mitophagy. Further, p62 accumulation can be seen in conditions of impaired mitophagy (157). As previously mentioned, the lipidated form of LC3 (LC3-II) is a surrogate marker of autophagosome formation (158); hence, the ratio of lipidated LC3-II to cytosolic LC3-I is a common marker for mitophagic flux as LC3-I should decrease while LC3-II increase upon mitophagic stimulation. However, LC3-II itself is degraded in the lysosome making interpretation of either total LC3-II or the ratio LC3-II/LC3-I difficult. To circumnavigate this, a much more robust and accurate measurement of mitophagy is monitoring levels of LC3-II between samples in the presence of lysosomal protease and enzymatic inhibitors such as leupeptin. Leupeptin is a membrane-permeable thiolprotease inhibitor that impairs the enzymatic and proteolytic activity of the lysosome, preventing the degradation and allowing accumulation of autophagosomes and their associated proteins.

Methods using dual-fluorescent probes that target the mitochondria and a key protein involved in mitophagy (often LC3) currently provide the most accurate method of active mitophagy, particularly if the fluorescents are pH dependent. The mt-Keima and mito-QC mouse model are the two prevailing methods using this dual-fluorescent approach for measuring mitophagy. As the Keima molecule is pH dependent and importantly resistant to degradation in the lysosome, it can be depicted at a red fluorescence in acidic conditions (pH ~4.5 in the lysosome), or fluoresce green in the relatively neutral acidity of the mitochondria (pH~8.0). Hence, the Keima molecule can be directed to the mitochondrial matrix in mice by a targeting sequence by COX VIII, and ultimately the

147

mt-Keima murine model allows detection of mitochondria in the acidic environment of the lysosome or not i.e. active mitophagy (159). This model detected a significant decrease in mitophagy in the livers of mice fed a high fat diet for 18 weeks compared to mice fed a low-fat diet. This suggests that mitophagy is decreased with a high fat diet/obesity, although does not rule out the possibility an initial compensatory increase in mitophagy during the diet.

The mito-QC model using a similar pH dependent, dual-fluorescent approach for mitophagy measurement, and was developed in part due to the limitations of the mt-Keima model such as the Keima protein's incompatibility with fixation and can also exhibit spectral overlap (160). The mito-QC model uses a dual mCherry-GFP tag (red and green, respectively) that fuses with an outer mitochondrial membrane (FIS1 for example). In basal conditions, both red and green colors fluoresce on the mitochondria, and upon mitophagic stimulation where the mitochondria are targeted and delivered to the autophagosome and ultimately the lysosome for degradation, the mCherry fluorescence remains stable whereas the green GFP is quenched in the acidic environment. Thus, just a red signal compared to a red/green (yellow) signal indicated active mitophagy. Interestingly, this model detected the kidney and liver to have the highest basal rate of mitophagy compared to the spleen, muscle, and heart (160). Currently, the dual fluorescence measurements of mitophagy are the gold standard, with lysosomal degradation inhibitors following closely behind due to their outcome of protein accumulation still a surrogate marker of flux. Despite the marked increase in ability to accurately measure mitophagy in recent years, the timeline of mitophagy and autophagy

148

during NAFLD development remains relatively unresolved, as well as the effect of using robust mitophagy measurements under different physiological conditions such as different diets and exercise.

Autophagy/mitophagy and NAFLD

Due to the high metabolic activity of the liver, autophagy becomes a vital component of facilitating the high turnover of cells and their cargo within the liver. Using perfused livers, it is estimated that basal autophagy degrades 1.5% of total hepatic protein per hour, with this increasing three-fold to 4.5% upon starvation (161). Additionally, glycophagy and lipophagy aid in the breakdown of hepatic glycogen and lipids respectively, during times of nutrient depravation to provide hepatocytes with energy (162). As such, livers deficient in autophagy develop pathophysiological issues. Mice lacking hepatic Atg7, a vital player in autophagosome formation, displayed impaired blood glucose regulation due the absence of autophagy-induced release of amino acids (163). Further, liver-specific Atg7 KO mice displayed grossly enlarged livers as well as altered morphology of mitochondria and peroxisomes, and the accumulation of polyubiquitinated proteins (164).

Due to the importance of a healthy mitochondrial pool within the liver, the role of mitophagy is vital in maintaining this pool via the removal of dysfunctional mitochondria. Indeed, impaired mitophagy in the liver leads to accumulation of dysfunctional mitochondria, increased oxidative stress, and elevated steatosis (57). Further, mice subjected to a methionine and choline deficient diet-induced NAFLD

149

displayed 'megamitochondria' and accumulation of mitophagy intermediates, indicative of impaired mitophagy (165). The authors went on to demonstrate mitophagy was significantly impaired in mice lacking liver-specific Drp1, a vital protein for mitochondrial division, as shown by the gold standard dual-florescence, pH sensitive mCherry-GFP mitochondrial tags (165). These mice also displayed enlarged mitochondria and accumulation of mitophagy intermediates, along with elevated serum ALT and hepatic triglyceride accumulation. Importantly, restoration of mitophagy in both mouse models reduced hepatic triglyceride and alleviated liver injury. These data demonstrate the importance of maintaining mitophagy in preventing NAFLD.

To further demonstrate the importance of mitophagy proteins in NAFLD prevention, whole body BNIP3 null mice were generated, a key protein in the docking of dysfunctional mitochondria to the autophagosome. These mice displayed elevated mitochondrial mass as measured by mitochondrial proteins and genome copy number (58). Despite elevated mass, these mitochondria exhibited reduced beta-oxidation, membrane potential, and oxygen consumption, suggesting an impaired ability to remove dysfunctional mitochondria compared to WT mice. This resulted in increased liver triglycerides, and elevated markers of hepatic lipogenesis and inflammation. These data further highlight the importance of mitophagy in limiting abnormal mitochondrial number and maintaining their integrity for the attenuation of hepatic steatosis development.

While it is clear that impairment of autophagy and mitophagy are detrimental to hepatic mitochondrial health and NAFLD development, how environmental/lifestyle factors such

as diet and exercise (discussed later) effect hepatic autophagy is an ongoing area of research. The prevailing notion is that hepatic autophagy is decreased with a high fat or western diet-induced hepatic steatosis and NAFLD development (166-168). Mechanisms of action include suppression of autophagic genes and reduced protein abundance with elevated steatosis, but also may be due to an impaired enzymatic activity and acidification of the lysosome to degrade its contents (169, 170). In isolated hepatocytes from *ob/ob* mice with confirmed steatosis via BODIPY staining, elevated autophagosome formation was observed along with elevated p62 compared to hepatocytes from control fed mice (169). Although fusion of the autophagosome with the lysosome was not impaired, the acidification of the autolysosome was significantly reduced in hepatocytes from *ob/ob* mice. This suggests that elevated autophagosome formation (commonly measured by LC3-II/LC3-I accumulation), may infer an artificially high rate of autophagy/mitophagy as these autophagosomes are not being degraded by the lysosome due to elevated hepatic steatosis. Thus, the results of investigating the effects of obesity/obesogenic diets on hepatic autophagy/mitophagy are equivocal; with some studies showing elevated hepatic autophagy with HFD or obesity (171, 172), and some showing hepatic autophagy is reduced with NAFLD development (169, 173). To fully elucidate the auto- and mitophagic capacity of the liver during diet-induced NAFLD, more robust autophagy and mitophagy techniques are required, such as dual fluorescent imaging and lysosomal degradation inhibitors. Both of these methods bypass the issue of impaired lysosomal acidification that can be seen with hepatic steatosis. As previously mentioned, the mT-Keima model showed reductions in murine hepatic mitophagy after 18 weeks of a western diet (159). However, measurements at multiple timepoints is

151

required to fully resolve the hepatic autophagy and mitophagy capacity in NAFLD development.

eNOS and autophagy/mitophagy

While there is clear evidence for a role of eNOS in the process of mitochondrial biogenesis as discussed previously, little is known about the ability of eNOS to regulate autophagy and mitophagy. Interestingly, an argument can be made for the requirement of functional autophagy and mitophagy for the induction of eNOS. The compound simvastatin is a well-established activator of eNOS (174, 175), possibly through the induction of mitophagy. Simvastatin administration had no effect on cardio protection in Parkin KO mice vs WT controls, where it suppressed mTOR and increased autophagy in cardiomyocytes (176). Further, decreases eNOS activity in endothelial cells was associated with impaired autophagic flux (177), while bafilomycin-induced inhibition of autophagy abrogated the insulin-induced activation of eNOS. Additionally, 10 weeks of rapamycin treatment in mice (autophagy activator) caused increases in total and phosphorylated eNOS protein expression in aortas (178). Collectively, these data suggest that intact autophagy is required for the activation of eNOS.

Recent work from our lab has demonstrated the reverse relationship between eNOS and autophagy/mitophagy; by identifying hepatocellular eNOS as a novel regulator of mitochondrial homeostasis and maintaining mitophagic capacity (1). Hepatic mitochondria from eNOS null mice displayed decreased markers of mitochondrial biogenesis (PGC1α, TFAM) and autophagy/mitophagy (BNIP3, LC3-II/LC3-I). In

152

addition, in vitro siRNA-induced knockdown of eNOS in primary hepatocytes reduced

fatty acid oxidation and impaired the induction of BNIP3 upon mitophagic stimulation.

Collectively, these data demonstrate a novel role for hepatocellular eNOS in maintaining

a healthy mitochondrial pool within the hepatocyte via the maintenance of mitophagic

capacity, and may contribute to curbing NAFLD development (**Figure 5.1**). These

studies taken together clearly outline a dynamic relationship between

autophagy/mitophagy and eNOS activity, with manipulation of one causing a knock-on

effect in the other. Further *in vivo* manipulation of hepatocellular eNOS is required to

tease out its significance in hepatic autophagy/mitophagy, and whether these effects are

mediated eNOS derived NO. The direct effects of NO on global autophagy and

mitophagy will be discussed in greater detail later in this extended literature review.

Nitric oxide and autophagy/mitophagy

It has been shown that oxidative stress and reactive oxygen species are inducers of

autophagy in response to damaged or limiting damage to organelles (179, 180). However,

the role of nitric oxide (NO) in the autophagy/mitophagy process is equivocal. As

previously stated, AMPK is a potent activator of Ulk1 (61) and one of the key initiators

of autophagy. NO was shown to increase AMPK activity when L6 myotubes treated with

nitric oxide donors (S-nitroso-N-penicillamine – SNAP 25 µM and DETA NONOate

50µM), while AICAR-induced AMPK phosphorylation was prevented by NOS-inhibitors

(l-NG-monomethyl arginine - L-NAME, 1mM) (60). Hence, it could be postulated that

NO may induce autophagy via AMPK activation. Indeed, enhanced NO production via

the NO donor sodium nitroprusside (SNP), increased protein markers of autophagy and

153

increased the number of acidic autophagolysosomal vacuoles in human dental pulp cells

(HDPCs) (181). Increased NO via SNP activated AMPK and Ulk1 signaling, while

inhibiting AMPK enhanced apoptotic cell death induced by SNP in the HDPCs, further

solidifying the NO/AMOK/Ulk1 dynamic. In breast cancer cells, the combination of

increased AMPK activation and decreased mTOR activity in response to NO exposure

led to increased Ulk1 phosphorylation and autophagy initiation (63). This initiation was

measured by an increase in LC3-II/LC3-I ratio as well as increased GFP-LC3 puncta

acidity of lysosomal vesicles, while p62 levels decreased as it got degraded with

increasing levels of lysosomal formation. Interestingly, increased NO (NONOate, an NO

donor) and over expression of eNOS (A23187, an eNOS activator), increased Ulk1

protein and stabilized SIRT1 protein, with this phenomenon abolished in Ulk1-siRNA-

treated endothelial cells or in embryonic fibroblasts from *Ulk1−/−* mice (182). Despite

increased Ulk1 phosphorylation, elevated NO and eNOS activation did not have a

significant effects on autophagy markers such as GFP-LC3 puncta, and p62 and LC3-II

protein expression. This suggests that regulation of Ulk1 by NO or eNOS may be

independent of autophagy, at least in endothelial cells.

Further confirming the effects of NO on autophagy, it was recently shown that NO

impairs autophagosome synthesis and ultimately autophagy in rat cortical neurons and

HeLa cells (183). In response to NO donors (NONOnate 500µM) in both basal and

starved conditions, authors demonstrated reduced LC3-II levels and reduced

autophagosome synthesis as measured by the dual fluorescent labelled autophagosomes

(mRFP-GFP-LC3) emitting more GFP signal because of reduced quenching of the GFP

154

in the acidic lysosomal environment. Interestingly, NO donors S-nitrosylated IKKβ and reduced its phosphorylation, resulting in decrease AMPK phosphorylation in mouse embryonic fibroblasts, leading to an increase in mTOR activity. Further, NOS overexpression in HEK293 cell lines, elevating their basal NO levels due to the absence of NO isoforms in control HEK293 cells, displayed decreased LC3-II levels and autophagosome synthesis compared to control cells; which was rescued L-NAME (100µM) exposure. At the same concentration, L-NAME increased autophagosome synthesis in mouse primary cortical neurons and HeLa cells under basal conditions, comparable to rapamycin. However, the authors only use DAF-2DA fluorescent dye to merely confirm the increase in NO in HEK293 cells with NOS overexpression, or its decrease with L-NAME administration. Given that varying NO levels can have extremely different physiological outcomes (nM for physiological levels, µM for pathophysiologic levels), precise measurement or surrogate markers of NO may be required to endure adequate conclusions can be drawn.

The results by Sakar and colleagues (183) are in stark discordance with the previous studies investigating the effects of NO on autophagy and AMPK phosphorylation (60, 63). These discrepancies may be due to variations in cell lines used; myotubes, HDPCs, endothelial cells, vs rat cortical neurons, HeLa cells, mouse embryonic fibroblasts, and HEK293 cell lines. Importantly, given that varying NO levels can have extremely different physiological outcomes (nM for physiological levels, µM for pathophysiologic levels), the concentrations of compounds used to manipulate NO can have profound effects on the outcome. One previously mentioned study increased AMPK activity in

155

myotubes with 50µM of DETA NONOate (NO donor) (60), while Sakar et al. showed

AMPK activity was decreased in mouse embryonic fibroblasts with 500µM of DETA

NONOate. While this may be due to differences in cell types, the 10-fold difference in

DETA NONOate added to the embryonic fibroblasts may have induced

pathophysiological levels of NO (which were not measured in either cell samples).

Similarly, decreased autophagy and AMPK phosphorylation was seen with

administration of 500µM of NONOate in cortical neurons and HeLa cells (183),

compared with Tripathi et al. showing exogenous NO (steady-state concentration of 11

µM NO over time) increased AMPK activity and LC3-II/LC3-I in MCF-7 breast cancer

cells (63). Of note, the cortical neurons and HeLa cells were stimulated with growth

media every 8 hours for 24 hours, and the increased nutrient load may have inhibited

autophagy initiation, and may explain the discordant observations with AMPK activity as

this is the energy sensor of the cell. Moreover, Sakar et al. saw NO-induced reductions in

autophagy when examined at 24 hours, as opposed to NO-induction of autophagy when

examined in a 2-8 hour window post exposure by Tripathi et al. (63). This suggests that

NO may be mediating its effect in a time dependent manner, with initial NO exposure

sufficient to induce autophagy, whereas over exposure or long duration exposure to NO

may inhibit autophagy.

Although speculative, these data suggest that while differences in cell types may account

for the opposite outcomes, at very high pathophysiological levels NO may act to inhibit

autophagy, whereas the regulation of autophagy via NO occurs at much lower

physiological levels. Hence, manipulating hepatocellular eNOS, which produces NO at

156

physiological levels, may be sufficiently sensitive to elicit alterations in hepatic autophagy/mitophagy. Similarly, NO's regulation of autophagy may be time sensitive, and the potential early effects of NO on autophagy may be missed if outcomes are examined at a later time. To truly determine the effects of NO of autophagy/mitophgay, NO would be titrated to various levels across multiple cell lines and multiple time points before manipulating NO *in vivo* and using gold standard measurements of autophagy/mitophagy.

Autophagy/mitophagy and exercise

There is well-established evidence for exercise as a potent inducer for autophagy and mitophagy across an array of tissues (106, 109). as mitophagy is induced to counteract the stress applied to the mitochondria during exercise (184). A key protein involved in this mitophagic induction is the energy sensing protein AMPK, whose activity is increased during exercise, and is known to promote autophagy by directly activating Ulk1 through phosphorylation of Ser 317 and Ser 777 (61). Following an acute bout and 90 min post exercise, gene expression of mitophagy related genes (p62 and LC3) were elevated in WT but not PGC-1α KO mice (185). Prior to the exercise bout, a subset of animals were injected with colchicine to block autophagosome degradation and cause an accumulation of mitophagy related proteins in order to assess mitophagic flux in these animals. Following gene expression trends, LC3-II accumulation was markedly elevated in both whole muscle and isolated muscle mitochondria in WT mice following exercise, although this effect was significantly attenuated in PGC-1α KO mice animals. These results indicate that exercise is an acute stimulator of mitophagy, which is mediated in

157

part by PGC-1α (185). Similar inductions in mitophagy are seen with longer-term exercise training. Basal autophagy/mitophagy was elevated in skeletal muscle after 4 weeks of VWR in mice, as measured by increased LC3-II/LC3-I ratio, BNIP3, and decreased p62 accumulation, indicative of higher rates of initiation and resolution of autophagic events (109). Notably, Atg6$^{+/-}$ mice, that have reduced expression of the Atg6 protein required for autophagosome formation, had completely attenuated exercise-induced increases in autophagy/mitophagy, mitochondrial content, and maximal endurance tests as compared to WT mice. These differences were seen despite similar basal autophagy and VWR distances between Atg6$^{+/-}$ and WT mice, indicating that fully functional autophagy/mitophagy is required for exercise training-induced improvements in skeletal muscle mitochondrial adaptations and physical performance.

Although limited studies have been conducted in this area, exercise is also a potent stimulator of autophagy/mitophagy in the liver. In one study, male mice were given either a LFD or WD for 4 weeks, then exposed to VWR or kept sedentary for an additional 4 weeks (35). Regardless of diet, VWR mice displayed 50% greater LC3-II/I ratio and 40% lower p62 protein content, indicative of increased basal mitophagy. Yet, with no autophagy/mitophagy inhibitor, basal autophagy measures do not provide an accurate indication of mitophagic flux or capacity. To provide a more accurate measure of autophagy/mitophagy, mice that transgenically express a green fluorescent protein (GFP)-labelled marker of autophagosomes (GFP–LC3), had elevated GFP-LC3 puncta in the liver after both acute and chronic exercise treadmill training (108). Further, mice with a mutated BCL2 gene (autophagy initiator) exhibited less exercise-induced hepatic LC3-

II conversion, p62 degradation, and hepatic steatosis resolution compared to WT mice, highlighting the importance of autophagy for exercise-induced amelioration of NAFLD. Overall, exercise seems to be an inducer of hepatic mitophagy, although the body of literature is limited. More recent studies investigating the dynamics of exercise and hepatic mitophagy in the context of sex differences are discussed below. As the exact mechanisms behind the exercise-induced benefit to the liver and liver mitochondria are relatively unresolved, the effect of exercise on hepatic autophagy/mitophagy may be a fruitful avenue of research into potential mechanisms of action.

Sex differences with hepatic mitophagy

There is a paucity of literature examining sex differences in hepatic mitophagy. Female rodents are known to be protected against hepatic steatosis development, while showing inherent differences in hepatic mitochondrial metabolism (64, 65). Despite this, the mechanisms conferring this protection against NAFLD development is unresolved. Female mice are not only protected from hepatic steatosis compared to male mice, but also displayed elevated markers of mitochondrial biogenesis and mitophagy, regardless of maternal condition (66). Similarly, we have shown that female rats have higher markers of mitochondrial biogenesis (TFAM), mitophagy (LC3-II/I, ATG12:5), and cellular energy homeostasis (AMPK) compared to males, regardless of diet (67).

To elucidate the importance of key proteins involved in mitochondrial biogenesis and mitophagy, BNIP3 and PGC-1α, in response to exercise, sex, and high fat diet, male and female hepatic-specific PGC-1α$^{+/-}$ and BNIP3 KO mice were fed either a low or high fat

diet for 16 weeks, with a third cohort having access to VWR for the final 8 weeks (68).

High fat diet feeding and VWR increased basal and maximal mitochondrial respiration,

although this ablated the response in BNIP3 null mice. Interestingly, BNIP3 null mice

maintained their ability to reduce H_2O_2 emissions via VWR, indicative of increased

mitochondrial coupling, regardless of sex. These data suggest that the mitochondrial

adaptive response to HFD and VWR is mediated in part by hepatic BNIP3, while

adaptive mitochondrial coupling efficiency may be facilitated by alternative mitophagy

pathways (Pink1, Parkin, Nix, etc.) maintaining mitochondrial function during BNIP3

deficiency. Regardless of condition or genotype, female mice possessed increased hepatic

mitochondrial respiratory coupling control, lower H_2O_2 emission, and protection against

steatosis and markers of fibrosis compared with males. In a similar study, male and

female liver-specific PGC-1$\alpha^{+/-}$ and BNIP3 KO were maintained in low fat diet

conditions with or without VWR for 4 weeks (69). Interestingly, PGC-1$\alpha^{+/-}$ and BNIP3

KO mice displayed similar VWR-induced mitochondrial adaptations to WT mice, but

BNIP3 KO mice had elevated mitochondrial content due to repressed mitochondrial

turnover. In concordance with the previous study, female mice displayed elevated

mitochondrial content, maximal mitochondrial respiration, reduced H_2O_2 emissions, and

reduced mitophagic flux, compared to males regardless of genotype or VWR. Female

mice had reduced accumulation of LC3-II and p62 in response to leupeptin injection

(autophagy inhibitor) compared to male mice, with authors suggesting that the increased

mitochondrial coupling efficiency in female mice requires less need for mitochondrial

turnover. For male mice, VWR was required to bring them to the level of LC3-II and p62

accumulation of sedentary female mice.

Taken together, both of these studies demonstrate that mitochondrial adaptations to VWR or HFD are mostly mediated by sex, and not solely dependent on hepatic PGC-1α and BNIP3. Further studies are required to determine if other pathways in mitochondrial dynamics are upregulated in order to maintain mitochondrial health in these conditions. These studies indicate that female mice possess elevated hepatic mitochondrial content, respiratory capacity, and lower reactive oxygen species emission compared to male mice, regardless of physical activity. As such, females had a lower need for mitophagy, reflected in lower mitophagy flux. Males required VWR to achieve the healthy hepatic mitochondrial phenotype seen in female mice; whereas, female mice had markedly fewer hepatic adaptations to VWR, and female mice may require further stressors to the system (such as treadmill training) in order to see VWR mitochondrial adaptions. Collectively, these data indicate that females confer some protection against hepatic steatosis, potentially due to their higher hepatic mitochondrial function compared to male mice. Further, while certain studies show mitophagic flux is lower in females (68, 69), this is likely due to a healthier mitochondrial pool within the hepatocyte, and females may possess a higher capacity for mitophagy given the marked increase in static content markers of mitophagy (66, 67). Further studies are warranted to elucidate the mechanisms behind the sexual dimorphisms of hepatic mitochondrial health.

Conclusion

Significant strides in recent years in teasing out the molecular mechanisms of NAFLD development and progression have been made, including the pathological role of hepatic

mitochondrial dysfunction. Given the well-characterized role of eNOS in mitochondrial dynamics in an array of tissues, including exercise-induced mitochondrial adaptations, one could speculate that eNOS is also functioning to maintain a healthy mitochondrial pool in hepatocytes. Indeed, data from our group have identified a novel role for hepatocellular eNOS in NAFLD development which furthers the understanding of the molecular mechanisms involved in NAFLD pathogenesis. Future studies should seek to further elucidate the role of hepatocellular eNOS via direct manipulation, i.e. in vivo hepatocyte-specific gain and loss of function studies, and whether hepatocellular eNOS is required for hepatic mitochondrial adaptations to exercise. Moreover, whether eNOS exerts its effects via NO-dependent mechanisms needs to be resolved, and to confirm the role of NO in hepatic autophagy/mitophagy during NAFLD development. Uncovering a role for hepatocellular eNOS may improve our knowledge of NAFLD pathogenesis, but more importantly, also may provide a potential therapeutic target to attenuate hepatic mitochondrial dysfunction and curb NAFLD development.

BIBLIOGRAPHY

1.   Sheldon RD, Meers GM, Morris EM, Linden MA, Cunningham RP, Ibdah JA, Thyfault JP, Laughlin MH, Rector RS. eNOS deletion impairs mitochondrial quality control and exacerbates Western diet-induced NASH. *American Journal of Physiology-Endocrinology and Metabolism*. 2019;317(4):E605-E16.

2.   Buzzetti E, Pinzani M, Tsochatzis EA. The multiple-hit pathogenesis of non-alcoholic fatty liver disease (NAFLD). *Metabolism*. 2016;65(8):1038-48.

3.   Brunt EM. Pathology of nonalcoholic fatty liver disease. *Nature Reviews Gastroenterology and Hepatology*. 2010;7(4):195-203.

4.   Vernon G, Baranova A, Younossi Z. Systematic review: the epidemiology and natural history of non-alcoholic fatty liver disease and non-alcoholic steatohepatitis in adults. *Alimentary pharmacology & therapeutics*. 2011;34(3):274-85.

5.   Chalasani N, Younossi Z, Lavine JE, Diehl AM, Brunt EM, Cusi K, Charlton M, Sanyal AJ. The diagnosis and management of non-alcoholic fatty liver disease: practice Guideline by the American Association for the Study of Liver Diseases, American College of Gastroenterology, and the American Gastroenterological Association. *Hepatology (Baltimore, Md.)*. 2012;55(6):2005-23.

6.   Lonardo A, Bellentani S, Argo CK, Ballestri S, Byrne CD, Caldwell SH, Cortez-Pinto H, Grieco A, Machado MV, Miele L. Epidemiological modifiers of non-alcoholic fatty liver disease: Focus on high-risk groups. *Digestive and Liver Disease*. 2015;47(12):997-1006.

7.   Lonardo A, Carani C, Carulli N, Loria P. 'Endocrine NAFLD'a hormonocentric perspective of nonalcoholic fatty liver disease pathogenesis. *Journal of hepatology*. 2006;44(6):1196-207.

8.   Wong RJ, Aguilar M, Cheung R, Perumpail RB, Harrison SA, Younossi ZM, Ahmed A. Nonalcoholic steatohepatitis is the second leading etiology of liver disease among adults awaiting liver transplantation in the United States. *Gastroenterology*. 2015;148(3):547-55.

9.   Targher G, Marra F, Marchesini G. Increased risk of cardiovascular disease in non-alcoholic fatty liver disease: causal effect or epiphenomenon? *Diabetologia*. 2008;51(11):1947-53.

10.   Stepanova M, Rafiq N, Makhlouf H, Agrawal R, Kaur I, Younoszai Z, McCullough A, Goodman Z, Younossi ZM. Predictors of all-cause mortality and liver-related mortality in patients with non-alcoholic fatty liver disease (NAFLD). *Digestive diseases and sciences*. 2013;58(10):3017-23.

11. Musso G, Gambino R, Cassader M, Pagano G. Meta-analysis: natural history of non-alcoholic fatty liver disease (NAFLD) and diagnostic accuracy of non-invasive tests for liver disease severity. *Annals of medicine*. 2011;43(8):617-49.

12. Fang YL, Chen H, Wang CL, Liang L. Pathogenesis of non-alcoholic fatty liver disease in children and adolescence: From "two hit theory" to "multiple hit model". *World Journal of Gastroenterology : WJG*. 2018;24(27):2974-83.

13. Donnelly KL, Smith CI, Schwarzenberg SJ, Jessurun J, Boldt MD, Parks EJ. Sources of fatty acids stored in liver and secreted via lipoproteins in patients with nonalcoholic fatty liver disease. *The Journal of clinical investigation*. 2005;115(5):1343-51.

14. Panasevich MR, Meers GM, Linden MA, Booth FW, Perfield JW, Fritsche KL, Wankhade UD, Chintapalli SV, Shankar K, Ibdah J. High fat, high fructose, high cholesterol feeding causes severe NASH and cecal microbiota dysbiosis in juvenile Ossabaw swine. *American Journal of Physiology-Endocrinology and Metabolism*. 2017.

15. Panasevich MR, Morris EM, Chintapalli SV, Wankhade UD, Shankar K, Britton SL, Koch LG, Thyfault JP, Rector RS. Gut Microbiota are Linked to Increased Susceptibility to Hepatic Steatosis in Low Aerobic Capacity Rats Fed an Acute High Fat Diet. *American Journal of Physiology-Heart and Circulatory Physiology*. 2016.

16. Poeta M, Pierri L, Vajro P. Gut-Liver Axis Derangement in Non-Alcoholic Fatty Liver Disease. *Children (Basel, Switzerland)*. 2017;4(8).

17. Nassir F, Ibdah JA. Role of mitochondria in nonalcoholic fatty liver disease. *International journal of molecular sciences*. 2014;15(5):8713-42.

18. Pessayre D, Fromenty B. NASH: a mitochondrial disease. *Journal of hepatology*. 2005;42(6):928-40.

19. Caldwell SH, Swerdlow RH, Khan EM, Iezzoni JC, Hespenheide EE, Parks JK, Parker WD, Jr. Mitochondrial abnormalities in non-alcoholic steatohepatitis. *Journal of hepatology*. 1999;31(3):430-4.

20. Wei Y, Rector RS, Thyfault JP, Ibdah JA. Nonalcoholic fatty liver disease and mitochondrial dysfunction. *World Journal of Gastroenterology : WJG*. 2008;14(2):193-9.

21. Rector RS, Thyfault JP, Uptergrove GM, Morris EM, Naples SP, Borengasser SJ, Mikus CR, Laye MJ, Laughlin MH, Booth FW. Mitochondrial dysfunction precedes insulin resistance and hepatic steatosis and contributes to the natural history of non-alcoholic fatty liver disease in an obese rodent model. *Journal of hepatology*. 2010;52(5):727-36.

22.   Sunny NE, Parks EJ, Browning JD, Burgess SC. Excessive hepatic mitochondrial TCA cycle and gluconeogenesis in humans with nonalcoholic fatty liver disease. *Cell metabolism*. 2011;14(6):804-10.

23.   Fletcher JA, Deja S, Satapati S, Fu X, Burgess SC, Browning JD. Impaired ketogenesis and increased acetyl-CoA oxidation promote hyperglycemia in human fatty liver. *JCI insight*. 2019;5.

24.   Koliaki C, Szendroedi J, Kaul K et al. Adaptation of hepatic mitochondrial function in humans with non-alcoholic fatty liver is lost in steatohepatitis. *Cell Metab*. 2015;21(5):739-46.

25.   Morris EM, Rector RS, Thyfault JP, Ibdah JA. Mitochondria and redox signaling in steatohepatitis. *Antioxidants & redox signaling*. 2011;15(2):485-504.

26.   Guo R, Liong EC, So KF, Fung M-L, Tipoe GL. Beneficial mechanisms of aerobic exercise on hepatic lipid metabolism in non-alcoholic fatty liver disease. *Hepatobiliary & Pancreatic Diseases International*. 2015;14(2):139-44.

27.   Shojaee-Moradie F, Cuthbertson D, Barrett M, Jackson N, Herring R, Thomas E, Bell J, Kemp G, Wright J, Umpleby A. Exercise training reduces liver fat and increases rates of VLDL clearance but not VLDL production in NAFLD. *The Journal of Clinical Endocrinology & Metabolism*. 2016;101(11):4219-28.

28.   Rabøl R, Petersen KF, Dufour S, Flannery C, Shulman GI. Reversal of muscle insulin resistance with exercise reduces postprandial hepatic de novo lipogenesis in insulin resistant individuals. *Proceedings of the National Academy of Sciences*. 2011;108(33):13705-9.

29.   Linden MA, Fletcher JA, Morris EM, Meers GM, Laughlin MH, Booth FW, Sowers JR, Ibdah JA, Thyfault JP, Rector RS. Treating NAFLD in OLETF rats with vigorous-intensity interval exercise training. *Med Sci Sports Exerc*. 2015;47(3):556-67.

30.   Rector RS, Uptergrove GM, Morris EM, Borengasser SJ, Laughlin MH, Booth FW, Thyfault JP, Ibdah JA. Daily exercise vs. caloric restriction for prevention of nonalcoholic fatty liver disease in the OLETF rat model. *Am J Physiol Gastrointest Liver Physiol*. 2011;300(5):G874-83.

31.   Keating SE, Hackett DA, George J, Johnson NA. Exercise and non-alcoholic fatty liver disease: a systematic review and meta-analysis. *Journal of hepatology*. 2012;57(1):157-66.

32.   Hallsworth K, Fattakhova G, Hollingsworth KG, Thoma C, Moore S, Taylor R, Day CP, Trenell MI. Resistance exercise reduces liver fat and its mediators in non-alcoholic fatty liver disease independent of weight loss. *Gut*. 2011:gut. 2011.242073.

33.   Fletcher JA, Meers GM, Linden MA, Kearney ML, Morris EM, Thyfault JP, Rector RS. Impact of various exercise modalities on hepatic mitochondrial function. *Med Sci Sports Exerc*. 2014;46(6):1089-97.

34.   Rector RS, Thyfault JP, Morris RT, Laye MJ, Borengasser SJ, Booth FW, Ibdah JA. Daily exercise increases hepatic fatty acid oxidation and prevents steatosis in Otsuka Long-Evans Tokushima Fatty rats. *Am J Physiol Gastrointest Liver Physiol*. 2008;294(3):G619-26.

35.   Rosa-Caldwell ME, Lee DE, Brown JL, Brown LA, Perry RA, Jr., Greene ES, Carvallo Chaigneau FR, Washington TA, Greene NP. Moderate physical activity promotes basal hepatic autophagy in diet-induced obese mice. *Appl Physiol Nutr Metab*. 2017;42(2):148-56.

36.   Dethlefsen MM, Kristensen CM, Tøndering AS, Lassen SB, Ringholm S, Pilegaard H. Impact of liver PGC-1α on exercise and exercise training-induced regulation of hepatic autophagy and mitophagy in mice on HFF. *Physiological reports*. 2018;6(13):e13731-e.

37.   Martínez-Ruiz A, Cadenas S, Lamas S. Nitric oxide signaling: classical, less classical, and nonclassical mechanisms. *Free Radical Biology and Medicine*. 2011;51(1):17-29.

38.   Förstermann U, Sessa WC. Nitric oxide synthases: regulation and function. *European heart journal*. 2012;33(7):829-37, 37a-37d.

39.   Bendall JK, Alp NJ, Warrick N, Cai S, Adlam D, Rockett K, Yokoyama M, Kawashima S, Channon KM. Stoichiometric relationships between endothelial tetrahydrobiopterin, endothelial NO synthase (eNOS) activity, and eNOS coupling in vivo: insights from transgenic mice with endothelial-targeted GTP cyclohydrolase 1 and eNOS overexpression. *Circulation research*. 2005;97(9):864-71.

40.   Kietadisorn R, Juni RP, Moens AL. Tackling endothelial dysfunction by modulating NOS uncoupling: new insights into its pathogenesis and therapeutic possibilities. *American journal of physiology. Endocrinology and metabolism*. 2012;302(5):E481-95.

41.   Fleming I, Busse R. Molecular mechanisms involved in the regulation of the endothelial nitric oxide synthase. *American Journal of Physiology-Regulatory, Integrative and Comparative Physiology*. 2003;284(1):R1-R12.

42.   Takahashi S, Mendelsohn ME. Synergistic activation of endothelial nitric-oxide synthase (eNOS) by HSP90 and Akt Calcium-independent eNOS activation involves formation of an HSP90-Akt-CaM-bound eNOS complex. *Journal of Biological Chemistry*. 2003;278(33):30821-7.

43. Rockey DC, Chung JJ. Reduced nitric oxide production by endothelial cells in cirrhotic rat liver: endothelial dysfunction in portal hypertension. *Gastroenterology*. 1998;114(2):344-51.

44. Shah V, Toruner M, Haddad F, Cadelina G, Papapetropoulos A, Choo K, Sessa WC, Groszmann RJ. Impaired endothelial nitric oxide synthase activity associated with enhanced caveolin binding in experimental cirrhosis in the rat. *Gastroenterology*. 1999;117(5):1222-8.

45. Nozaki Y, Fujita K, Wada K, Yoneda M, Shinohara Y, Imajo K, Ogawa Y, Kessoku T, Nakamuta M, Saito S. Deficiency of eNOS exacerbates early-stage NAFLD pathogenesis by changing the fat distribution. *BMC gastroenterology*. 2015;15(1):177.

46. Sheldon RD, Padilla J, Jenkins NT, Laughlin MH, Rector RS. Chronic NOS inhibition accelerates NAFLD progression in an obese rat model. *American Journal of Physiology-Gastrointestinal and Liver Physiology*. 2015;308(6):G540-G9.

47. Sheldon RD, Laughlin MH, Rector RS. Reduced hepatic eNOS phosphorylation is associated with NAFLD and type 2 diabetes progression and is prevented by daily exercise in hyperphagic OLETF rats. *J Appl Physiol* 2014;116(9):1156-64.

48. Jiang R, Wang S, Takahashi K, Fujita H, Fruci CR, Breyer MD, Harris RC, Takahashi T. Generation of a conditional allele for the mouse endothelial nitric oxide synthase gene. *Genesis (New York, N.Y. : 2000)*. 2012;50(9):685-92.

49. Nisoli E, Carruba MO. Nitric oxide and mitochondrial biogenesis. *J Cell Sci*. 2006;119(Pt 14):2855-62.

50. Nisoli E, Clementi E, Paolucci C, Cozzi V, Tonello C, Sciorati C, Bracale R, Valerio A, Francolini M, Moncada S, Carruba MO. Mitochondrial biogenesis in mammals: the role of endogenous nitric oxide. *Science*. 2003;299(5608):896-9.

51. Nisoli E, Falcone S, Tonello C et al. Mitochondrial biogenesis by NO yields functionally active mitochondria in mammals. *Proc Natl Acad Sci U S A*. 2004;101(47):16507-12.

52. Nisoli E, Tonello C, Cardile A et al. Calorie restriction promotes mitochondrial biogenesis by inducing the expression of eNOS. *Science*. 2005;310(5746):314-7.

53. Trevellin E, Scorzeto M, Olivieri M et al. Exercise training induces mitochondrial biogenesis and glucose uptake in subcutaneous adipose tissue through eNOS-dependent mechanisms. *Diabetes*. 2014;63(8):2800-11.

54. Vettor R, Valerio A, Ragni M et al. Exercise training boosts eNOS-dependent mitochondrial biogenesis in mouse heart: role in adaptation of glucose

metabolism. *American journal of physiology. Endocrinology and metabolism*. 2014;306(5):E519-28.

55.   Sansbury BE, Cummins TD, Tang Y, Hellmann J, Holden CR, Harbeson MA, Chen Y, Patel RP, Spite M, Bhatnagar A, Hill BG. Overexpression of endothelial nitric oxide synthase prevents diet-induced obesity and regulates adipocyte phenotype. *Circulation research*. 2012;111(9):1176-89.

56.   Kim I, Rodriguez-Enriquez S, Lemasters JJ. Selective degradation of mitochondria by mitophagy. *Archives of biochemistry and biophysics*. 2007;462(2):245-53.

57.   Dorn GW. Mitochondrial pruning by Nix and BNip3: an essential function for cardiac-expressed death factors. *Journal of cardiovascular translational research*. 2010;3(4):374-83.

58.   Glick D, Zhang W, Beaton M, Marsboom G, Gruber M, Simon MC, Hart J, Dorn GW, Brady MJ, Macleod KF. BNip3 regulates mitochondrial function and lipid metabolism in the liver. *Molecular and cellular biology*. 2012;32(13):2570-84.

59.   Li Y, Chen Y. AMPK and Autophagy. *Advances in experimental medicine and biology*. 2019;1206:85-108.

60.   Lira VA, Brown DL, Lira AK, Kavazis AN, Soltow QA, Zeanah EH, Criswell DS. Nitric oxide and AMPK cooperatively regulate PGC-1α in skeletal muscle cells. *The Journal of physiology*. 2010;588(18):3551-66.

61.   Kim J, Kundu M, Viollet B, Guan K-L. AMPK and mTOR regulate autophagy through direct phosphorylation of Ulk1. *Nature cell biology*. 2011;13(2):132-41.

62.   Laker RC, Drake JC, Wilson RJ et al. Ampk phosphorylation of Ulk1 is required for targeting of mitochondria to lysosomes in exercise-induced mitophagy. *Nature communications*. 2017;8(1):548.

63.   Tripathi DN, Chowdhury R, Trudel LJ, Tee AR, Slack RS, Walker CL, Wogan GN. Reactive nitrogen species regulate autophagy through ATM-AMPK-TSC2– mediated suppression of mTORC1. *Proceedings of the National Academy of Sciences*. 2013;110(32):E2950-E7.

64.   Hart-Unger S, Arao Y, Hamilton KJ, Lierz SL, Malarkey DE, Hewitt SC, Freemark M, Korach KS. Hormone signaling and fatty liver in females: analysis of estrogen receptor α mutant mice. *International Journal of Obesity*. 2017;41(6):945-54.

65.   Reue K. Sex differences in obesity: X chromosome dosage as a risk factor for increased food intake, adiposity and co-morbidities. *Physiology & behavior*. 2017;176:174-82.

66.   Cunningham RP, Moore MP, Meers GM, Ruegsegger GN, Booth FW, Rector RS. Maternal Physical Activity and Sex Impact Markers of Hepatic Mitochondrial Health. *Med Sci Sports Exerc*. 2018;50(10):2040-8.

67.   Moore MP, Cunningham RP, Kelty TJ, Boccardi LR, Nguyen NY, Booth FW, Rector RS. Ketogenic diet in combination with voluntary exercise impacts markers of hepatic metabolism and oxidative stress in male and female Wistar rats. *Appl Physiol Nutr Metab*. 2020;45(1):35-44.

68.   McCoin CS, Von Schulze A, Allen J, Fuller KN, Xia Q, Koestler DC, Houchen CJ, Maurer A, Dorn 2nd GW, Shankar K. Sex modulates hepatic mitochondrial adaptations to high-fat diet and physical activity. *American Journal of Physiology-Endocrinology and Metabolism*. 2019;317(2):E298-E311.

69.   Von Schulze A, McCoin CS, Onyekere C, Allen J, Geiger P, Dorn GW, Morris EM, Thyfault JP. Hepatic mitochondrial adaptations to physical activity: impact of sexual dimorphism, PGC1α and BNIP3-mediated mitophagy. *The Journal of physiology*. 2018;596(24):6157-71.

70.   Fuller KNZ, McCoin CS, Allen J, Bell-Glenn S, Koestler DC, Dorn GW, Thyfault JP. Sex and BNIP3 genotype, rather than acute lipid injection, modulate hepatic mitochondrial function and steatosis risk in mice. *Journal of applied physiology (Bethesda, Md. : 1985)*. 2020;128(5):1251-61.

71.   Momken I, Lechene P, Ventura-Clapier R, Veksler V. Voluntary physical activity alterations in endothelial nitric oxide synthase knockout mice. *American journal of physiology. Heart and circulatory physiology*. 2004;287(2):H914-20.

72.   Younossi Z, Anstee QM, Marietti M, Hardy T, Henry L, Eslam M, George J, Bugianesi E. Global burden of NAFLD and NASH: trends, predictions, risk factors and prevention. *Nature reviews. Gastroenterology & hepatology*. 2018;15(1):11-20.

73.   Le Gouill E, Jimenez M, Binnert C, Jayet P-Y, Thalmann S, Nicod P, Scherrer U, Vollenweider P. Endothelial nitric oxide synthase (eNOS) knockout mice have defective mitochondrial β-oxidation. *Diabetes*. 2007;56(11):2690-6.

74.   Winn NC, Acin-Perez R, Woodford ML et al. A Thermogenic-Like Brown Adipose Tissue Phenotype Is Dispensable for Enhanced Glucose Tolerance in Female Mice. *Diabetes*. 2019;68(9):1717-29.

75.   Guguen-Guillouzo C. Isolation and culture of animal and human hepatocytes. *Culture of epithelial cells*. 2002;2:337-79.

76.   Morris EM, Meers GME, Booth FW, Fritsche KL, Hardin CD, Thyfault JP, Ibdah JA. PGC-1α overexpression results in increased hepatic fatty acid oxidation with

reduced triacylglycerol accumulation and secretion. *Am J Physiol Gastrointest Liver Physiol*. 2012;303(8):G979-G92.

77.   Azimifar SB, Nagaraj N, Cox J, Mann M. Cell-type-resolved quantitative proteomics of murine liver. *Cell metabolism*. 2014;20(6):1076-87.

78.   Werner M, Driftmann S, Kleinehr K et al. All-In-One: Advanced preparation of Human Parenchymal and Non-Parenchymal Liver Cells. *PLoS One*. 2015;10(9):e0138655.

79.   Win S, Than TA, Le BHA, García-Ruiz C, Fernandez-Checa JC, Kaplowitz N. Sab (Sh3bp5) dependence of JNK mediated inhibition of mitochondrial respiration in palmitic acid induced hepatocyte lipotoxicity. *Journal of hepatology*. 2015;62(6):1367-74.

80.   Muoio DM, Way JM, Tanner CJ, Winegar DA, Kliewer SA, Houmard JA, Kraus WE, Dohm GL. Peroxisome proliferator-activated receptor-alpha regulates fatty acid utilization in primary human skeletal muscle cells. *Diabetes*. 2002;51(4):901-9.

81.   Haspel J, Shaik RS, Ifedigbo E, Nakahira K, Dolinay T, Englert JA, Choi AM. Characterization of macroautophagic flux in vivo using a leupeptin-based assay. *Autophagy*. 2011;7(6):629-42.

82.   Klionsky DJ, Abdelmohsen K, Abe A et al. Guidelines for the use and interpretation of assays for monitoring autophagy (3rd edition). *Autophagy*. 2016;12(1):1-222.

83.   Bryan NS, Grisham MB. Methods to detect nitric oxide and its metabolites in biological samples. *Free radical biology & medicine*. 2007;43(5):645-57.

84.   Syed AA, Lahiri S, Mohan D, Valicherla GR, Gupta AP, Kumar S, Maurya R, Bora HK, Hanif K, Gayen JR. Cardioprotective Effect of Ulmus wallichiana Planchon in β-Adrenergic Agonist Induced Cardiac Hypertrophy. *Front Pharmacol*. 2016;7:510-.

85.   Roy DG, Chen J, Mamane V et al. Methionine Metabolism Shapes T Helper Cell Responses through Regulation of Epigenetic Reprogramming. *Cell Metabolism*. 2020;31(2):250-66.e9.

86.   Yamada T, Murata D, Adachi Y et al. Mitochondrial Stasis Reveals p62-Mediated Ubiquitination in Parkin-Independent Mitophagy and Mitigates Nonalcoholic Fatty Liver Disease. *Cell Metab*. 2018;28(4):588-604.e5.

87.   Pucino V, Bombardieri M, Pitzalis C, Mauro C. Lactate at the crossroads of metabolism, inflammation, and autoimmunity. *European journal of immunology*. 2017;47(1):14-21.

88. Mándi Y, Vécsei L. The kynurenine system and immunoregulation. *Journal of neural transmission (Vienna, Austria : 1996)*. 2012;119(2):197-209.

89. Shah V, Haddad FG, Garcia-Cardena G, Frangos JA, Mennone A, Groszmann RJ, Sessa WC. Liver sinusoidal endothelial cells are responsible for nitric oxide modulation of resistance in the hepatic sinusoids. *The Journal of clinical investigation*. 1997;100(11):2923-30.

90. Shah V, Cao S, Hendrickson H, Yao J, Katusic ZS. Regulation of hepatic eNOS by caveolin and calmodulin after bile duct ligation in rats. *American Journal of Physiology-Gastrointestinal and Liver Physiology*. 2001;280(6):G1209-G16.

91. Pasarín M, La Mura V, Gracia-Sancho J, García-Calderó H, Rodríguez-Vilarrupla A, García-Pagán JC, Bosch J, Abraldes JG. Sinusoidal endothelial dysfunction precedes inflammation and fibrosis in a model of NAFLD. *PloS one*. 2012;7(4):e32785.

92. McNaughton L, Puttagunta L, Martinez-Cuesta MA, Kneteman N, Mayers I, Moqbel R, Hamid Q, Radomski MW. Distribution of nitric oxide synthase in normal and cirrhotic human liver. *Proceedings of the National Academy of Sciences*. 2002;99(26):17161-6.

93. Mei Y, Thevananther S. Endothelial nitric oxide synthase is a key mediator of hepatocyte proliferation in response to partial hepatectomy in mice. *Hepatology (Baltimore, Md.)*. 2011;54(5):1777-89.

94. Abudukadier A, Fujita Y, Obara A et al. Tetrahydrobiopterin has a glucose-lowering effect by suppressing hepatic gluconeogenesis in an endothelial nitric oxide synthase-dependent manner in diabetic mice. *Diabetes*. 2013;62(9):3033-43.

95. Mason MG, Nicholls P, Wilson MT, Cooper CE. Nitric oxide inhibition of respiration involves both competitive (heme) and noncompetitive (copper) binding to cytochrome c oxidase. *Proceedings of the National Academy of Sciences*. 2006;103(3):708-13.

96. Clementi E, Brown GC, Feelisch M, Moncada S. Persistent inhibition of cell respiration by nitric oxide: crucial role of S-nitrosylation of mitochondrial complex I and protective action of glutathione. *Proceedings of the National Academy of Sciences*. 1998;95(13):7631-6.

97. Brown GC, Borutaite V. Inhibition of mitochondrial respiratory complex I by nitric oxide, peroxynitrite and S-nitrosothiols. *Biochimica et Biophysica Acta (BBA)-Bioenergetics*. 2004;1658(1-2):44-9.

98. Seth RK, Das S, Pourhoseini S, Dattaroy D, Igwe S, Ray JB, Fan D, Michelotti GA, Diehl AM, Chatterjee S. M1 polarization bias and subsequent nonalcoholic

steatohepatitis progression is attenuated by nitric oxide donor DETA NONOate via inhibition of CYP2E1-induced oxidative stress in obese mice. *The Journal of pharmacology and experimental therapeutics*. 2015;352(1):77-89.

99. Langer DA, Das A, Semela D, Kang-Decker N, Hendrickson H, Bronk SF, Katusic ZS, Gores GJ, Shah VH. Nitric oxide promotes caspase-independent hepatic stellate cell apoptosis through the generation of reactive oxygen species. *Hepatology (Baltimore, Md.)*. 2008;47(6):1983-93.

100. Zhang J, Ney PAJCD, Differentiation. Role of BNIP3 and NIX in cell death, autophagy, and mitophagy. 2009;16(7):939-46.

101. Quinsay MN, Thomas RL, Lee Y, Gustafsson AB. Bnip3-mediated mitochondrial autophagy is independent of the mitochondrial permeability transition pore. *Autophagy*. 2010;6(7):855-62.

102. Kubli DA, Ycaza JE, Gustafsson AB. Bnip3 mediates mitochondrial dysfunction and cell death through Bax and Bak. *Biochem J*. 2007;405(3):407-15.

103. Lund J, Aas V, Tingstad RH, Van Hees A, Nikolić N. Utilization of lactic acid in human myotubes and interplay with glucose and fatty acid metabolism. *Sci Rep*. 2018;8(1):9814-.

104. Castro-Portuguez R, Sutphin GL. Kynurenine pathway, NAD(+) synthesis, and mitochondrial function: Targeting tryptophan metabolism to promote longevity and healthspan. *Experimental gerontology*. 2020;132:110841.

105. Sarkar S, Floto RA, Berger Z, Imarisio S, Cordenier A, Pasco M, Cook LJ, Rubinsztein DC. Lithium induces autophagy by inhibiting inositol monophosphatase. *The Journal of cell biology*. 2005;170(7):1101-11.

106. Yan Z, Lira VA, Greene NP. Exercise training-induced regulation of mitochondrial quality. *Exercise and sport sciences reviews*. 2012;40(3):159-64.

107. Fu T, Xu Z, Liu L et al. Mitophagy Directs Muscle-Adipose Crosstalk to Alleviate Dietary Obesity. *Cell reports*. 2018;23(5):1357-72.

108. He C, Bassik MC, Moresi V et al. Exercise-induced BCL2-regulated autophagy is required for muscle glucose homeostasis. *Nature*. 2012;481(7382):511-5.

109. Lira VA, Okutsu M, Zhang M, Greene NP, Laker RC, Breen DS, Hoehn KL, Yan Z. Autophagy is required for exercise training-induced skeletal muscle adaptation and improvement of physical performance. *FASEB journal : official publication of the Federation of American Societies for Experimental Biology*. 2013;27(10):4184-93.

110. Ojaimi C, Li W, Kinugawa S, Post H, Csiszar A, Pacher P, Kaley G, Hintze TH. Transcriptional basis for exercise limitation in male eNOS-knockout mice with

age: heart failure and the fetal phenotype. *American journal of physiology. Heart and circulatory physiology*. 2005;289(4):H1399-407.

111. Egan DF, Shackelford DB, Mihaylova MM et al. Phosphorylation of ULK1 (hATG1) by AMP-activated protein kinase connects energy sensing to mitophagy. *Science*. 2011;331(6016):456-61.

112. Decker B, Pumiglia K. mTORc1 activity is necessary and sufficient for phosphorylation of eNOS(S1177). *Physiol Rep*. 2018;6(12):e13733-e.

113. Fritzen AM, Madsen AB, Kleinert M, Treebak JT, Lundsgaard A-M, Jensen TE, Richter EA, Wojtaszewski J, Kiens B, Frøsig C. Regulation of autophagy in human skeletal muscle: effects of exercise, exercise training and insulin stimulation. *The Journal of physiology*. 2016;594(3):745-61.

114. Besse-Patin A, Léveillé M, Oropeza D, Nguyen BN, Prat A, Estall JL. Estrogen Signals Through Peroxisome Proliferator-Activated Receptor-γ Coactivator 1α to Reduce Oxidative Damage Associated With Diet-Induced Fatty Liver Disease. *Gastroenterology*. 2017;152(1):243-56.

115. Klinge CM. Estrogenic control of mitochondrial function and biogenesis. *Journal of cellular biochemistry*. 2008;105(6):1342-51.

116. Fletcher JA, Linden MA, Sheldon RD, Meers GM, Morris EM, Butterfield A, Perfield JW, 2nd, Thyfault JP, Rector RS. Fibroblast growth factor 21 and exercise-induced hepatic mitochondrial adaptations. *Am J Physiol Gastrointest Liver Physiol*. 2016;310(10):G832-43.

117. Cunningham RP, Moore MP, Moore AN, Healy JC, Roberts MD, Rector RS, Martin JS. Curcumin supplementation mitigates NASH development and progression in female Wistar rats. *Physiol Rep*. 2018;6(14):e13789.

118. Rolo AP, Teodoro JS, Palmeira CM. Role of oxidative stress in the pathogenesis of nonalcoholic steatohepatitis. *Free radical biology & medicine*. 2012;52(1):59-69.

119. Bauer PM, Fulton D, Boo YC, Sorescu GP, Kemp BE, Jo H, Sessa WC. Compensatory phosphorylation and protein-protein interactions revealed by loss of function and gain of function mutants of multiple serine phosphorylation sites in endothelial nitric-oxide synthase. *Journal of Biological Chemistry*. 2003;278(17):14841-9.

120. Mount PF, Kemp BE, Power DA. Regulation of endothelial and myocardial NO synthesis by multi-site eNOS phosphorylation. *Journal of molecular and cellular cardiology*. 2007;42(2):271-9.

121. Chen Z-P, Mitchelhill KI, Michell BJ, Stapleton D, Rodriguez-Crespo I, Witters LA, Power DA, Ortiz de Montellano PR, Kemp BE. AMP-activated protein kinase phosphorylation of endothelial NO synthase. *FEBS letters*. 1999;443(3):285-9.

122. Fulton D, Gratton J-P, McCabe TJ, Fontana J, Fujio Y, Walsh K, Franke TF, Papapetropoulos A, Sessa WC. Regulation of endothelium-derived nitric oxide production by the protein kinase Akt. *Nature*. 1999;399(6736):597.

123. Michell BJ, Harris MB, Chen Z-p, Ju H, Venema VJ, Blackstone MA, Huang W, Venema RC, Kemp BE. Identification of regulatory sites of phosphorylation of the bovine endothelial nitric-oxide synthase at serine 617 and serine 635. *Journal of Biological Chemistry*. 2002;277(44):42344-51.

124. Smith BK, Marcinko K, Desjardins EM, Lally JS, Ford RJ, Steinberg GR. Treatment of nonalcoholic fatty liver disease: role of AMPK. *American Journal of Physiology-Endocrinology and Metabolism*. 2016;311(4):E730-E40.

125. Lee-Young RS, Ayala JE, Hunley CF, James FD, Bracy DP, Kang L, Wasserman DH. Endothelial nitric oxide synthase is central to skeletal muscle metabolic regulation and enzymatic signaling during exercise in vivo. *American Journal of Physiology-Regulatory, Integrative and Comparative Physiology*. 2010;298(5):R1399-R408.

126. Zou M-H, Kirkpatrick SS, Davis BJ, Nelson JS, Wiles WG, Schlattner U, Neumann D, Brownlee M, Freeman MB, Goldman MH. Activation of the AMP-activated protein kinase by the anti-diabetic drug metformin in vivo role of mitochondrial reactive nitrogen species. *Journal of Biological Chemistry*. 2004;279(42):43940-51.

127. Zhang J, Xie Z, Dong Y, Wang S, Liu C, Zou M-H. Identification of nitric oxide as an endogenous activator of the AMP-activated protein kinase in vascular endothelial cells. *Journal of Biological Chemistry*. 2008;283(41):27452-61.

128. Shankar RR, Wu Y, Shen H-q, Zhu J-S, Baron AD. Mice with gene disruption of both endothelial and neuronal nitric oxide synthase exhibit insulin resistance. *Diabetes*. 2000;49(5):684-7.

129. Persico M, Masarone M, Damato A, Ambrosio M, Federico A, Rosato V, Bucci T, Carrizzo A, Vecchione C. "Non alcoholic fatty liver disease and eNOS dysfunction in humans". *BMC gastroenterology*. 2017;17(1):35-.

130. Mohan S, Reddick RL, Musi N, Horn DA, Yan B, Prihoda TJ, Natarajan M, Abboud-Werner SL. Diabetic eNOS knockout mice develop distinct macro-and microvascular complications. *Laboratory investigation*. 2008;88(5):515.

131.   Bates T, Loesch A, Burnstock G, Clark J. Immunocytochemical evidence for a mitochondrially located nitric oxide synthase in brain and liver. *Biochemical and biophysical research communications*. 1995;213(3):896-900.

132.   Kobzik L, Stringer B, Balligand J-L, Reid MB, Stamler JS. Endothelial-type nitric oxide synthase (ec-NOS) in skeletal muscle fibers: mitochondrial relationships. *Biochemical and biophysical research communications*. 1995;211(2):375-81.

133.   Gao S, Chen J, Brodsky SV, Huang H, Adler S, Lee JH, Dhadwal N, Cohen-Gould L, Gross SS, Goligorsky MS. Docking of Endothelial Nitric Oxide Synthase (eNOS) to the Mitochondrial Outer Membrane A PENTABASIC AMINO ACID SEQUENCE IN THE AUTOINHIBITORY DOMAIN OF eNOS TARGETS A PROTEINASE K-CLEAVABLE PEPTIDE ON THE CYTOPLASMIC FACE OF MITOCHONDRIA. *Journal of Biological Chemistry*. 2004;279(16):15968-74.

134.   Ghafourifar P, Cadenas E. Mitochondrial nitric oxide synthase. *Trends in pharmacological sciences*. 2005;26(4):190-5.

135.   Persichini T, Mazzone V, Polticelli F, Moreno S, Venturini G, Clementi E, Colasanti M. Mitochondrial type I nitric oxide synthase physically interacts with cytochrome c oxidase. *Neuroscience letters*. 2005;384(3):254-9.

136.   Tatoyan A, Giulivi C. Purification and characterization of a nitric-oxide synthase from rat liver mitochondria. *Journal of Biological Chemistry*. 1998;273(18):11044-8.

137.   Stadler J, Billiar TR, Curran RD, Stuehr DJ, Ochoa JB, Simmons RL. Effect of exogenous and endogenous nitric oxide on mitochondrial respiration of rat hepatocytes. *American Journal of Physiology-Cell Physiology*. 1991;260(5):C910-C6.

138.   Lin HZ, Yang SQ, Chuckaree C, Kuhajda F, Ronnet G, Diehl AM. Metformin reverses fatty liver disease in obese, leptin-deficient mice. *Nature medicine*. 2000;6(9):998.

139.   Valerio A, Cardile A, Cozzi V, Bracale R, Tedesco L, Pisconti A, Palomba L, Cantoni O, Clementi E, Moncada S. TNF-α downregulates eNOS expression and mitochondrial biogenesis in fat and muscle of obese rodents. *The Journal of clinical investigation*. 2006;116(10):2791-8.

140.   Tateya S, Rizzo NO, Handa P, Cheng AM, Morgan-Stevenson V, Daum G, Clowes AW, Morton GJ, Schwartz MW, Kim F. Endothelial NO/cGMP/VASP signaling attenuates Kupffer cell activation and hepatic insulin resistance induced by high-fat feeding. *Diabetes*. 2011;60(11):2792-801.

141. Xie G, Wang X, Wang L, Wang L, Atkinson RD, Kanel GC, Gaarde WA, Deleve LD. Role of differentiation of liver sinusoidal endothelial cells in progression and regression of hepatic fibrosis in rats. *Gastroenterology*. 2012;142(4):918-27 e6.

142. Liu J, Li C, Waalkes MP, Clark J, Myers P, Saavedra JE, Keefer LK. The nitric oxide donor, V-PYRRO/NO, protects against acetaminophen-induced hepatotoxicity in mice. *Hepatology (Baltimore, Md.)*. 2003;37(2):324-33.

143. Moal F, Veal N, Vuillemin E et al. Hemodynamic and antifibrotic effects of a selective liver nitric oxide donor V-PYRRO/NO in bile duct ligated rats. *World Journal of Gastroenterology : WJG*. 2006;12(41):6639-45.

144. Maslak E, Zabielski P, Kochan K et al. The liver-selective NO donor, V-PYRRO/NO, protects against liver steatosis and improves postprandial glucose tolerance in mice fed high fat diet. *Biochemical pharmacology*. 2015;93(3):389-400.

145. Lee K-C, Hsieh Y-C, Chan C-C, Sun H-J, Huang Y-H, Hou M-C, Lin H-C. Human relaxin-2 attenuates hepatic steatosis and fibrosis in mice with non-alcoholic fatty liver disease. *Laboratory Investigation*. 2019;99(8):1203-16.

146. Nixon RA. The role of autophagy in neurodegenerative disease. *Nature medicine*. 2013;19(8):983.

147. Levine B. Autophagy and cancer. *Nature*. 2007;446(7137):745-7.

148. Rubinsztein DC, Mariño G, Kroemer G. Autophagy and aging. *Cell*. 2011;146(5):682-95.

149. Rabinowitz JD, White E. Autophagy and metabolism. *Science*. 2010;330(6009):1344-8.

150. Takamura A, Komatsu M, Hara T, Sakamoto A, Kishi C, Waguri S, Eishi Y, Hino O, Tanaka K, Mizushima N. Autophagy-deficient mice develop multiple liver tumors. *Genes & development*. 2011;25(8):795-800.

151. Amir M, Czaja MJ. Autophagy in nonalcoholic steatohepatitis. *Expert review of gastroenterology & hepatology*. 2011;5(2):159-66.

152. Youle RJ, Narendra DP. Mechanisms of mitophagy. *Nature reviews Molecular cell biology*. 2011;12(1):9-14.

153. Mizushima N, Klionsky DJ. Protein turnover via autophagy: implications for metabolism. *Annu. Rev. Nutr.* 2007;27:19-40.

154. He C, Klionsky DJ. Regulation mechanisms and signaling pathways of autophagy. *Annual review of genetics*. 2009;43:67-93.

155.	Ashrafi G, Schwarz T. The pathways of mitophagy for quality control and clearance of mitochondria. *Cell Death & Differentiation*. 2013;20(1):31-42.

156.	Zhang T, Xue L, Li L, Tang C, Wan Z, Wang R, Tan J, Tan Y, Han H, Tian R. BNIP3 protein suppresses PINK1 kinase proteolytic cleavage to promote mitophagy. *Journal of Biological Chemistry*. 2016;291(41):21616-29.

157.	Mizushima N, Yoshimori T. How to interpret LC3 immunoblotting. *Autophagy*. 2007;3(6):542-5.

158.	Kabeya Y, Mizushima N, Ueno T, Yamamoto A, Kirisako T, Noda T, Kominami E, Ohsumi Y, Yoshimori T. LC3, a mammalian homologue of yeast Apg8p, is localized in autophagosome membranes after processing. *The EMBO journal*. 2000;19(21):5720-8.

159.	Sun N, Yun J, Liu J, Malide D, Liu C, Rovira II, Holmström KM, Fergusson MM, Yoo YH, Combs CA. Measuring in vivo mitophagy. *Molecular cell*. 2015;60(4):685-96.

160.	McWilliams TG, Prescott AR, Allen GF, Tamjar J, Munson MJ, Thomson C, Muqit MM, Ganley IG. mito-QC illuminates mitophagy and mitochondrial architecture in vivo. *Journal of Cell Biology*. 2016;214(3):333-45.

161.	Schworer CM, Shiffer K, Mortimore G. Quantitative relationship between autophagy and proteolysis during graded amino acid deprivation in perfused rat liver. *Journal of Biological Chemistry*. 1981;256(14):7652-8.

162.	Madrigal-Matute J, Cuervo AM. Regulation of liver metabolism by autophagy. *Gastroenterology*. 2016;150(2):328-39.

163.	Ezaki J, Matsumoto N, Takeda-Ezaki M, Komatsu M, Takahashi K, Hiraoka Y, Taka H, Fujimura T, Takehana K, Yoshida M. Liver autophagy contributes to the maintenance of blood glucose and amino acid levels. *Autophagy*. 2011;7(7):727-36.

164.	Komatsu M, Waguri S, Ueno T, Iwata J, Murata S, Tanida I, Ezaki J, Mizushima N, Ohsumi Y, Uchiyama Y. Impairment of starvation-induced and constitutive autophagy in Atg7-deficient mice. *The Journal of cell biology*. 2005;169(3):425-34.

165.	Yamada T, Murata D, Adachi Y, Itoh K, Kameoka S, Igarashi A, Kato T, Araki Y, Huganir RL, Dawson TM. Mitochondrial stasis reveals p62-mediated ubiquitination in Parkin-independent mitophagy and mitigates nonalcoholic fatty liver disease. *Cell metabolism*. 2018;28(4):588-604. e5.

166. Singh R, Kaushik S, Wang Y, Xiang Y, Novak I, Komatsu M, Tanaka K, Cuervo AM, Czaja MJ. Autophagy regulates lipid metabolism. *Nature*. 2009;458(7242):1131-5.

167. Yang L, Li P, Fu S, Calay ES, Hotamisligil GS. Defective hepatic autophagy in obesity promotes ER stress and causes insulin resistance. *Cell metabolism*. 2010;11(6):467-78.

168. Czaja MJ. Function of Autophagy in Nonalcoholic Fatty Liver Disease. *Dig Dis Sci*. 2016;61(5):1304-13.

169. Inami Y, Yamashina S, Izumi K, Ueno T, Tanida I, Ikejima K, Watanabe S. Hepatic steatosis inhibits autophagic proteolysis via impairment of autophagosomal acidification and cathepsin expression. *Biochemical and biophysical research communications*. 2011;412(4):618-25.

170. Czaja MJ. Functions of autophagy in hepatic and pancreatic physiology and disease. *Gastroenterology*. 2011;140(7):1895-908.

171. Trevaskis JL, Griffin PS, Wittmer C, Neuschwander-Tetri BA, Brunt EM, Dolman CS, Erickson MR, Napora J, Parkes DG, Roth JD. Glucagon-like peptide-1 receptor agonism improves metabolic, biochemical, and histopathological indices of nonalcoholic steatohepatitis in mice. *American Journal of Physiology-Gastrointestinal and Liver Physiology*. 2012;302(8):G762-G72.

172. Hsu H-C, Liu C-H, Tsai Y-C, Li S-J, Chen C-Y, Chu C-H, Chen M-F. Time-dependent cellular response in the liver and heart in a dietary-induced obese mouse model: the potential role of ER stress and autophagy. *European journal of nutrition*. 2016;55(6):2031-43.

173. Gonzalez-Rodriguez A, Mayoral R, Agra N, Valdecantos M, Pardo V, Miquilena-Colina M, Vargas-Castrillón J, Iacono OL, Corazzari M, Fimia G. Impaired autophagic flux is associated with increased endoplasmic reticulum stress during the development of NAFLD. *Cell death & disease*. 2014;5(4):e1179-e.

174. Trocha M, Merwid-Ląd A, Szuba A, Chlebda E, Pieśniewska M, Sozański T, Szeląg A. Effect of simvastatin on nitric oxide synthases (eNOS, iNOS) and arginine and its derivatives (ADMA, SDMA) in ischemia/reperfusion injury in rat liver. *Pharmacological Reports*. 2010;62(2):343-51.

175. Zhang Z, Wang M, Xue S-J, Liu D-H, Tang Y-B. Simvastatin ameliorates angiotensin II-induced endothelial dysfunction through restoration of Rho-BH4-eNOS-NO pathway. *Cardiovascular drugs and therapy*. 2012;26(1):31-40.

176. Andres AM, Hernandez G, Lee P, Huang C, Ratliff EP, Sin J, Thornton CA, Damasco MV, Gottlieb RA. Mitophagy is required for acute cardioprotection by simvastatin. *Antioxidants & redox signaling*. 2014;21(14):1960-73.

177. Fetterman JL, Holbrook M, Flint N, Feng B, Bretón-Romero R, Linder EA, Berk BD, Duess M-A, Farb MG, Gokce N. Restoration of autophagy in endothelial cells from patients with diabetes mellitus improves nitric oxide signaling. *Atherosclerosis*. 2016;247:207-17.

178. Naoum JJ, Zhang S, Woodside KJ, Song W, Guo Q, Belalcazar LM, Hunter GC. Aortic eNOS expression and phosphorylation in Apo-E knockout mice: differing effects of rapamycin and simvastatin. *Surgery*. 2004;136(2):323-8.

179. Kiffin R, Bandyopadhyay U, Cuervo AM. Oxidative stress and autophagy. *Antioxidants & redox signaling*. 2006;8(1-2):152-62.

180. Chen Y, Azad M, Gibson S. Superoxide is the major reactive oxygen species regulating autophagy. *Cell death and differentiation*. 2009;16(7):1040.

181. Park SY, Park MY, Park HG, Lee KJ, Kook MS, Kim WJ, Jung JY. Nitric oxide-induced autophagy and the activation of activated protein kinase pathway protect against apoptosis in human dental pulp cells. *International endodontic journal*. 2017;50(3):260-70.

182. Xing J, Liu H, Yang H, Chen R, Chen Y, Xu J. Upregulation of Unc-51-like kinase 1 by nitric oxide stabilizes SIRT1, independent of autophagy. *PLoS One*. 2014;9(12):e116165.

183. Sarkar S, Korolchuk VI, Renna M, Imarisio S, Fleming A, Williams A, Garcia-Arencibia M, Rose C, Luo S, Underwood BR. Complex inhibitory effects of nitric oxide on autophagy. *Molecular cell*. 2011;43(1):19-32.

184. Guan Y, Drake JC, Yan Z. Exercise-Induced Mitophagy in Skeletal Muscle and Heart. *Exercise and sport sciences reviews*. 2019;47(3):151-6.

185. Vainshtein A, Tryon LD, Pauly M, Hood DA. Role of PGC-1α during acute exercise-induced autophagy and mitophagy in skeletal muscle. *American Journal of Physiology-Cell Physiology*. 2015;308(9):C710-C9.

APPENDIX A – CURRICULUM VITAE

CURRICULUM VITAE

Rory P. Cunningham
Exercise Physiology PhD Candidate
Department of Nutrition and Exercise Physiology
University of Missouri - Columbia
Email: rorycunningham@mail.missouri.edu
Office: 573-814-6000-Ext.53728
Cell: +1-989-944-1797
Nationality: Ireland

EDUCATION

Degree	Institution	Field	Date
PhD	University of Missouri-Columbia, MO, USA; Mentor Dr. R. Scott Rector	Exercise Physiology	2016-Present
MS	Central Michigan University, MI, USA; Mentor - Dr. Naveen Sharma	Exercise Physiology	2014-2016
BS	University of Limerick, Ireland	Exercise Science	2010-2014

DOCTORAL COMMITTEE

R. Scott Rector, PhD (Mentor)
Jill A. Kanaley, PhD (Chair)
Victoria J. Vieira-Potter, PhD
Frank W. Booth, PhD

SCIENTIFIC TRAINING

2016-present	Research Assistant, Department of Nutrition and Exercise Physiology, University of Missouri, Columbia, MO, USA
2014-2016	Research/Teaching Assistant, Department of Health Sciences, Central Michigan University, MI, USA

TEACHING EXPERIENCE

Central Michigan University

2014-2016	HSC 637: Advanced Exercise Physiology – Lab Instructor
2015-2016	HSC 212 Applied Physiology & Kinesiology- Lab instructor
2015-2016	HSC 216 Biomechanics and Kinesiology - Lab instructor
2015	HSC 220 Basics in Health Fitness - Lab Instructor

HONORS AND AWARDS

2020	Edward J. O'Brien Scholarship, University of Missouri, Columbia MO
2020	M. Harold Laughlin Scholarship, University of Missouri, Columbia MO
2020	Mizzou 18 Award Class of 2020 – Campus Wide Outstanding Graduate Student,

	University of Missouri, Columbia MO
2020	Keystone Symposia Conference: New Insights into the Biology of Exercise – Selected Oral Presentation, University of Missouri, Columbia, MO
2019	Graduate Student Professional Development Travel Grant, University of Missouri, Columbia, MO
2019	Ben R. Londeree/Tom R. Thomas Award for Outstanding Graduate Student, University of Missouri, Columbia, MO
2019	Experimental Biology Annual Meeting - Selected Oral Presentation, University of Missouri, Columbia, MO
2018	American College of Sports Medicine Annual Meeting - Selected Oral Presentation, University of Missouri, MO
2017	Experimental Biology Annual Meeting - Poster of Distinction, University of Missouri, Columbia, MO

RESEARCH INTERESTS

- Understanding the molecular mechanisms behind of nonalcoholic fatty liver disease development, particularly hepatic mitochondrial dysfunction.
- Understanding exercise-induced adaptations to metabolism and how it pertains to chronic disease.
- The role of mitochondrial dynamics in chronic disease.

CURRENT RESEARCH PROJECTS

2019-Present
"Role of hepatic endothelial nitric oxide synthase and exercise-induced hepatic mitochondrial adaptations"
ACSM Foundation Doctoral Student Research Grant #18-00754
PI: **RP Cunningham**
- The goal of this project is to determine whether the beneficial effects of exercise on hepatic mitochondria occur through hepatocellular eNOS-dependent mechanisms.

2018-Present
"Nutrient overload, insulin resistance, and hepatic mitochondrial dysfunction"
NIH R01 DK113701-01
MPI: RS Rector, EJ Parks, JA Ibdah
- The goal of this project is to examine the role of hepatic mitochondrial dysfunction in the development and progression of NASH in humans and to determine whether hepatic mitochondria function is modifiable with lifestyle intervention therapies.
- This involves collaborating with bariatric surgeons to collect liver samples from patients, and also an intensive nine-month long lifestyle intervention study.

2017-Present
"Hepatic eNOS and Mitochondrial Function in NASH"
VA Merit Grant 1 I01 BX003271-01
PI: RS Rector
- The goal of this project is to examine the role of hepatocellular endothelial nitric oxide synthase in the regulation of NRF2 and BNIP2 in the progression of NASH.
- This involves cell culture and genetic manipulation in murine models of NASH.

PUBLICATIONS

Peer-Reviewed Publications (most recent listed first)

Primary articles
*co-first author

1) **Cunningham, R.P**., Moore, M.P., Meers, G.M., Jepkemoi, V., Boccardi, L., Takahashi, K., Sheldon, R.D., Ibdah, J.A., Thyfault, J.P., Rector, R.S. 2020. Manipulation of hepatocellular eNOS uncovers its vital role in NAFLD and NASH development. *Diabetes* (to be submitted to)

2) **Cunningham, R.P**., Moore, M.P., Dashek, R.J., Meers, G.M., Jepkemoi, V., Boccardi, L., Takahashi, K., Sheldon, R.D., Vieira-Potter, V.J., Kanaley, J.A., Booth, F.W., Rector, R.S. 2020. Deletion of hepatocellular eNOS impairs exercise-induced improvements in hepatic mitochondrial function and autophagy markers *Journal of Physiology* (to be submitted to)

3) **Cunningham, R.P**., Sheldon, R., and Rector, R.S. 2020. The emerging role of hepatocellular endothelial nitric oxide synthase in the development and progression of nonalcoholic fatty liver disease. *Frontiers in Physiology: Gastrointestinal Sciences*

4) *Moore, M.P., ***Cunningham, R.P**., Dashek, R., Mucinski J., and Rector, R.S., 2020. Dietary strategies for the management of nonalcoholic fatty liver disease. *Obesity*

5) Sheldon, R.D., Meers, G.M., Morris, E.M., Linden, M.A., **Cunningham, R.P**., Ibdah, J.A., Thyfault, J.P., Laughlin, M.H. and Rector, R.S., 2019. eNOS deletion impairs mitochondrial quality control and exacerbates Western diet-induced NASH. *American Journal of Physiology-Endocrinology and Metabolism*, *317*(4), pp.E605-E616.

6) Moore, M.P., **Cunningham, R.P**., Kelty, T.J., Boccardi, L.R., Nguyen, N.Y., Booth, F.W. and Rector, R.S., 2019. Ketogenic diet in combination with voluntary exercise impacts markers of hepatic metabolism and oxidative stress in male and female Wistar rats. *Applied Physiology, Nutrition, and Metabolism*.

7) Gremminger, V.L., Jeong, Y., **Cunningham, R.P**., Meers, G.M., Rector, R.S. and Phillips, C.L., 2019. Compromised Exercise Capacity and Mitochondrial Dysfunction in the Osteogenesis Imperfecta Murine (oim) Mouse Model. *Journal of Bone and Mineral Research*.

8) Winn, N.C., Jurrissen, T.J., Grunewald, Z.I., **Cunningham, R.P**., Woodford, M.L., Kanaley, J.A., Lubahn, D.B., Manrique-Acevedo, C., Rector, R.S., Vieira-Potter, V.J. and Padilla, J., 2018. Estrogen receptor-α signaling maintains immunometabolic function in males and is obligatory for exercise-induced amelioration of nonalcoholic fatty liver. *American Journal of Physiology-Endocrinology and Metabolism*, *316*(2), pp.E156-E167.

9) **Cunningham, R.P**., Moore, M.P., Moore, A.N., Healy, J.C., Roberts, M.D., Rector, R.S. and Martin, J.S., 2018. Curcumin supplementation mitigates NASH development and progression in female Wistar rats. *Physiological reports*, *6*(14), p.e13789.

10) **Cunningham, R.P**., Moore, M.P., Meers, G.M., Ruegsegger, G.N., Booth, F.W. and Rector, R.S., 2018. Maternal Physical Activity and Sex Impact Markers of Hepatic Mitochondrial Health. *Medicine and science in sports and exercise*, *50*(10), pp.2040-2048.

Selected Abstracts

1) Moore M.P., **Cunningham R.P.**, Meers G.M., Johnson S.A., Wheeler A.A., Ganga R.R. Spencer N.M., Pitt J.B., Diaz-Arias A., Swi A. I. A., Ibdah J.A., Parks E.J., Rector R.S. 2020. Reduced Hepatic Mitochondrial Metabolism and Markers of Mitochondrial Turnover in Humans Are Linked to NAFLD Progression. *American Diabetes Association*

2) **Cunningham, R.P.**, Moore, M.P., Meers, G.M., Jepkemoi, V., and Rector, R.S. 2020. Deletion of hepatocellular eNOS impairs exercise-induced improvements in hepatic mitochondrial function. *Keystone Symposia Conference: New Insights into the Biology of Exercise.*

3) **Cunningham, R.P.**, Linden, M.A., Meers, G.M., and Rector, R.S. 2019. Moderate and high intensity exercise prevents the NAFLD-induced impairment in markers of hepatic lactate metabolism. *North East ACSM Annual Conference.*

4) Moore, M.P., **Cunningham, R.P.**, Kelty, T.J., Boccardi, L.R., Nguyen, N., Booth, F.W., and Rector, R.S. 2019. Combining a ketogenic diet with voluntary exercise impacts markers of hepatic metabolism in male and female Wistar rats. *Cell Symposia Exercise Metabolism.*

5) **Cunningham, R.P.**, Moore, M.P., Nguyen, N., Dashek, R., Boccardi, L.R., Jepkemoi, V., Meers, G.M., Chandrasekar, B., and Rector, R.S. 2019. Hepatic Knockdown of RECK Increases NASH. *The FASEB Journal.*

6) **Cunningham, R.P.**, Moore, M.P., Meers, G.M., Nguyen, N., Boccardi, L.R., Jepkemoi, V., Takahashi, T., and Rector, R.S. 2019 Hepatocyte-Specific Deletion of eNOS Impairs Mitochondrial Function and Exacerbates Hepatic Steatosis. *The FASEB Journal.*

7) Moore, M.P., **Cunningham, R.P.**, Kelty, T.J., Boccardi, L.R., Nguyen, N., Booth, F.W., and Rector, R.S. 2019 Ketogenic diet in combination with voluntary exercise impacts markers of hepatic metabolism and oxidative stress in male and female Wistar rats. *The FASEB Journal.*

8) **Cunningham, R.P.**, Meers, G.M., Ruegsegger, G., Booth, F. and Rector, R.S., 2018. Effects of Maternal Exercise on Hepatic Steatosis in Young Adult Rats: 2527 June 1 2. *Medicine & Science in Sports & Exercise*, 50(5S), p.626.

9) Moore, M., **Cunningham, R.P.**, Moore, A.N., Healy, J.C., Roberts, M.D., Rector, S. and Martin, J.S., 2018. Curcumin Supplementation Mitigates Nash Development and Progression in Female Wistar Rats: 2926 Board# 209 June 1 3. *Medicine & Science in Sports & Exercise*, 50(5S), p.724.

10) Meers, G., **Cunningham, R.P.**, Panasevich, M. and Rector, R.S., 2018. In Vivo Knockdown of Hepatocellular enos Reduces Cellular Anti-oxidant Defense and Mitochondria Biogenesis/Function: 1075 Board# 7 May 31 8. *Medicine & Science in Sports & Exercise*, 50(5S), p.249.

11) Gremminger, V., Jeong, Y., **Cunningham, R.P.**, Meers, G., Rector, R.S. and Phillips, C., 2018. Potential mitochondrial dysfunction in skeletal muscle of mouse models of Osteogenesis imperfecta. *The FASEB Journal*, 32(1_supplement), pp.543-20.

12) Noble, N.D., Pettit-Mee, R.J., **Cunningham, R.P.** and Sharma, N., 2017. High Protein Diets Blunt Insulin-Stimulated Akt Phosphorylation While Enhancing Fibroblast Growth Factor Receptor Phosphorylation in Rat Liver. *The FASEB Journal*, 31(1_supplement), pp.1036-10.

13) Pettit-Mee, R.J., **Cunningham, R.P.** and Sharma, N., 2017. High Casein Diet Differentially Alters FGF21 Levels in Plasma and Cardiac Tissue in Rats. *The FASEB Journal*, 31(1_supplement), pp.885-6.

14) **Cunningham, R.P.**, Sheldon, R., Meers, G., Kandikattu, H.K., Chandrasekar, B. and Rector, R.S., 2017. Western diet feeding downregulates hepatic RECK expression and induces NASH with fibrosis. *The FASEB Journal*, 31(1_supplement), pp.887-5.

PROFESSIONAL AFFILIATIONS

2015-Present	American College of Sports Medicine (ACSM)
2016-Present	American Society for Nutrition (ASN)
2015-Present	American Physiologic Society (APS)
2015-2016	Endocrine Society

PROFESSIONAL SERVICE

Co-reviewer under Scott Rector, PhD

- *American Journal of Physiology - Regulatory, Integrative and Comparative Physiology*
- *American Journal of Physiology – Endocrinology*
- *Applied Physiology, Nutrition, and Metabolism*
- *Journal of Applied Physiology*

LECTURES AND INVITED TALKS

"*The role of hepatocellular eNOS in NAFLD development and hepatic mitochondrial adaptations to exercise*""
Invited Talk; National Institute of Health, June 2020

"*Excess Weight and Chronic Disease in Adults*"
The Landscape of Obesity; Instructor: Sara Gable, PhD, University of Missouri, February 2020

"*Deletion of hepatocellular eNOS impairs exercise-induced improvements in hepatic mitochondrial function*"
Keystone Symposia Conference 2020: New Insights into the Biology of Exercise, March 2020

"*Exercise and Weight Management*"
The Landscape of Obesity; Instructor: Sara Gable, PhD, University of Missouri, April 2019

"*Hepatocyte-Specific Deletion of eNOS Impairs Mitochondrial Function and Exacerbates Hepatic Steatosis*"
Experimental Biology Annual Meeting 2019, Orlando FL, April 2019

"*Navigating Mitophagy – Mechanisms and Interpretation*"
Etiology of Obesity; Instructor: Scott Rector, PhD, University of Missouri, March 2018

"*The Effect of Maternal Exercise on Offspring Hepatic Steatosis*"
Department of Nutrition and Exercise Physiology Seminar Series, University of Missouri, February 14, 2019

"*The Effect of Maternal Exercise on Offspring Hepatic Steatosis*"
ACSM Annual Meeting 2018, Milwaukee, WC, June 2018

"The Effect of High Protein Diets on Circulating Cytokine Levels"
Michigan Chapter ACSM Meeting, Gaylord, MI, 2016

UNIVERSITY SERVICE

2019-2020	Diabetes and Metabolism Journal Club Coordinator
2019	Assisted with student recruitment for the Nutrition and Exercise Physiology Department at regional ACSM chapter meetings, University of Missouri
2018-Present	Graduate Student Representative and founding member for 'Exercise is Medicine on Campus', University of Missouri
2016-Present	Graduate Profession Council Representative for Department of Nutrition and Exercise Physiology, University of Missouri
2017-2018	Graduate Student Association President for Department of Nutrition and Exercise Physiology, University of Missouri
2016-2017	Graduate Student Association Head of Fundraising for Department of Nutrition and Exercise Physiology, University of Missouri

LAY CONTRIBUTIONS

2020	Rockbridge High School Tour and Demonstration of Nutrition and Exercise Physiology Department, University of Missouri, MO, USA
2018	Bradford Agricultural Education Field Day, "Exercise is Medicine" Booth, Columbia, MO, USA
2018	Rockbridge High School Tour and Demonstration of Nutrition and Exercise Physiology Department, University of Missouri, MO, USA
2017	Rockbridge High School Newsletter, Columbia, MO, USA

CERTIFICATIONS & ACHIEVEMENTS

2012-Present	I.A.W.L.A. Olympic Weightlifting Instructor Level 1, Ireland
2014-Present	CPR and First Aid, USA
2008-2010	Pool Lifeguard, Galway, Ireland
2017	Science Communication Course, University of Missouri, MO
2008-2012	Ireland International Rugby Team u18/u19/u20

PREVIOUS WORK EXPERIENCE

2018-2019	Personal Trainer for Older Women on Weights (OWOW), Optimus Center for Health, Columbia, MO, USA
2015	Head Rugby 7s Coach, Boston Irish Wolfhounds, Boston, MA, USA
2014-2015	Head Rugby 7s Coach, Central Michigan University, Mt. Pleasant, MO, USA
2012-2014	Strength and Conditioning Intern, Connacht Rugby, Ireland
2013	Strength and Conditioning Intern, Chiefs Super Rugby Franchise, New Zealand

VOLUNTEER EXPERIENCE

2015-2016	Michigan Special Olympics – State Winter Games Ski Coach, MI, USA
2015-2016	Michigan Special Olympics – State Poly Hockey Volunteer, MI, USA
2012	Jacinta O' Brein 10km Run – Volunteer, Limerick, Ireland

REFERENCES

R. Scott Rector, PhD
Associate Professor
Internal Medicine-Division of Gastroenterology and Hepatology/Nutrition and Exercise Physiology
CE443 Clinical Support Education Building
University of Missouri
Columbia, MO 65211
Phone: (573) 814-6000 ext 53779 | Fax: (573) 884-4595
E-mail: rectors@health.missouri.edu
http://nep.missouri.edu/faculty_rector.html

Jill A. Kanaley, PhD
Professor and Associate Chair
Nutrition and Exercise Physiology
204D Gwynn Hall
University of Missouri,
Columbia, MO 65211
Phone: (573) 882-2519
E-mail: kanaleyj@missouri.edu
http://nep.missouri.edu/faculty_kanaley.html

Last Update – June, 2020

VITA

Rory Cunningham was born on October 18th 1991 in Galway, Ireland. He completed his undergraduate degree in Sports and Exercise Science at the University of Limerick in Ireland, focusing on strength and conditioning for sports performance while completing multiple internships in Ireland and New Zealand. During his Master's in Exercise Physiology at Central Michigan University, he became more interested in research related to exercise physiology's role in obesity and chronic disease. It was this foray into research that led him to pursue a PhD in Exercise Physiology at the University of Missouri, under the mentorship of Dr. Scott Rector. Rory obtained his doctorate degree in 2020, and plans to pursue a post-doctoral degree in mitochondrial dynamics at the National Cancer Institute.